UNIVERZITET U BEOGRADU
MAŠINSKI FAKULTET

Abdalla S. Ahmed Tawengi

Određivanje zavarljivosti niskolegiranih čelika povišene čvrstoće primenom Tagučijeve metode planiranja eksperimenta

doktorska disertacija

Beograd, 2014

EXAMINATION COMMITTEE

Supervisor:	Prof. Dr. Aleksandar Sedmak University of Belgrade, Faculty of Mechanical Engineering
Members:	Prof. Dr. Radica Prokić-Cvetković University of Belgrade, Faculty of Mechanical Engineering
	Prof. Dr. Vidosav Majstorovic University of Belgrade, Faculty of Mechanical Engineering
	Dr. Ljubica Milović, Assistant Professor Faculty of Technology and Metallurgy in Belgrade
	Dr. Snezana Kirin, Research Associate, Innovation Center, Faculty of Mechanical Engineering in Belgrade

Date of defence:

06 MAR 2014

Комисијазаоцену и одбранудисертације:

Ментор: ПрофесордокторАлександарСедмак,
Универзитет у Београду, Машинскифакултет

Члановикомисије: ПрофесордокторРадицаПрокић,
Универзитет у Београду, Машинскифакултет

ПрофесордокторvidosavMajstorovic,
Универзитет у Београду, Машинскифакултет

ДрЉубицаМиловић, доцентдоцент,
Технолошко-металуршкомфакултету у Београду

ДрСнежанаКирин, истраживачсарадник,
Иновационицентар-Машинскифакултету Београду

Датумодбране:

To my parents

Acknowledgments

I would like to express my enormous gratitude to all of those who stood by me regarding this work; particularly my supervisor Professor Dr. Aleksandar Sedmak for his generous support and assistance. Without him, I would not have been capable to bring this to an end.

Appreciation is also extended to Dr. Lujbica Milovic from the Faculty of Technology and Metallurgy of Belgrade University for her advices and help.

Special thanks to my colleague Muamar Bin Isa, who was willing to help in whatever he could during my study period. I would also like to thank all of the teaching staff members of the Mechanical Engineering Faculty of Belgrade University whose insightful wide knowledge of the field helped me to go ahead and finish my study.

My final gratitude always goes to my beloved wife and my four lovely kids for being so patient to keep me cheerful during my whole study periods.

Abdalla

Belgrade, Serbia

2014

Abstract

Group of high strength low alloy steel, signs NIONIKRAL60 and NIONIKRAL70, created as the need to replace the steel HY-80 and HY-100, is a serious breakthrough to designers and manufacturers of metal structures, especially pressure vessels, enabling to design and produce light steel structure. The main problem in the application of high strength low alloy steels, especially NIONIKRAL 70, their weldability, especially in the case of thicker base material, which is dictated by the requirements of the appropriate structures.

The reliability of welds cannot be ensured without proper understanding of weldability therefore the literature reporting the research on cold cracking phenomenon and weldability of HSLA steel is reviewed and studied in the first part of this thesis in order to lay the theoretical foundations of this study.

However in view of the importance of high strength low alloy (HSLA) NIONIKRAL-70 steel, particularly for critical applications such as offshore platforms, pipeline and pressure vessels, the second part of this current work reports on an investigation of how to weld this type of steel economically without cold cracking. Using manual metal arc (MMA) welding process and thicker plates of NIONIKRAL-70 steel (up to 30 mm), many experiments through various technological tests such as Controlled Thermal Severity (CTS) test, Y-Groove test and Cabelka-Million test have been carried out both to observe this phenomenon, and to investigate the influencing factors, such as preheating technique, heat input, and electrode type. In addition to detecting cracks themselves, as an indirect indicator of weldability, and as a result of experimental research, the distribution of hardness in the welded joints, as well as toughness and fracture toughness of typical cross-sections of the welded joints have been tested. However, it has been found that there is a risk of cold cracking in NIONIKRAL-70 steel welds.

For NIONIKRAL-70 steel the optimum energy input has been determined, providing maximum crack propagation energy due to parametric combination of 200 °C preheating temperature, 15 KJ/cm heat input and TENACITO-80 electrode type.

Moreover Taguchi philosophy has been successfully applied to obtain optimal welding parametric combinations to evaluate the weldability of NIONIKRAL-70 steel joints produced by manual metal arc (MMA) welding. Based on Taguchi approach the present study centers around adoption of L4 orthogonal array and design experiments have been accordingly conducted with two different levels of welding process parameters e.g. preheating temperature, heat input and electrode strength. Weld toughness and fracture toughness measured for each experiment trial. With respect to the obtained results by Taguchi method and ANOVA it has been found that preheating is the most influencing parameter on weldability of the selected steel.

Keywords: HSLA (NIONIKRAL-70) steel, cold cracks, weldability testing, preheating, hardness, toughness, Taguchi approach, ANOVA.

Scientific field:

Technical science, Mechanical Engineering.

Narrow scientific field:

Welding and Materials Engineering

UDC

апстрактан

Група високе чврстоће низак легираног челика , потписује НИОНИКРАЛ60 и НИОНИКРАЛ70 , настао као потреба да се замени челика ХИ - 80 и ХИ - 100 , јеозбиљан пробој на дизајнера и произвођача металних конструкција , посебно судова под притиском, што омогућава да дизајнира и произведе лака челична конструкција . Основни проблем у примени високе чврстоће нисколегираних челика , посебно НИОНИКРАЛ 70 , њихова способност заваривања , посебно у случају дебљег основног материјала , који је диктиран захтевима одговарајућих структура .

Поузданост варова не може обезбедити без правилног разумевања заварљивости стогалитература извештавање истраживање о феномену и хладних прслина заварљивости од ХСЛА челика је прегледан и студирао у првом делу ове тезе како би се поставили теоријске основе ове студије .

Међутим, с обзиром на важност високе чврстоће ниског легуре (ХСЛА) НИОНИКРАЛ - 70 челика , нарочито за критичне апликације као што су оф шор платформи , цевовода и посуда под притиском , у другом делу овог извештаја текућих раде на истрази о томе како за варење ова врста челика економски без хладних прслина . Користећи упутство метални лук (ММА) процес заваривања и дебљих плоча за НИОНИКРАЛ - 70 челика (до 30 мм) , многим експериментима путем разних технолошких тестова , као што су Контролисано топлотно предострожности (ЦТС) тест , И - Гроове теста и Цабелка милиона теста имају Спроведено је да посматра овај феномен , и да испитају фактори утицаја , као што су предгревање технике , улаз топлоте , и типа електроде . Поред откривања пукотине себе , као индиректног показатељ заварљивост , и као резултат експерименталних истраживања ,расподела тврдоће у заварених спојева , као и жилавости и лома жилавост типичних пресека заварених спојева су тестирани . Међутим , нађено је да постојиризик од хладног пукотина у НИОНИКРАЛ - 70 челичних заварених спојева .

За НИОНИКРАЛ - 70 челикаоптималан унос енергије је одређен , обезбеђујући максималну енергију прслине услед параметарског комбинације 200 ° Ц температуре предгревања , 15 КЈ / цм улаз топлоте и ТЕНАЦИТО - 80 типа електрода .

Штавише Тагучи филозофија је успешно примењена за добијање оптималне комбинације за заваривање параметарске да процени заварљивост од НИОНИКРАЛ-70 челичних спојева насталих ручним метал арц (ММА) заваривање. На основу Тагуцхи прићи овом раду центара око усвајања Л4 матрице широке и дизајн експеримената су сходно томе спроведено са два различита нивоа процесних параметара заваривања нпр. предгревање температура, унос топлоте и електрода снаге. Вара жилавост и жилавост лома измерена за сваки експеримент суђење. У погледу резултата добијених методом Тагуцхи и АНОВА је утврђено да је загревање највише вршење утицаја на параметар заварљивост изабраног челика.

Кључне речи: ХСЛА (НИОНИКРАЛ-70) челик, хладно пукотине, способност заваривања тестирање, предгревање, тврдоћа, жилавост, Тагучи приступ, АНОВА.

Научна област:

Техничкенауке, Машинство

Ужа научна област:

Заваривање и инжењерство материјала

UDC

TABLE OF CONTENTS

LIST OF FIGURES

LIST OF TABLES

List of abbreviations and symbols

α	Ferrite
σ	Tightening (MPa)
γ	Austenite
η	Welding efficiency
A	Amperes
A1	Eutectoid temperature
A3	Dissolution temperature of ferrite in austenite
AHSS	Advanced high strength steels
ANOVA	Analysis of variance
A.M	Additional material
AF	Acicular ferrite
AWS	American welding society
ASTM	American society for testing and materials
BM	Base material, parent material
C.C	Cold crack
CCT	Continues cooling temperature diagram
CE	Carbon equivalent (IIW) (%)
Ce	Carbon equivalent (Ito and Bessy) (%)
CEN	Carbon equivalent (chart method) based on chemical composition (%)

CTWD	Contact-tip to workpiece distance
ΔCEN	Change in carbon equivalent
CP	Complex phase steel
CTS	Controlled thermal severity test
D	Diffusion coefficient – general expression
DOE	Design of experiment
DP	Dual phase steels
FA	Austenitic stainless steel weld metal (closely confirming to AWS E307T1-1)
FCAW	Flux cored arc welding
FF	Low hydrogen ferritic steel weld metal (AWS E110T5-K4)
FS	Ferrite with second phase
G-BOP	Gapped bead on plate test
GF	Grain boundary ferrite
GMAW	Gas metal arc welding
GTAW	Gas tungsten arc welding
H10	low Hydrogen, conforming to standard weld metal containing not more 10 cm3 of hydrogen in 100g of weld deposit.
HAZ	Heat affected zone
HACC	Hydrogen assisted cold cracking
H.C	Hot crack

H_{cr}	Weld critical hydrogen content with respect to cracking (ml/100g DM IIW)
HD	Weld diffusible hydrogen content per deposited weld metal (DM) conforming to ISO/IIW 3690-1977 (ml/100 g DM IIW)
HI	Heat input of welding (J/cm)
HICC	Hydrogen induced cold cracking
HSLA	High strength low alloy steel
HSS	High strength steel
HTLA	Heat treatable low allow steel
HV	Vickers pyramid hardness (HV)
K	Stiffness coefficient
Lij	The loss function of the ith quality characteristic in the jth experiment
LTT	Low transformation temperature
m	Mean of sum of main characteristic
MAG	Metal Arc Active Gas
MIG	Metal Arc Inert Gas
NDT	Nondestructive inspection test
nj	Signal to noise ratio in the jth experiment
P_p	Parameter found by Ito&Bessyo
PWHT	Post weld heat treatment
R_m	Tensile strength (MPa)

R_p	Yield strength (MPa)
$R_{p0.2}$	Yield strength at 0.2 mm elongation (MPa)
S	Plate thickness (mm)
SAW	Sub-merged Arc Welding
SMAW	Shielded metal arc welding
S/N	Signal-to-noise ratio
TIG	Tungsten inert gas
TSN	Thermal severity number
TTT	Time temperature transformation diagram
$\Delta t8/5$	Cooling time from 800 to 500°C (sec)
T_i	weld interpass temperature (°C)
TMCP	Thermo mechanical controlled processed
T_0	Preheat temperature, in general (°C)
TRIP	Transformation-induced plasticity steels
UHSS	Ultra high strength steels
UTS	Ultimate tensile strength (MPa)
V	Voltage
WM	Weld metal
WS	Welding speed
YS	Yield strength (MPa)

1. Introduction

1.1 Background

High-strength low-alloy (HSLA) steels were originally developed in the 1960s for large-diameter oil and gas pipelines. The line pipe used in these projects required higher strength and toughness than mild carbon steel, and good weldability provided by a low carbon equivalent (CE).[1] The last four decades have seen remarkable progress in the development of High Strength Low Alloy (HSLA) steels for structural applications in pipelines, offshore structures, ships and buildings. These developments have been driven by the need to obtain improved combinations of weldability, toughness and strength in tonnage quantities at affordable prices. They have engaged all sectors of the industry; steelmakers, manufacturers, constructors, operators and safety regulators, and have spanned disciplines from theoretical modeling to manufacturing and site construction activities. At the heart of these developments has been the understanding of the physical and chemical metallurgy of the steel product, how the joining process influences it and how this in turn determines the performance, integrity and reliability of the final installation. Interest has focused particularly on the weld heat affected zone, its microstructure and properties, especially the effect of steel chemistry, weld process and heat input, preheat and post-weld heat treatment on weldability and toughness. While significant improvements in weldability have been achieved over the years through reductions in the carbon equivalent, a consequence of this has been the increased reliance on thermo-mechanical processing and a shift to microalloy-dominated strengthening mechanisms, away from the carbon-dominated mechanisms on which the original understanding was based.[2]

High-strength low-alloy (HSLA) steels, or microalloyed steels, are designed to provide better mechanical properties and/or greater resistance to atmospheric corrosion than conventional carbon steels. They are not considered

to be alloy steels in the normal sense because they are designed to meet specific mechanical properties rather than a chemical composition (HSLA steels have yield strengths greater than 275 MPa.

The chemical composition of specific HSLA steel may vary for different product thicknesses to meet mechanical property requirements. The HSLA steels in sheet or plate form have low carbon content (0.05 to−0.25% C) in order to produce adequate formability and weldability, and they have manganese content up to 2.0%. Small quantities of chromium, nickel, molybdenum, copper, nitrogen, vanadium, niobium, titanium, and zirconium are used in various combinations.[3]

Further decreases in CE became possible with the introduction of improved processing procedures such as controlled rolling and quenching and tempering. These procedures, together with more recent developments such as water cooling directly after hot rolling, have played a major role in decreasing welding costs and in improving weldment properties, thus contributing towards maintaining the dominate position of steel as the world's major structural material.[4]

Just over 20 years ago, it was estimated that, in Britain alone, costs amounting to £260 million were annually incurred as a result of manufacturing problems directly attributable to welding. At least £40 million of this total arose from the need to repair hydrogen-induced cracks and adjacent to welds. Although much more is known about how to avoid hydrogen cracking when welding conventional steels, new steels and unexpected problems have arisen, so that further research and guidance has been needed. The weldability of steel, with regard to hydrogen-induced cold cracking, is inversely proportional to the hardenability of the steel, which measures the ease of forming martensite during heat treatment. The hardenability of steel depends on its chemical composition, with greater quantities of carbon and other alloying elements resulting in a higher hardenability and thus a lower

weldability. In order to be able judge alloys made up of many distinct materials, a measure known as the carbon equivalent content (CE) is used to compare the relative weldabilities of different alloys by comparing their properties to plain carbon steel. [5]

1.2 Defining the problem

Hydrogen-induced [3,4,5,6,7] cracking is also referred as cold cracking, delayed cracking or underbead cracking. It is a mechanical fracture caused by the penetration and diffusion of atomic hydrogen into the internal structure of steel, which changes into molecular hydrogen in the internal interface between non-metallic inclusion and base material.

The presence of hydrogen in material is a potential source of defects and must be detected before it reaches a critical size which can result in severe damage and expensive repairs. Cracking may occur in the HAZ or weld metal, and it may be longitudinal or transverse see (**Figure 1.1**and **Figure 1.2**). A cold cracking is generally referred to as a spontaneous crack that occurs at temperature below 200 °C after solidification is complete in welding. It is likely to occur in all ferritic and martensitic steels such as carbon steel, low alloy steel and high alloy steel.

Figure 1.1Hydrogen-induced cracks in low carbon steel.[5]

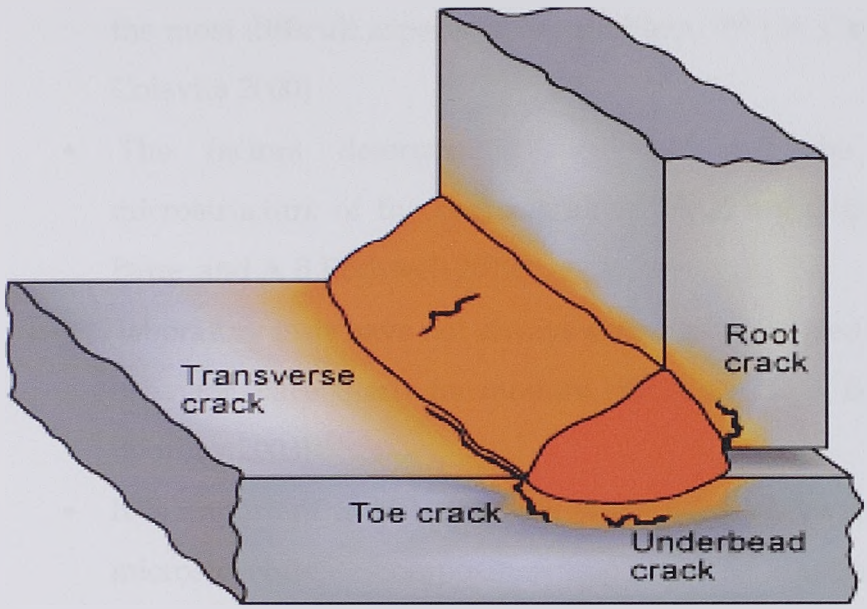

Figure 1.2Hydrogen cracks originating in the HAZ and weld metal. [6]

Despite that many papers have been written in the last decades exploring the influence of different parameters, on properties and microstructure of both the HAZ and the weld metal of HSLA steel welded joints in order to avoid cold cracks, this phenomenon is still present for welding engineers especially that cold cracks had accounted for more than 90% of weld cracks in actual steel structures. This crack type study importance has arisen from the following notes according to researchers around the world:

- Understanding hydrogen embrittlement is still an issue on a global scale. [7] (FERA 2000)
- At least £40 million arose from the need to repair hydrogen-induced cracks and adjacent to welds. [8] (PHM Hart, Granta Park 1999)
- Cold cracks had accounted for more than 90% of the weld cracks in actual steel structures. [9] (Kunihiko and Shigetomo)
- Presently this phenomenon is not completely understood and hydrogen embrittlement detection, in particular, seems to be one of

the most difficult aspects of the problem. [10] (R. Capriotti and M. Colavita 2000)

- The factors determining the size and the transformed microstructure of the coarse-grained HAZ are critical. [11] (A D Batte and A B Rothwell 2012)
- laboratory tests have not always accurately modeled field-welding behavior, particularly for modern HSLA steels.(A D Batte and P J Boothby 2003)
- It is important to note that the relationships between weld metal microstructure, composition and welding conditions are even more complex than in the HAZ (A D Batte and P J Boothby)
- HSLA-65 (ASTM A945) is a new structural steel of interest to the Navy shipbuilding community. [12] (Konkol P.J.; Mathers J.A 2003)

For these reasons the research community has paid attention in improving the possibilities of reducing the susceptibility of the steels to this dangerous phenomenon by controlling welding parameters, preheating, and applying low hydrogen level consumables and welding processes.

Generally speaking, the goal is to maintain the hydrogen levels as lower as possible at HAZ and WM by reducing cooling rate ($t_{8/5}$) which provides an opportunity for hydrogen that may be present to diffuse out harmlessly, reducing the potential for cold cracking.

However, there is a growing interest around the world in improving weldability of high strength low alloy (HSLA) steels. For example (HSLA-65 (ASTM A945)) is a new structural steel of interest to the Navy shipbuilding community.

Applying friction stir welding single-pass weldments in 6.4 mm plates and two-pass weldments in 12.7-mm plates of this HSLA steel were successfully made. The weldments exhibited satisfactory transverse weld tensile strength,

ductility, Charpy V notch toughness, and hardness (Konkol P.J; Mathers J.A 2003).

However, the previous factors and more subjects about weldability of HSLA steel are presented with more details in the fourth chapter of this thesis. In general, the following are the factors which cause cold cracking:

- Hard, brittle martensitic structure
- High carbon equivalent
- No preheat
- Hydrogen trapped in martensite
- Hydrogen diffusion to base metal
- Fast cooling of base metal Low amperage, high speed
- Low weld heat
- Poor joint design and fit-up
- Dirty, greasy, or contaminated surface

However this thesis studies the affect of some of the above factors that govern hydrogen induced (cold cracking) e.g. weldability of high-strength low alloy (HSLA) NIONIKRAL-70 steel.

1.3 Objective of the thesis

The overall objective of this work is directed towards obtaining a more coherent understanding of the effects of welding parameters such as (preheating, heat input and electrode strength) on cold cracking avoidance and to better define the key parameters involved in hydrogen induced cracking (HIC) in welded joints of HSLA (NIONIKRAL 70) steel.

Beside the theoretical background this objective intrinsically comprises several experiments e.g. Controlled Thermal Severity (CTS) test, Y-Groove test and Cabelka-Million test with different welding parameters that should be done to attain the final goal of testing weldability of the selected steel.

Taguchi method for design of experiment (DOE) will be adopted to analyze the effect of individual welding process parameters on toughness and fracture toughness of the welded joints of the selected HSLA steel.

1.4 Methodology used

In brief, the methodology employed goes along as follows: first, the reliability of welds cannot be ensured without proper understanding of weldability therefore the literature reporting the research on cold cracking phenomenon and weldability of HSLA NIONIKRAL 70 steel is reviewed and studied in order to lay the theoretical foundations of the thesis; second; the experiments will be concerned with different cold cracking susceptibility tests such as the Oblique-Y-Groove comparative test, controlled thermal severity (CTS) test, and Cabelka-Million test of flux cored arc welding (FCAW) in order to investigate this phenomenon in the selected HSLA steel welded joints. However the Taguchi approach for DOE will be applied to predict the optimal factor "factors" that affect the outcome of the manual metal arc (MMA) welding process experiments of NIONIKRAL 70.

The present thesis is organized in seven chapters and a few appendices. Some of these chapters are based on developments from former chapters, but in general, all of them can be read independently as self-contained entities

Chapter 2 presents a deep revision of the cold cracking phenomenon research during the last ten years.

Chapter 3 looks deeply into the fundamentals of HSLA steels.

Chapter 4 presents the weldability and welding rules of HSLA Steels.

Chapter 5 presents weldability testing through several tests of the Oblique-Y-Groove comparative test, CTS test, and Cabelka-Million test. All of them are achieved under different welding conditions and the results are

analyzed in terms of establishing the best solution for this serious welding problem. However chapter 6 presents the evaluation of HSLA NIONIKRAL 70 steel weldabilty using Taguchi method for design of experiment (DOE).

With respect to the conclusions of the thesis, they are presented in detail at the end of each chapter and the most important concepts are summarized in Chapter 7, as a conclusion and further future work.

2. Literature Review

As has been previously remarked in Chapter 1, the control of cold cracking is not an easy task to carry out without solid background knowledge on the theme. Fortunately, this subject has attracted the attention of many researchers around the world in the last decades. This chapter summarizes the most important developments and results found in the specialized research literature on avoidance of cold cracking in the last years.

2.1 Hydrogen-induced cracking in weldments

In OULU (2003) [13]there was a study about the prevention of weld metal hydrogen cracking, weld hydrogen cracking is attributable to three main factors:

- Microstructure
- Hydrogen
- Stress

The truth is that the causal factors governing the occurrence of hydrogen-induced cold cracking in welded joints of ferritic structural steels are: (i) crack-sensitive, hardened microstructure containing martensitic and/or bainitic transformation products, (ii) sufficiently high, local weld hydrogen concentration in terms of weld diffusible hydrogen content and (iii) elevated stress caused by high structural restraint that is determined by structural rigidity, i.e., plate thickness and weld bead height (or weld build-up thickness).

They studied controlling factors that govern transverse hydrogen cracking in high-strength multipass weld metal (WM). The experiments were concerned with heavy-restraint Y- and U-Groove multipass crack tests of shielded-metal arc (SMAW) and submerged-arc (SAW) weld metals.

Results of tensile tests, hardness surveys, weld residual stress measurements and microstructural investigations are discussed. The analytical

phase comprised numerical calculations for analyzing the interactions between crack-controlling factors.

The objectives were: (i) the assessment of WM hydrogen cracking risk by defining the Crack-No Crack boundary conditions in terms of 'safe line' description giving the desired lower-bound estimates, and (ii) to derive predictive equations capable of giving reliable estimates of the required preheat/interpass temperature T_0/T_i for the avoidance of cracking. However, the above study showed that the Hydrogen cracking occurred predominantly in high strength weld metals of $R_{p0.2} \approx$ 580-900 MPa. Low strength WMs of Rp0.2 ≤ 480 MPa did not exhibit cracking under any conditions examined. Hydrogen cracking occurred predominantly in high strength weld metals of $R_{p0.2} \approx$ 580-900 MPa. At intermediate strengths of $R_{p0.2} \approx$ 500-550 MPa, cracking took place in the cases where the holding time from welding to NDT inspection was prolonged to 7 days. Low strength WMs of $R_{p0.2} \leq$ 480 MPa did not exhibit cracking under any conditions examined. Cracking occurrence was, above all, governed by WM tensile strength, weld diffusible hydrogen and weld residual stresses amounting to the yield strength. The appearance of cracking vanished when transferring from 40 to 6 mm thick welds. The implications of the holding time were more significant than anticipated previously. A period of 16 hrs in accordance with SFS-EN 1011 appeared much too short for thick multipass welds. Interpass time and heat input showed no measurable effect on cracking sensitivity, hence being of secondary importance. Equations were derived to assess the weld critical hydrogen content H_{cr} corresponding to the Crack-No Crack conditions as a function of either weld metal P_{cm} or yield strength $R_{p0.2}$.

2.2 Weldability Control

In Stockholm (2004) [14],Control of weldability was studied and they found that, although the overall results indicate that the weld metal susceptibility to cold cracking corresponds to the relevant levels of HD, this relationship was found to be ambiguous in welds deposited at the shortest

CTWD of 15 mm, using CO2 shielding gas at all welding currents investigated. While the amount of diffusible hydrogen was marginally increased from 11.7 to 12.8 ml/100g, resulting from the welding current increase from 280 to 320 A, the amount of cold cracking at room temperature was significantly decreased from 89 to 25 %RTC (room temperature crack). This is explained by a significant difference in the cross section of the weld beads, suggesting a need to more closely evaluate the G-BOP testing, particularly examining the effects of weld bead profiles on the weld susceptibility to HACC.

Preheat was found to decrease the amount of cold cracking in the H10 welds and it was concluded that preheat significantly reduces the main contributor to decrease the HD in the weld metal. Although the cracking susceptibility of welds using 75Ar-25CO2 shielding gas decreased more slowly with an increasing preheat temperature, compare to those deposited using CO2, no cracking was observed at 120 °C in welds under both shielding gases. This indicates that the same welding consumable (H10) deposited using different shielding gases can result in a different response to preheat temperature. Based on the results of this work, a number of changes are proposed to hydrogen testing standards AS 3752-1996 and ISO 3690-2000, particularly with respect to the effects of CTWD and shielding gases on levels of diffusible hydrogen in weld metal deposited using gas shielded rutile flux-cored wire.

2.2.1 Effect of weld microstructure on cold cracking susceptibility

Korea Institute of Industrial Technology, published a study in (2008) [15] titled as microstructural parameter controlling weld metal cold cracking. It was aimed to identify and evaluate the effect of weld microstructure on cold cracking susceptibility of FCAW weld metals, and then to give a basic guideline for designing new welding consumables from the microstructural point of view.

In order to figure out the parameter(s) that can quantify the microstructural susceptibility of multi-pass weld deposit, two sets of FCAW deposits having tensile strength of about 600MPa were prepared by controlling the Ni content to allow a sufficient variation in weld microstructure but with little change in weld metal strength. Cold crack susceptibility of those two chemistries was evaluated by 'multi-pass weld metal cracking test' at various levels of diffusible hydrogen content.

All of the cold cracks developed were Chevron-type cracks and the occurrence of such cracks was depending on the proportion of grain boundary ferrite as well as the diffusible hydrogen content. In fact, at the same level of diffusible hydrogen, 1.5%Ni wire showed better resistance to cold cracking than the 0%Ni even though that was higher in strength and carbon equivalent. This result could be explained by the difference in grain boundary ferrite content between those two welds based on the microstructural characteristics of Chevron cracking that preferentially propagates along grain boundary ferrite.

In addition to hydrogen control approach, microstructural modification in a way to reduce the proportion of grain boundary ferrite can be pursued for developing welding consumables with improved resistance to cold cracking.

In a very recent study done in Turkey (2010) [16] where have been clearly demonstrated that LTT welding consumables produces fully martensitic structure or martensitic structure containing some retained beta. Residual tensile stresses are lowered or compressive residual stresses are generated within the weld region due to martensitic expansion when the transformation takes place at lower temperatures. Thus, weld properties such as fatigue strength and cold cracking resistance are increased without any costly post-weld treatment.

In Poland (2006) [17] a research showed that shielded metal arc welded (SMAW) joint is more susceptible than base metal. Differences in resistance to hydrogen delayed cracking could be explained by variations of microstructure

present in steel and welded joints. The various microstructures, resulting in different mechanical properties (strength, hardness), and different susceptibility to hydrogen degradation.

In Dillingen-Germany (2002) [18] A low carbon TMCP steel with minimum yield strength of 500 MPa was developed in two plate thickness, 30 mm and 70 mm (for off sure constructions). The chemical compositions were optimized relative to each thickness. The 70 mm plate contained some molybdenum but bad 0.02 % lower carbon content. Tensile properties were exactly hitting the target, yield to tensile ratios were below 0.90 thereby assuring appropriate work hardening an excellent toughness was obtained the S500 test plates were suitable for high amounts of cold deformation the steel is suitable for PWHT. Both steel types have proven excellent weldability, in particular:

- Very low HAZ hardenability
- Little cold cracking susceptibility allowing welding without preheat
- High HAZ toughness through the complete rangeof usual welding beat inputs
- No need for PWHT to achieve appropriate brittle fracture resistance

Another study of the effect of shielding gas mixture on gas metal arc welding of HSLA steel using solid and flux-cored wires was published in London (2005) [19]. The above study showed that the microstructural constituents such as AF, GF and FS in HSLA weld metals are influenced by the oxygen and carbon dioxide content in the shielding gas. In the case of solid wire welds, both YS and UTS increased with increasing oxygen content (up to 4%) in the shielding gas. Further increase in oxygen content resulted in reduction in UTS and % elongation of the weld metal. In the case of flux-cored wire, both YS and UTS decreased with increasing oxygen content (up to 4%) in the shielding

gas without altering % elongation. Gas metal arc welding can achieve acceptable weld metal properties in HSLA steel with the proper combination of filler wire and shielding gas composition.

2.2.2 Effect of welding parameters and preheating on cold cracking

A study about the weld cracking susceptibility of High Hardness Armoursteel (S.J. Alkemade) [20] showed that the 10 mm thick, Bisalloy 500 steel plate can be readily welded by the pulsed- GMAW process using the three electrodes trialed in this work, if precautions are taken to limit potential hydrogen sources and appropriate levels of heat input and preheat are used. However, it is recommended that either of the austenitic consumables examined in this work should be used in preference to the ferritic consumable due to their greater resistance to hydrogen induced cracking. Based on this work and the Bisalloy Steels handbook it is recommended that heat input levels should be 1.0 - 2.5 kJ/mm and the preheat should be 50 - 75 °C. These limits are considered to be reasonably conservative and should allow for welding in workshop conditions. Significant softening is caused by welding these steels, especially in the fusion zones when using undermatched electrodes such as those utilized in this work.

The greatest hardness reduction was measured in the austenitic stainless steel fusion zone where the hardness measured was as low as 31% of that of the original plate. With the other electrodes used, the reduction in hardness was less severe.

The minimum hardness of the ferritic fusion zones ranged from 42% to 49% of the original plate hardness, depending on the level of heat input and preheat used. The hardness of the duplex stainless steel fusion zone approached the lower hardness level of the ferritic fusion zones.

Last years in Japan[21] there was a study about determination of necessary preheat temperature to avoid cold cracking under varying ambient temperature . The experimental results of y-groove weld cracking tests of that study were compared with the prediction methods of minimum preheat temperatures to avoid cold cracking in the heat affected zones, which include the BS-5135, the AWSD1.1, the JSSC procedure and the CEN chart method. The effects of steel chemical compositions, plate thicknesses, diffusible hydrogen contents and ambient temperatures on cold cracking susceptibility were investigated in that study.

The CEN chart method can predict minimum preheat temperatures most precisely as long as homogeneous preheating is conducted and the ambient temperature is 20°C. When local preheating is conducted, cooling time down to 100°C (t100) must be used. The minimum preheat temperature for local preheating was selected so that t100 of local preheating is equal to or longer than that of the minimum preheat temperature for homogeneous preheating. Ambient temperatures greatly affect cold cracking susceptibility more than expected from its effect on t100. As ambient temperature becomes lower, minimum preheat temperature to avoid cold cracking becomes higher. However, all the previous prediction methods cannot estimate this effect. In the above study, the effects of ambient temperatures on necessary preheat temperatures were converted into CEN increments, which were determined from the experimental results. Using these CEN increments, the CEN chart method can estimate the effect of ambient temperature.

Fukuhisa Matsuda,Hiroji Nakagawa, Kenji Shinozaki [22]while studying in order to reveal the criterion under which cold cracking in root pass welding occurs alternatively in HAZ or weld metal and hardness of HAZ concluded that there is definite upper limit temperature of cold cracking. The upper limit temperature was about 170°C in HY130 weldment and about 300 °C to 250 °C in HT60 weldment.

Tadashi Kasuya Nobutaka Yurioka, Makoto Okumura[23] while comparing the results of y-groove weld cracking tests with the prediction methods of minimum preheat temperatures to avoid cold cracking in the heat affected zones, which include the BS-5135, the AWSD1.1 and CEN chart method concluded that ambient temperatures greatly affect cold cracking susceptibility more than expected from its effect on t_{100}, also as ambient temperature becomes lower, minimum preheat temperature to avoid cold cracking becomes higher. . Also the T_{cr}, of the steel when it was preheated by a gas burner, was higher than 150 °C, while its T_{cr} under homogenous preheating was 125°C.

Raimundo Carlos Silverio Freire Junior, Theophilo MouraMaciel[24] while evaluating of cold crack susceptibility on HSLA steel welded joints they concluded that the effect of the preheating temperature on the microstructure depended on the specific weld joint/base metal combination, either decreasing or maintain the contents of acicular ferrite, The results indicated the presence of cracks in the welded metals with the combination of increased hardness 230 HV and the formation of high contents of acicular ferrite (above 93 %) in the welds without preheating. Higher crack susceptibility was also observed in the thickest welded metal plates.

Kunihiko Satoh, Shigetomo Matsui, KohsukeHorikawa[9] while the JSSC study group studying how to select reasonable preheating conditions for prevention of weld cracks as a result, cold cracks had accounted for more than 90% of the weld cracks in actual steel structures.

M. D. Rowe, T. W. Nelson, J. C. Lippold[25] while investigating the susceptibility of dissimilar austenitic/ferritic combinations to hydrogen-induced cracking they emphasized that cracking was always associated with hard, martensitic regions adjacent to the fusion boundary, therefore, minimizing the compositional regime within which martensite can form will reduce susceptibility.

Jose Hilton Ferreira da Silva, Hipolito CarvajalFals[26] while evaluating of a proposal for a gapped bead-on-plate (G-BOP) test, used for study of hydrogen cracks in relatively thin sheets of welded steel, concluded that preheating the API X80 steel to 100°C has a positive influence on the susceptibility to cracking of weld metals, avoiding the formation of hydrogen induced cracks.

Yoni Adonyi[27] while comparing weldability of the traditional steels with 480 and 689 MPa yield strength and high performance steels (A 709 Grade 485 HPS and Grade 785 HPS 100W), concluded that HPS steels needed preheat temperatures by about 38-79 °C lower than presently specified for the conventional steels to avoid heat affected zone cracking for up to 50.8 mm in thickness.

Richard E. Smith, David W. Gandy [28] while investigating ambient temperature preheat for machine GTAW temperbead applications, concluded that no preheat temperature or post-weld bake above ambient is required to achieve sound machine GTAW temperbead repairs that have high toughness and ductility. This conclusion is based on the fact that the GTAW process is an inherently low hydrogen process regardless of the welding environment.

2.2.3 Effect of diffusible hydrogen level on cold cracking

Jae Hak Kim, JunSeokSeo[29] while studying the effect of weld metal microstructures on cold crack susceptibility of FCAW weld metal concluded that the 1.5 %Ni wire showed substantially better resistance to HICC than 0 %Ni.

D. D. Harwig, D. P. Longenecker, J. H. Cruz [30] while investigating the effects of welding parameters and electrode atmospheric exposure on the diffusible hydrogen content of Gas Shielded Flux Cored Arc Welds, concluded that weld diffusible hydrogen content was found to increase almost linearly as the weld current increased for the E71T-1 electrode. Welds made with basic

(E71T-5) and metal cored electrodes appear to be more resistant to increased diffusible hydrogen contents after atmospheric exposure of the electrodes.

Pargeter[31] while studying evaluation of necessary delay before inspection for hydrogen cracks concluded that the behavior of the HY100 welds, which showed only very small differences in delayed cracking behavior between high and low hydrogen levels and between high and low restraint, indicate that these factors are indeed of little significance.

B. Swieczko-Zurek, S. Sobieszczyk, J. Cwiek[32] while studying the evaluation of susceptibility of high strength steels to hydrogen delayed cracking, concluded that two constructional middle carbon steel 26H2MF and 34HNM tested in used mineral engine oil at 80°C are not susceptible to hydrogen delayed cracking since hydrogen concentration was below critical value in this case.

G. Magudeeswaran, V. Balasubramanian and G. Madhusudhan Reddy [33] while investigating cold cracking of Flux Cored Arc welded armour grade high strength steel weldments, concluded that The presence of widely spaced delta ferrite in a large plain austenitic matrix, lower diffusible hydrogen level, lower weld metal strength, lower fusion boundary and HAZ hardness, softergrain boundary phase, and lower residual stress are the factors that contribute for the greater resistance of FA welds against cold cracking compared with FF joints.

M. Anis, DeniFerdian[34] while analyzing failure of 4 elbow pipe weld crack concluded that during welding process of the elbow, the source of hydrogen such water, oils, greases, and rust that containing hydrates must be eliminated.

J. W. Martin, J. Kittel T. Cassagne and C. Bosch [35] while studying hydrogen induced cracking (HIC) - laboratory testing assessment of low alloy steel line pipe, concluded that when the diffusible hydrogen concentration was below 0.5ppm, no HIC was found for the five steel types. Above 1ppm diffusible hydrogen, all steel types exhibit significant HIC.

2.3 Conclusion

- The study of the different previous work in this field reviews that preheating is necessary in welding some steel types to avoid cold cracking but it is also possible to weld without preheating in some other cases. According to the researchers results cold cracks had the higher percentage of the weld cracks in actual steel structures and the higher crack susceptibility was observed in the thickest welded metal plates. Some researchers concluded that the susceptibility toward cold cracking can be eliminated by using low hydrogen welding process and consumables.

- Moreover researchers observed that cracking was always associated with hard, martensitic regions adjacent to the fusion boundary. However other researchers emphasized that lower diffusible hydrogen level, lower weld metal strength, lower fusion boundary and HAZ hardness are quite important factors to prevent cold cracks. Some researches indicated that the presence of cracks in the welded metals with the combination of increased hardness 230 HV and the formation of high contents of acicular ferrite (above 93 %). In conclusion it is clear that resistance to cold cracking has generally improved in many different high strength steel types and the steps needed to avoid cold cracking through control of the welding parameters are well established.

- In brief, this chapter reviews the conceptual/theoretical dimension and the methodological dimension of the literature in cold cracking avoidance and discovers research questions or hypotheses that are worth researching in later chapters.

3. Fundamentals of HSLA Steel

3.1 Definition of High Strength Steels

The traditional[36, 37] route to high strength in steels is by quenching to form martensite that is subsequently reheated or tempered, at an intermediate temperature, increasing the toughness of the steel without too great a loss in strength. The ability of steel to form martensite on quenching is referred to as the hardenability. Therefore, for the optimum development of strength, steel must be first fully converted to martensite. To achieve this, the steel must be quenched at a rate sufficiently rapid to avoid the decomposition of austenite during cooling to such products as ferrite, pearlite and bainite. [36]

Industry, particularly in the transport sector, is constantly aiming to reduce weight, increase performance and safety and rationalize production methods. The use of high strength steels with good formability and weldability is increasingly seen as one important way in which these aims can be met. Quenched and tempered steels with yield strength levels up to 1100 MPa and hot rolled cold forming steels with yield strength levels up to 740 MPa are successfully used in cranes, trucks, dumpers, temporary bridges and similar products. For automotive applications rephosphorized, micro-alloyed and dual-phase cold rolled grades with tensile strengths of up to 1400 MPa and metalized grades with tensile strengths of up to 600 MPa have been introduced. On the basis of yield strength new types of high strength steels give a great potential for weight reduction and cost effective designs. To exploit the full potential of high strength steels the design philosophy and production techniques must take into account factors such as formability, weldability, stiffness, buckling, crush resistance and fatigue. [37]

3.2 Hardenability

There can be confusion [41,42]over what is meant hardenability and hardness. Hardenability is a steel property which describes the depth to which the steel may be hardened during quenching. It is important to note that hardenability is a material property, dependent on chemical composition and grain size, but independent of the quenchant or quenching system (cooling rate). However, the structures obtained across a quenched section are a function of both hardenability and the quenching process (severity of quench). [38]

However hardness is a measure of the resistance of a material to plastic deformation. This depends on the carbon content and microstructure of the steel. Hence the same steel can exhibit different hardness values depending upon its microstructure, which itself may depend on how the sample was quenched, etc. [38]

Starting in the 1930 with the development of hardenability concepts, a number of investigators have demonstrated that the hardness of as-quenched martensite increases in a relatively linear fashion from about 0.05 to 0.5 wt% carbon. **Figure 3.1** shows data from a number of investigators. Note that when the carbon content of the austeniteis >0.8%, the as quenched hardness drops. This is due to the presence of retained austenite which is much softer than plate martensite. [39]

3.3 Hardening Mechanisms [5]

The strength of steel is affected by the typical strengthening mechanisms-namely, grain refinement, solid-solution hardening, and precipitation hardening. Of these various strengthening mechanisms, the refinement of grain size is perhaps the most unique because it is the only strengthening mechanism that also increases toughness. However **Figure 3.2** shows the relationship between grain size and yield strength in C-Mn steels.

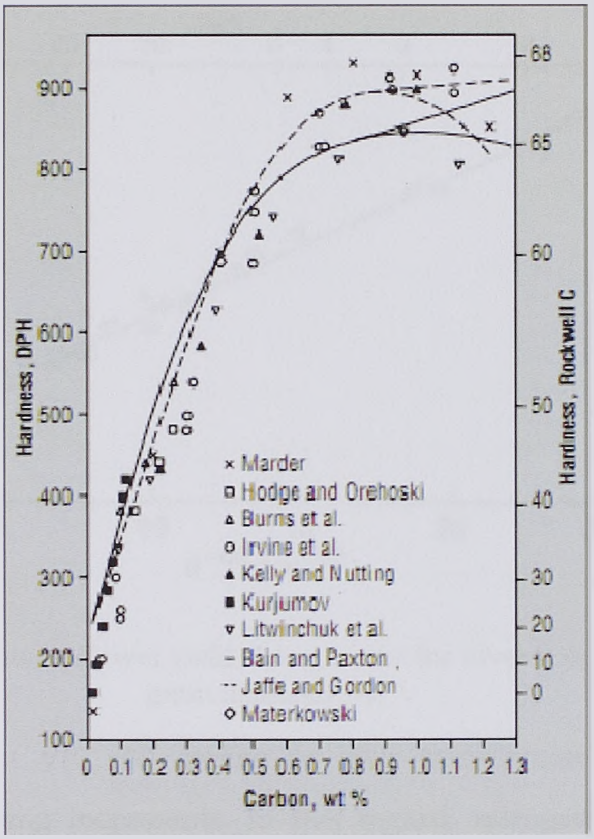

Figure3. 1Summary of extensive as-quenched hardness data from the literature for Fe-C alloys and steels by Krauss.[39]

3.3.1 Microalloyed steels [5]

Microalloying is the use of small amounts of elements such as vanadium and columbium. Because the degree of ferritic grain refinement possible in as-rolled microalloyed bar steels is somewhat limited, and because substructural strengthening is not possible, alternative strengthening mechanisms must be used to reach yield strength levels comparable to those of plate grades. For example, in the alloy design of microalloyed bar steels, precipitation and pearlite strengthening must be relied on to a greater extent than in the design of plates. In view of the limited solubility of columbium and titanium at the reheat temperatures used in bar processing, vanadium is usually used to obtain the required level of precipitation strengthening in HSLA bar grades.

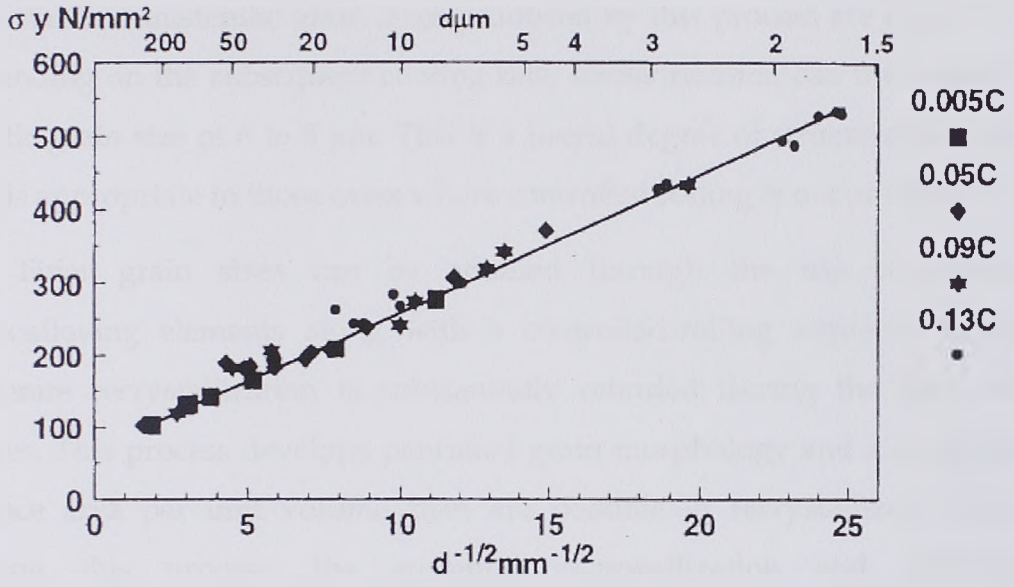

Figure3. 2Relation between lower yield strength and the inverse square root of the grain diameter.[40]

Precipitation of V(C, N) during or after transformation can provide significant strengthening increments. In this regard, nitrogen level is also of importance. Judicious selection of both the vanadium and nitrogen level is required to produce the desired level of precipitation strengthening.

3.3.2 Thermomechanical Treatment (Rolling)

Typically [5, 41, 42], the initial rolling passes are conducted at relatively high temperatures, just below the slab-reheating temperature. At these temperatures, each deformation step is usually followed by rapid recrystallization and grain growth. Recently, a thermomechanical processing procedure called recrystallization controlled rolling has been proposed. It combines repeated deformation and recrystallization steps with the addition of austenite grain-growth inhibitors such as titanium nitride to refine the starting austenitic grain size and to restrict growth after recrystallization. Such processing would obviate the need for low-temperature controlled rolling. However, even with optimal compositions and the adoption of rather difficult reduction schedules, there seems to be a limit to the degree of austenitic refinement that can be achieved by repeated recrystallization, the finest

recrystallized austenitic grain sizes produced by this process are about 15 μm. depending on the subsequent cooling rate, transformation can then result in a ferritic grain size of 6 to 8 μm. This is a useful degree of structural refinement and is appropriate in those cases where controlled rolling is not possible. [5]

Finer grain sizes can be attained through the use of additional microalloying elements along with a controlled-rolling sequence in which austenite recrystallization is substantially retarded during the later rolling passes. This process develops pancaked grain morphology and a much higher surface area per unit volume than are possible in recrystallized austenite. During this process, the austenite recrystallization and carbonitride precipitation reactions are coupled in the sense that each is greatly influenced by the other. [5]

However as shown in **Figure 3.3** in the seventies, the hot rolling and normalizing was replaced by thermo-mechanical rolling. The latter process enables materials up to X70 to be produced from steels that are microalloyed with niobium and vanadium and have reduced carbon content. By this method, it has become possible to produce higher strength materials like X80, having a further reduced carbon content and excellent field weldability. Additions of molybdenum, copper and nickel enable the strength level to be raised to that of grade X100, when the steel is processed to plate by thermo-mechanical rolling plus modified accelerated cooling. [41]

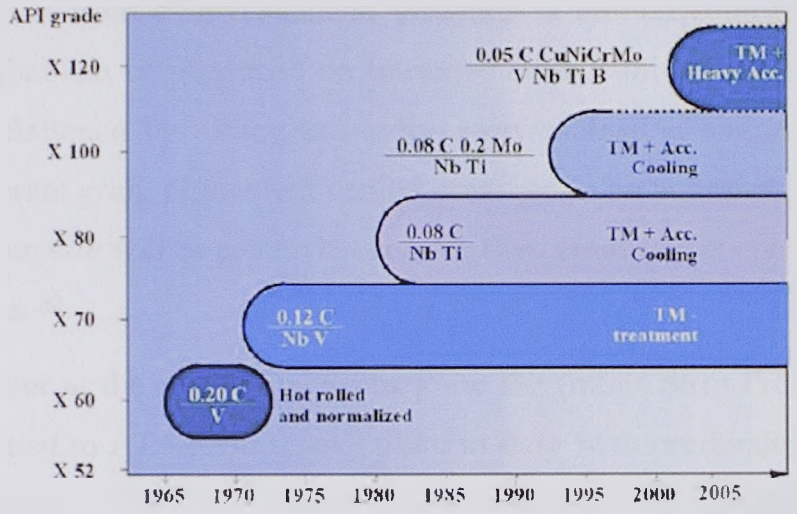

Figure3. 3History in Line Pipe Steels (Large Diameter Pipe) [41]

Transformation to ferrite

The transformation of the austenite structure into ferritic microstructures determines the final grain size and associated mechanical properties of the microalloyed plate. The effects of austenitic morphology and the transformation temperature range (as governed by alloy content, rolling deformation, and cooling rate) are of the greatest importance.

Even after the minimum austenitic grain thickness has been produced, the temperature range of the austenite-to-ferrite transformation must be controlled to determine the reaction kinetics. Increasing the ferritic growth rate can produce a finer ferritic grain size. These effects are generally achieved by alloying or controlled cooling. [5]

Consequently, recrystalliztion controlled rolling becomes quite important in bar rolling, and the rolling strategy must be designed to produce the finest possible recrystallized austenitic grain size. **Figure 3.4** shows the influence of accelerated cooling on the microstructure of low-carbon microalloyed steel products during controlled rolling. Subsequent control of the austenite-to-ferrite transformation range is still important to maximize ferritic grain refinement. Nevertheless, the ferritic grain size that can be produced on

transformation from a recrystallized austenite is limited compared with the grain size that can be produced on transformation from austenitic grains that have been flattened by rolling below the recrystallization temperature. Thus, while moderate grain refinement can be achieved in an as-rolled microalloyed bar, this grain size will be somewhat coarser than grain size of controlled-rolled HSLA plates. [5]

However at the end of last century the ISP (Inline Strip Production) line was developed in ATA Averdi steel plant in Italy with production capacity of 5.10^5 tons/year. This line (**Figure 3.5**) consists of the continuous casting machine for concast slabs 60 mm thick with the burnishing mill stand for squashing the slab with the liquid core to 43 mm, roughing train, furnace for inductive heating of the strand, Cremon-type furnace with the strand coiler and decoiler, ensuring maintaining the correct feedstock temperature, mill scale breaker, finishing train, laminar flow cooling, and a coiler for the finished product.[42]

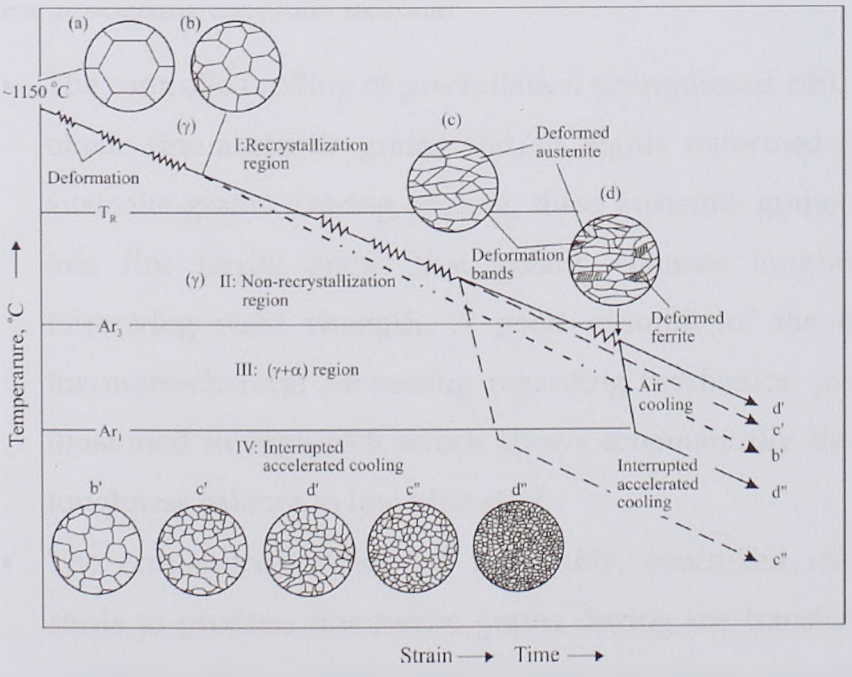

Figure3. 4Schematic diagram of the influence of accelerated cooling on the microstructure of low-carbon microalloyed steel products during controlled rolling.[42]

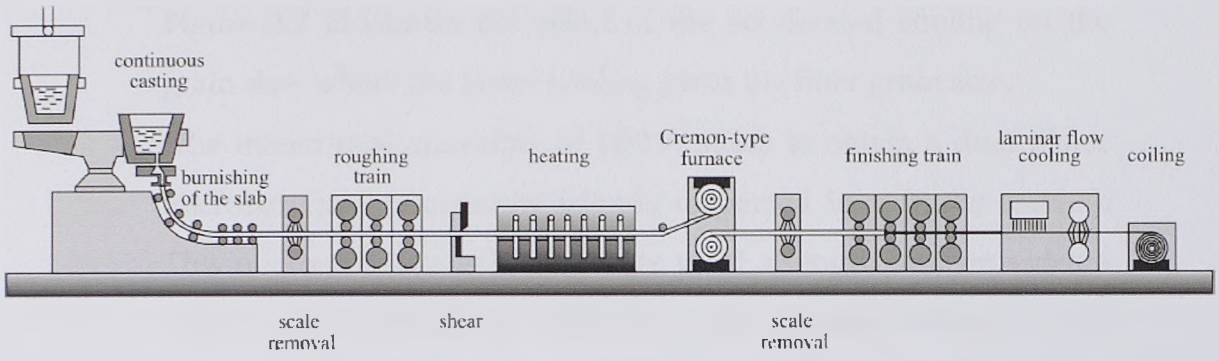

Figure3. 5Schematic diagram of an integrated production line of rolled plates in the ISP (In-line Strip Production) process. The steel sheets rolled by this line may be up to 1 mm thick). [42]

3.3.3 Processing methods of HSLA Steels [5]

High strength low alloy steels are primarily hot rolled into the usual wrought product forms (sheet, strip, bar, plate and structural sections) and are commonly furnished in the as-rolled condition. However, the production of hot-rolled HSLA products may also involve special hot-mill processing that further improves the mechanical properties of some HSLA steels and product forms. These processing methods include:

- The controlled rolling of precipitation strengthened HSLA steels to obtain fine austenite grains and/or highly deformed (pancaked) austenite grains. During cooling, these austenite grains transform into fine ferrite grains that greatly enhance toughness while improving yield strength. A good example of the benefits of thermomechanical processing regarding mechanical properties is illustrated in **Figure3.6** which shows schematically the strength-toughness balance in line pipe steel.
- The accelerated cooling of, preferably, controlled rolled HSLA steels to produce fine ferrite grains during the transformation of austenite. These cooling rates cannot be rapid enough to form acicular ferrite, nor can they be slow enough that high cooling temperature result thereby causing the over aging precipitates.

Figure 3.7 illustrates the effect of the accelerated cooling on the grain size, where the faster cooling gives the finer grain size.

- The intercritical annealing of HSLA steels to obtain a dual phase microstructure (martensite islands dispersed in a ferrite matrix). This microstructure exhibits lower yield strength but, provides a better combination of ductility and tensile strength than conventional HSLA steels and also improved formability. HSLA steels are also furnished as cold-rolled sheet and forgings. The main advantage of HSLA forgings (as that of as hot rolled HSLA products) is that yield strengths in the range of 275 to 485 MPa or perhaps higher can be achieved without heat treatment. Base compositions of these microalloyed ferrite-pearlite forgings are typically 0.3 to 0.5% C and 1.4 to 1.6% Mn. Low-carbon bainitic HSLA steel forgings have also been developed.

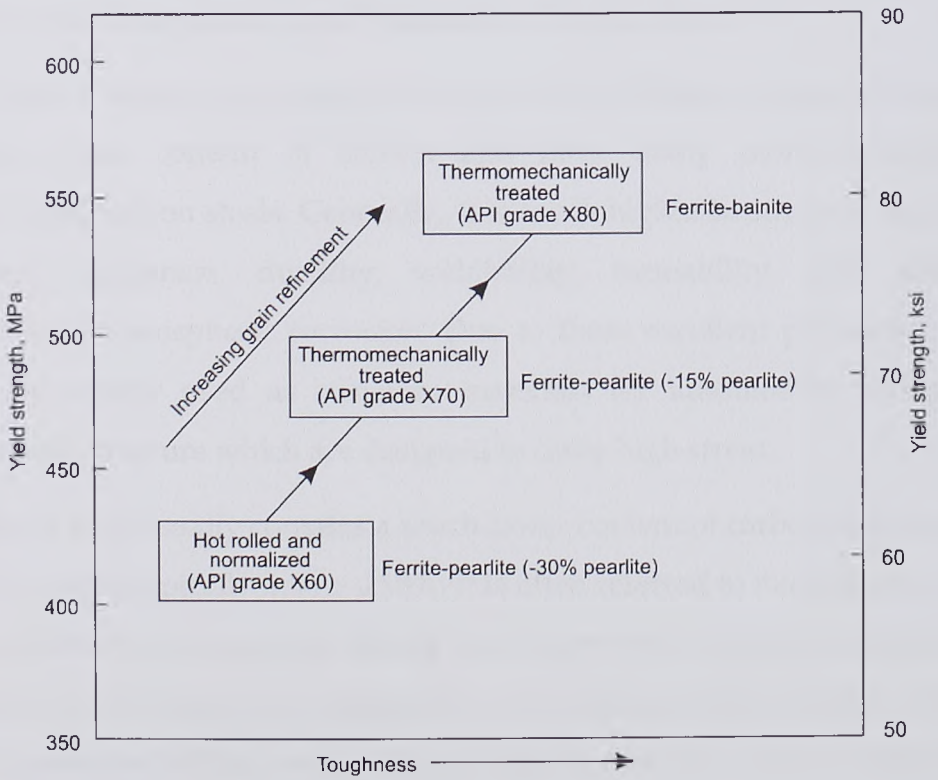

Figure3. 6Effect of microstructure and production process on the mechanical properties of line pipe steels. [5]

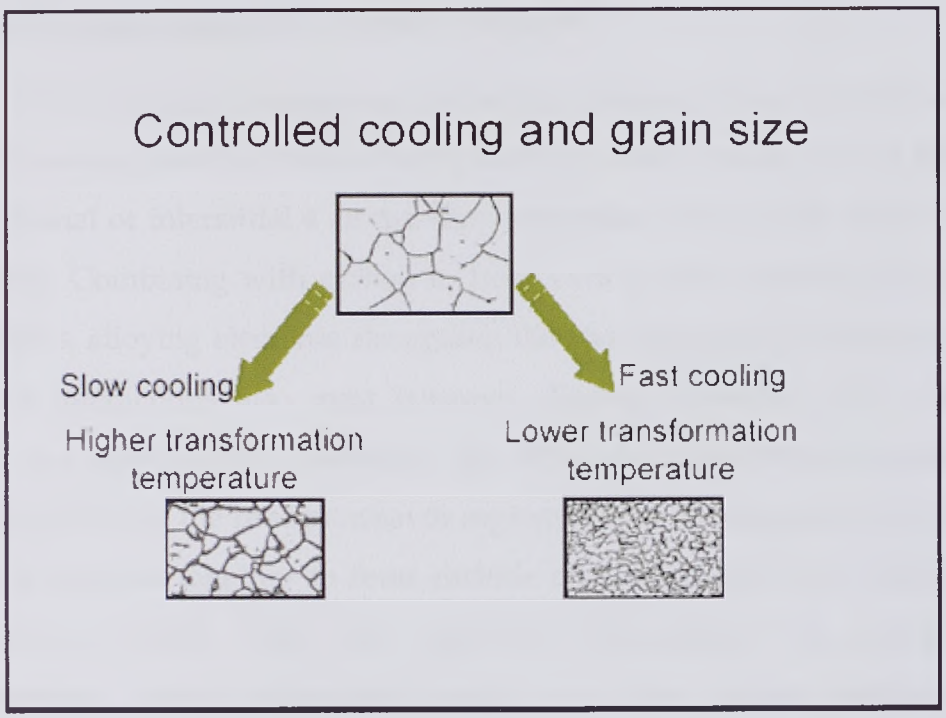

Figure3. 7Controlled cooling and grain size. [43]

3.4 Chemical Composition and Properties of HSLA Steels [44]

High strength low alloyed (HSLA) steel specifies a group of steels that contain a low content of carbon and have many more benefits than conventional carbon steels. Generally, it is much higher in strength, along with improved toughness, ductility, weldability, formability, and additional resistance to atmospheric corrosion. Due to these excellent properties, HSLA steels are widely used as structure materials for automobiles, bridges, oil storage and structure which are designed to carry high stress.

HSLA steel usually contains a much lower content of carbon than regular carbon steels, typically below 0.15%. It is often referred to microalloyed steel since its excellent properties usually come from various alloying elements in extremely small amounts compared to conventional steels. Besides carbon, manganese and silicon, over ten kinds of other elements, such as chromium, nickel, niobium, boron, molybdenum, titanium and copper, can be added to steels to achieve extra strength through various strengthening mechanisms.

3.4.1 Multivariate Interaction in HSLA Steel [44]

When alloying elements are added into the steel, their interactions with iron and carbon result in various strengthening effects. Solved in iron lattice as substitutional or interstitial 4 atoms, they strengthen the steel by solid-solution hardening. Combining with carbon to from various fine and disperse carbide precipitates, alloying elements strengthen the steel by precipitation hardening. Complex interactions also exist between alloying elements. For example, adding one element may influence the diffusion of existing elements and therefore influence the precipitation or segregation of existing elements. Several elements combine together to form carbide compound and then enhance the precipitation. HSLA steels are typically strengthened by precipitation strengthening, grain refinement, and, to a less extent, solid-solution strengthening due to the small amounts of alloying elements. All of these strengthening effects are sensitive to the processing environment, such as temperature, time, deformation extent and cooling rate. For example, temperature controls the solubility and diffusions of microalloying elements, and therefore greatly influences the formation of precipitates. Since grain growth is a thermal activated process, the grain size is strongly dependent on the both temperature and time during steel processing.

The challenge to design HSLA is to systematically understand the complex composition-processing-property relationship. Not only does each element strengthen steel through more than one mechanism, but sometimes two or three elements can combine together to influence the strength. In addition, the realization of strengthening effects of these elements strongly relies on the processing conditions. Coupled effects and intensive interaction of alloying elements and processing routes make metallurgy of HSLA steel very complicated to understand. Microalloyed steel metallurgy is a typical multidimensional problem, as shown in **Figure 3.8**.

Material specifications for most HSLA steels that are used in the as-rolled or normalized condition are provided by American Society for Testing and Materials (ASTM). For example **Table 3.1**lists a number of ASTM specifications covering structural-quality HSLA steels with their alloying elements. ASTM, ASI, API, and MIL specifications cover chemical compositions and additional testing and procedures relevant to each application.

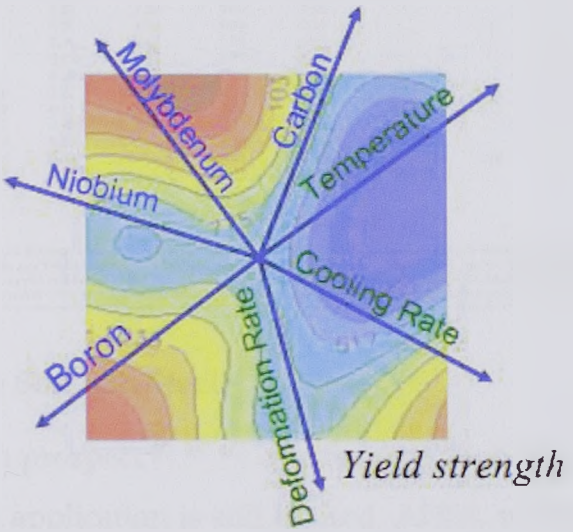

Figure3. 8 Multidimensional nature of microalloyed steel metallurgy.Various composition and processing parameters have complex interactions and different contributions to the final mechanical property. [44]

A user for special or critical applications may order supplementary testing. [5] However the selected high strength low alloy steel that will be tested in this work and its specification will be described in the fifth chapter.

Table 3.1Compositional limits for HSLA steel grades described in ASTM specifications properties. [3]

ASTM specification(a)	Type or grade	UNS designation	Heat compositional limits, % (b)									
			C	Mn	P	S	Si	Cr	Ni	Cu	V	Other
A 242	Type 1	K11510	0.15	1.00	0.45	0.05	...	...	...	0.20 min	...	...
A 572	Grade 42	...	0.21	1.35(c)	0.04	0.05	0.30(c)	...	...	0.20 min(d)	...	(e)
	Grade 50	...	0.23	1.35(c)	0.04	0.05	0.30(c)	...	...	0.20 min(d)	...	(e)
	Grade 60	...	0.26	1.35(c)	0.04	0.05	0.30	...	...	0.20 min(d)	...	(e)
	Grade 65	...	0.23(c)	1.65(c)	0.04	0.05	0.30	...	...	0.20 min(d)	...	(e)
A 588	Grade A	K11430	0.10–0.19	0.90–1.25	0.04	0.05	0.15–0.30	0.40–0.65	...	0.25–0.40	0.02–0.10	...
	Grade B	K12043	0.20	0.75–1.25	0.04	0.05	0.15–0.30	0.40–0.70	0.25–0.50	0.20–0.40	0.01–0.10	...
	Grade C	K11538	0.15	0.80–1.35	0.04	0.05	0.15–0.30	0.30–0.50	0.25–0.50	0.20–0.50	0.01–0.10	...
	Grade D	K11552	0.10–0.20	0.75–1.25	0.04	0.05	0.50–0.90	0.50–0.90	...	0.30	...	0.04 Nb, 0.05–0.15 Zr
	Grade K	...	0.17	0.5–1.20	0.04	0.05	0.25–0.50	0.40–0.70	0.40	0.30–0.50	...	0.10 Mo, 0.005–0.05 Nb
A 606	...	...	0.22	1.25	...	0.05	...	...	...	...	...	...
A 607	Grade 45	...	0.22	1.35	0.04	0.05	...	...	...	0.20 min(d)	...	(e)
	Grade 50	...	0.23	1.35	0.04	0.05	...	...	...	0.20 min(d)	...	(e)
	Grade 55	...	0.25	1.35	0.04	0.05	...	...	...	0.20 min(d)	...	(e)
	Grade 60	...	0.26	1.50	0.04	0.05	...	...	...	0.20 min(d)	...	(e)
	Grade 65	...	0.26	1.50	0.04	0.05	...	...	...	0.20 min(d)	...	(e)
	Grade 70	...	0.26	1.65	0.04	0.05	...	...	...	0.20 min(d)	...	(e)
A 618	Grade Ia	...	0.15	1.00	0.15	0.05	...	...	...	0.20 min	...	...
	Grade Ib	...	0.20	1.35	0.04	0.05	...	...	...	0.20 min(f)	...	...
	Grade II	K12609	0.22	0.85–1.25	0.04	0.05	0.30	...	...	...	0.02 min	...
	Grade III	K12700	0.23	1.35	0.04	0.05	0.30	...	...	...	0.02 min	0.005 Nb min(g)
A 633	Grade A	K01802	0.18	1.00–1.35	0.04	0.05	0.15–0.30	...	...	...	...	0.05 Nb
	Grade C	K12000	0.20	1.15–1.50	0.04	0.05	0.15–0.50	...	...	...	...	0.01–0.05 Nb
	Grade D	K02003	0.20	0.70–1.60(e)	0.04	0.05	0.15–0.50	0.25	0.25	0.35	...	0.08 Mo
	Grade E	K12202	0.22	1.15–1.50	0.04	0.05	0.15–0.50	...	...	...	0.04–0.11	0.01–0.05 Nb(d), 0.01–0.03 N

(continued)

(a) For characteristics and intended uses, see Table 2. (b) If a single value is shown, it is a maximum unless otherwise stated. (c) Values may vary, or maximum value may exist, depending on product size and mill form. (d) Optional or when specified. (e) May be purchased as type 1 (0.005–0.05 Nb), type 2 (0.01–0.15 V), type 3 (0.05 Nb, max, plus 0.02–0.15 V) or type 4 (0.015 N, max, plus V ≥ 4N). (f) If chromium and silicon are each 0.50% min, the copper minimum does not apply. (g) May be substituted for all or part of V. (h) Niobium plus vanadium, 0.02 to 0.15%. (i) Nitrogen with vanadium content of 0.015% (max) with a minimum vanadium-to-nitrogen ratio of 4:1. (j) When silicon-killed steel is specified. (k) For plate under 40 mm (1.5 in.), manganese contents are 0.70 to 1.35% or up to 1.60% if carbon equivalents do not exceed 0.47%. For plate thicker than 40 mm (1 to 5 in.), ASTM A 841 specifies manganese contents of 1.00 to 1.60%.

3.5 Advanced High Strength Steels

The future's prospect [5, 45, 46] of advanced high strength steels is bright though the present application is still limited. AHSS, which is strengthened by microstructure change during phase transformation, includes the following varieties:

- Dual phase steel (DP)

The microstructure of DP steel consists of a soft ferrite matrix and discreet hard martensitic islands, as shown in **Figure 3.9**. The ferrite is continuous for many grades up to DP780, but as volume fractions of martensite exceed 50 percent (as might be found in DP 980 or higher strengths), the ferrite may become discontinuous. The combination of hard and soft phases results in an excellent strength-ductility balance, with strength increasing with increasing amount of martensite. DP steels can be hot-or cold-formed and also have high bake hardening behavior. If hot-rolled, cooling is carefully controlled to produce the ferritic-martensitic structure from austenite. If continuously annealed or hot-dipped, the final structure is produced from a dual phase

ferritic-austenitic structure that is rapidly cooled to transform some of the austenite to martensite.

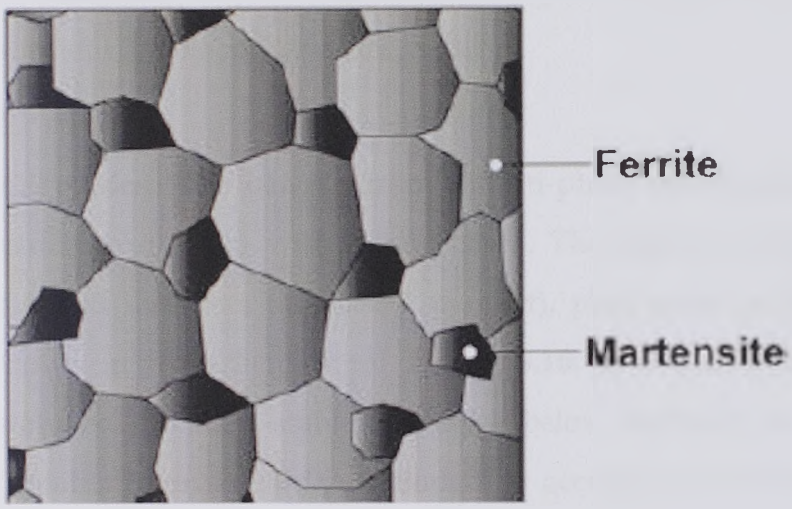

Figure3. 9DP microstructure schematic [45]

The soft ferrite in the final DP material is exceptionally ductile and absorbs strain around the martensitic islands, enabling uniform elongation with high work hardening rate and fatigue strength. Additionally, DP steels can absorb a lot of strain energy. Unlike conventional steels (even the traditional BH steels), bake hardening does not decrease with increasing pre-strain for DP steels.

DP is currently one of the most widely used AHSS. Automakers are increasingly employing DP to increase strength and down gauge HSLA structural components. Important to consider when designing with DP, as with other AHSS, is the effect of strain and bake hardening. DP steels may be developed with low to high yield strength (YS) to ultimate tensile strength (UTS) ratios, allowing for a broad range of applications from crumple zone to body structure. DP is sometimes selected for visible body parts and closures, such as doors, hoods, front and rear rails. Other popular applications include: beams and cross members; rocker, sill, and pillar reinforcements; cowl inner and outer; crush cans; shock towers, fasteners, and wheels.

DP is increasingly used by automakers in current car models. For example, in the 2011 Chevrolet Volt, the overall upper body structure is six percent DP by mass, and the lower structure is 15 percent, including such parts as the reinforcement for the rocker outer panel.

- TRIP steel

Like CP grades, TRIP benefits from a multi-phase microstructure with a soft ferrite matrix embedded with hard phases. The matrix contains a high amount of retained austenite (at least 5 percent), plus some martensite and bainite, as shown in the schematic of **Figure 3.10**. TRIP has a high carbon content to stabilize the meta-stable austenite below ambient temperatures. Silicon and/or aluminum are often included to accelerate the ferrite/bainite formation while suppressing carbide formation in this region.

TRIP steel received its name for its unique behavior during plastic strain: in addition to the dispersal of hard phases, the austenite transforms to martensite. This transformation allows the high hardening rate to endure at very high strain levels,hence"Transformation- Induced Plasticity." The amount of strain required to initiate this transformation may be managed by regulating the stability of the austenite by controlling its carbon content, size, morphology or alloy content. With less stability, the transformation begins almost as soon as deformation transpires.

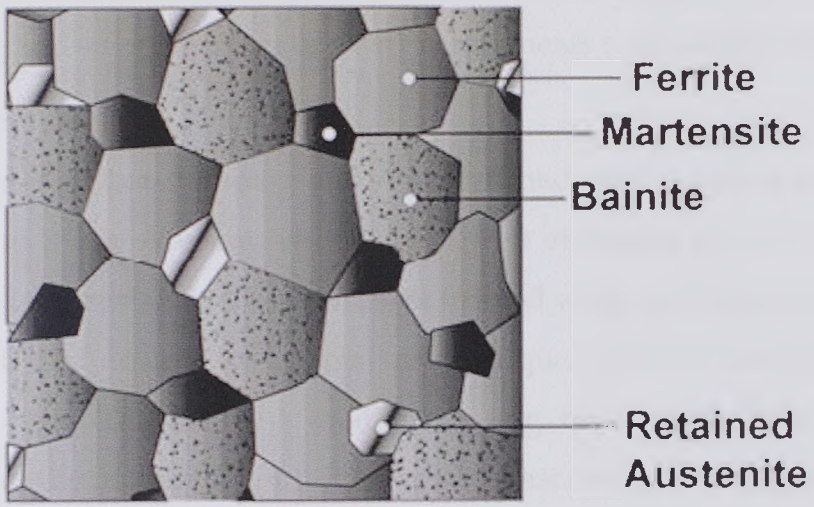

Figure3. 10Schematic of a typical TRIP microstructure [45]

With more stability, the austenitic transformation to martensite is delayed until higher levels of strain are reached, typically beyond those of the forming process. In highly stabilized TRIP steel automotive parts, this delay can allow austenite to remain until a crash event transforms it to martensite. Other factors also affect the transformation, including the specific conditions of deformation, such as the strain rate, the mode of deformation, the temperature, and the object causing the deformation. When the austenite-martensite transformation occurs, the resulting structure is toughened by the hard martensite.

- Complex phase steel (CP)

CP steel has similar microstructure with the TRIP steel except that CP steel has no retained austenite. With the hard phases like martensite and bainite and some help from precipitation hardening, the strength of CP steel ranges from 800 to 1000MPa, which makes the steel excellent for anti-crash rod, bumper and B pillar making.

- Martensite steel (M)

M steel is produced by fast quenching from austenite temperature to obtain lath martensite. M steel, no matter whether it is hot rolled, cold rolled

and annealed or formed and post heat treated, is the highest in strength for auto-making and suits the needs of safety components such as anti-crash rod.

- MnB steel

MnB steel or hot-stamping and die-quenched steel contains mainly Mn and Boron, so it has excellent hardenability. Hot stamping process consists of heating blanks to austenization, then press formed while the blanks are still red hot and soft, and at last, the formed parts is quenched to hard phases like martensite within the die. The total processing time takes about 15 to 25 seconds. Since the production of AHSS requires fast cooling, inadequate cooling capacity has to be compensated by adding more alloying elements. The addition of alloying elements deteriorates both the properties and increases environmental problem.

However dual phase (DP) and transformation induced plasticity (TRIP) steels are very promising approach to increase the ductility of high strength steels for automotive applications. In low alloyed DP and TRIP steels, the retained austenite is mainly stabilized by carbon. Thus carbon enrichment in the austenite and the prevention of precipitation of iron carbides, are achieved by lowering the activity of carbon in cementite, by addition of alloying elements such as Si and appropriate heat treatment of the cold-rolled strips. Addition of aluminum accelerates formation of ferrite in the (α, γ) temperature range thus enables creation of bainite-martensite islands from retained austenite when fast cooling is applied. Synergetic effect of alloying elements on phase transformation occurrence is shown in **Figure 3.11**. [46]

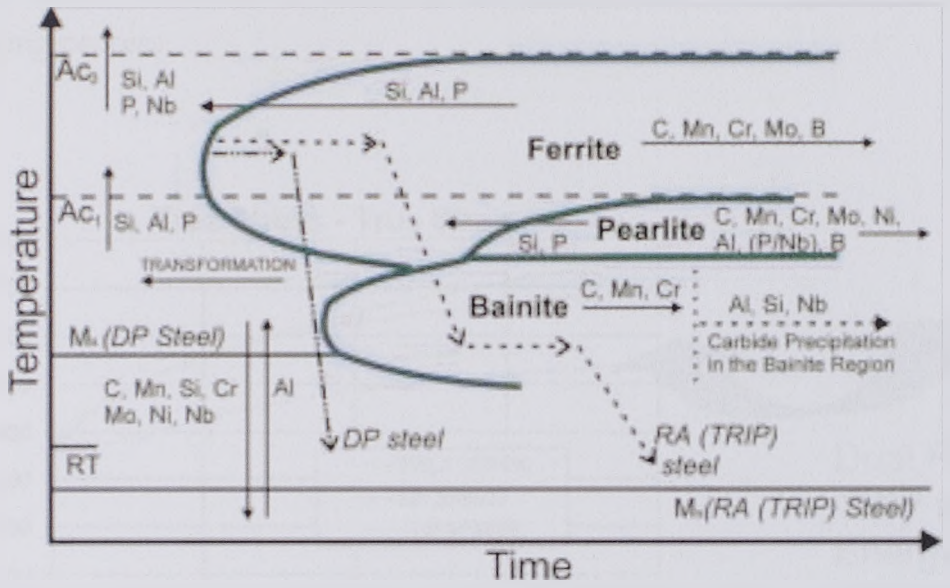

Figure3. 11 Influence of alloying elements on TTT behavior. [46]

However Stress-strain behavior of HSLA, DP and TRIP steels of approximately similar yield strengths are compared in **Figure 3.12**. The TRIP steel has lower initial work hardening rate than the DP steel, but the hardening rate persists at higher strains where that of the DP begins to diminish. The work hardening rates of DP and TRIP steels are substantially higher than for conventional HSS, providing DP and TRIP with significant formability advantages. This is particularly useful when designers take advantage of the high work hardening rate (and increased Bake Hardening effect) to design a part utilizing the as-formed mechanical properties. High work hardening rate persists to higher strains in TRIP steels, providing a slight advantage over DP in the most severe stretch forming applications. TRIP steels uses higher quantities of carbon and silicon and /or aluminum than DP steels to lower the martensite finish temperature to below ambient temperatures to form the retained austenite phase. [5]

The strain level at which retained austenite begins to transform to martensite can be designed by adjusting carbon content. At lower carbon levels, the retained austenite begins to transform almost immediately upon

deformation, increasing work hardening rate and formability during the stamping process.

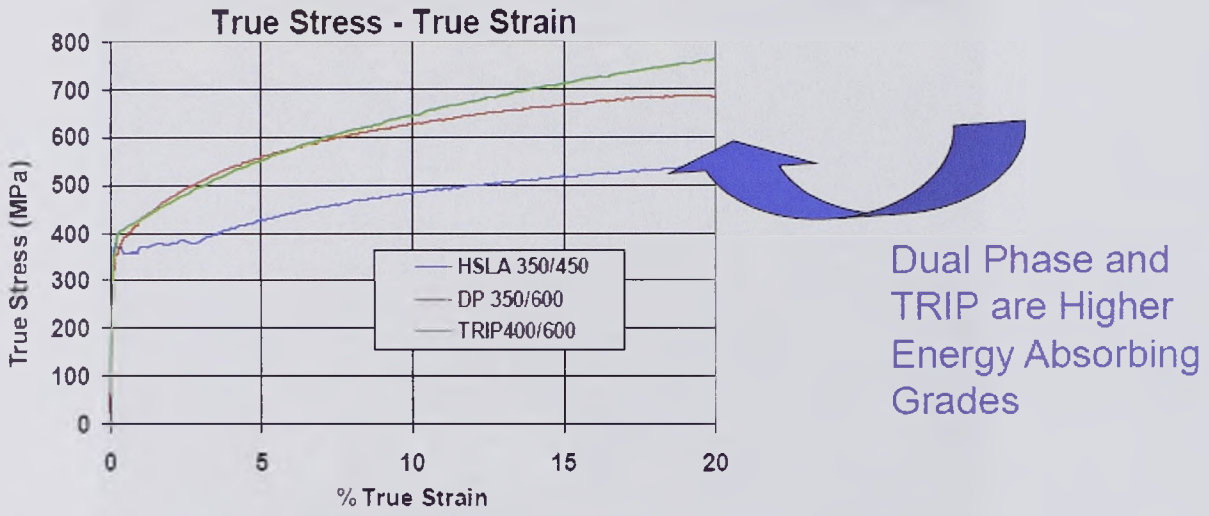

HSLA, DP, and TRIP comparisons [47]

Figure3. 12Advanced High Strength Steel Processing

All AHSS [48] are produced by controlling the cooling rate from the austenite or austenite plus ferrite phase, either on the run out table of the hot mill (for hot rolled products) or in cooling section of the continuous annealing furnace (continuously annealed or hot dip coated products). AHSS cooling patterns and resultant microstructures are schematically illustrated in **Figure 3.13**. Martensatic steels are produced from the austenite phase by rapid quenching to transform most of the austenite to martensite. Dual phase ferrite+ martensite steels are produced by controlled cooling from the austenite phase (in hot rolled products) or from the two-phase ferrite + austenite phase (for continuously annealed and hot dip coated products) to transform some austenite to ferrite before rapid cooling to transform the remaining austenite to martensite. TRIP steels typically require the use of an isothermal hold at an intermediate temperature, which produces some bainite. The higher silicon and carbon content of TRIP steels also results in significant volume fractions of retained austenite in the final microstructure. Complex phase steels also follow

a similar cooling pattern, but here, the chemistry is adjusted to produce less retained austenite and form fine precipitates to strengthen the martensite and bainite phases.

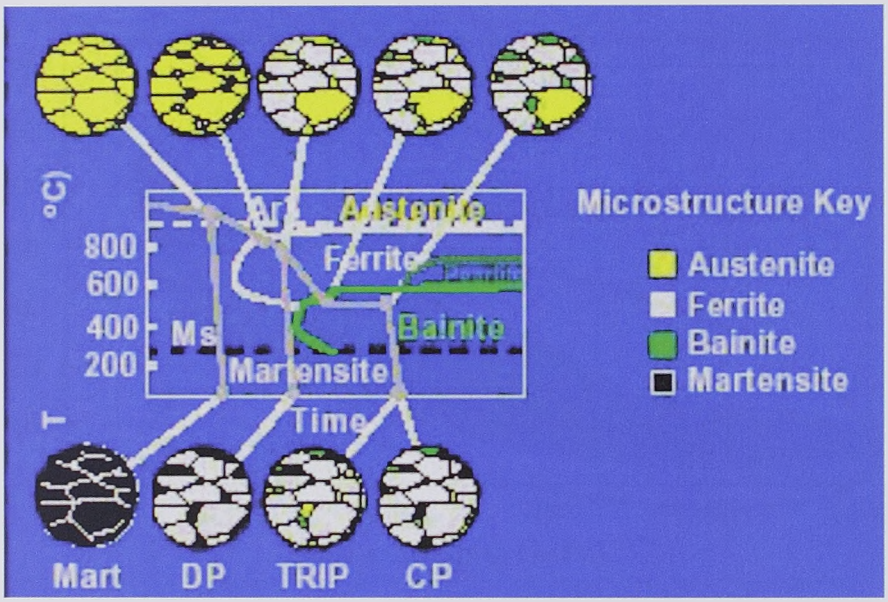

Figure3. 13 AHSS cooling patterns [48]

Figure 3.14 illustrates conventional strengthsteels suchasmild and IF steels, conventional high-strength steels such as carbon-manganese, bake hardenable, isotropic, high-strength IF, high strength, low alloy steels (HSLA) and the newer grades of advanced high strength steels such as Dual Phase, Transformation Induced Plasticity, Complex Phase, and Martensite-steel as "AHSS"-"Advanced High Steels". High strength steels (HSS) are defined as those steels with yield strengths from 210-550 MPa; Ultra High Strength Steels (UHSS) are defined as steels with yield strengths greater than 550 MPa. The yield strengths of advanced High Strength Steels (AHSS) overlap the range of strengths between HSS and UHSS. The principal differences between conventional HSS and UHSS are due to their microstructures. AHSS are multi phase steels, which contain martensite, bainite, and/ or retained austenite in quantities sufficient to produce unique mechanical properties. Compared to conventional micro-alloyed steels; AHSS exhibit a superior combination of high strength with good formability. This combination arises primarily from their

high strain hardening capacity as a result of their lower yield strength to ultimate tensile strength ratio. However **Figure 3.15** illustrates the third generation of AHSS steel. [49]

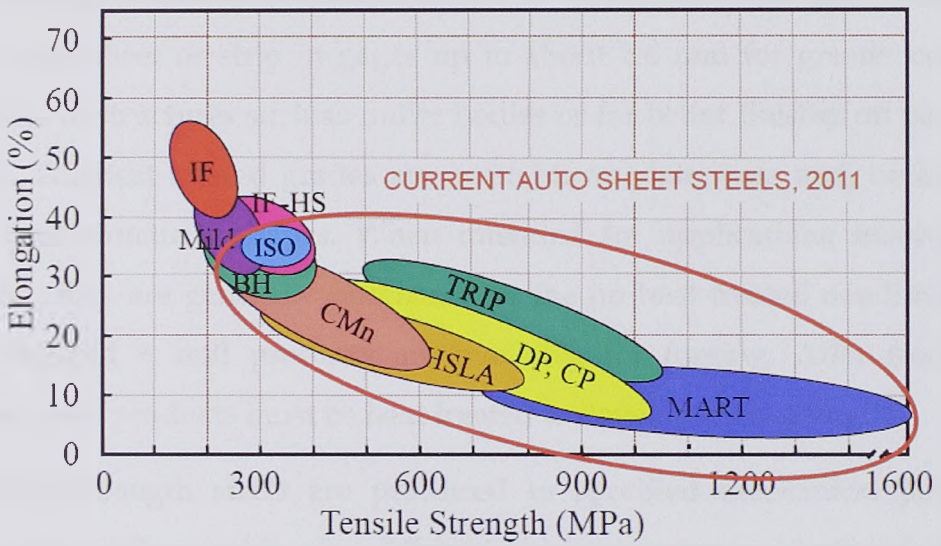

Figure3. 14 Tensile strength and elongation relationship of different HSS. [47]

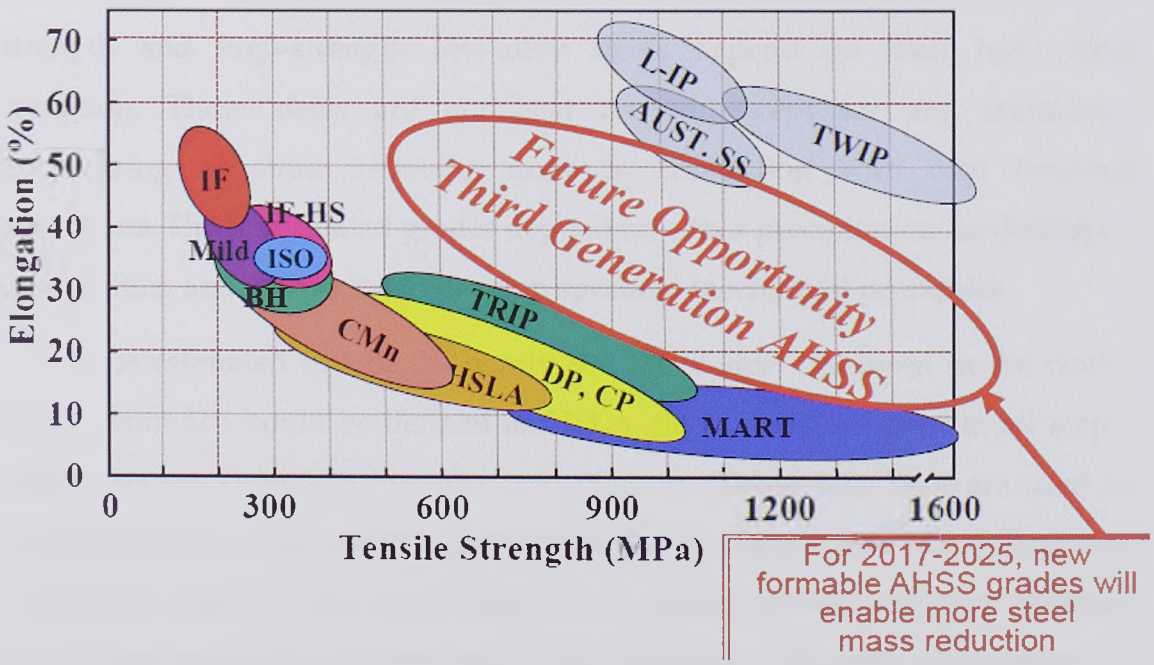

Figure3. 15 Third Generation of AHSS. [47]

3.6 High Strength Steel Availability

High strength [49, 40] and high strength low alloy steels are generally available in all standard wrought forms: sheet, strip, plate, structural shapes, bars, bar-size shapes and spherical sections. These steels are also furnished as cold rolled sheet or strip in gages up to about 1.6 mm for greater control of thickness in structures such as trailer bodies or for better finishes on parts to be plated. The heat treated grades are available as plate, bars and, occasionally, sheet and structural shapes. When intended for applications involving hot forming, they are generally purchased in the no heat-treated condition. Also, semi finished + mill products are available for forging. After forming or forging, such products must be heat treated to develop high strength.

High-strength steels are produced to specified mechanical properties, which may differ slightly for different thickness ranges. Limits of chemical composition are generally published for information only because the carbon and alloy contents vary as necessary to maintain mechanical properties of high-strength and high-strength low-alloy steels depend on their hot rolled condition. These steels are not heat treated except for any annealing, normalizing or stress relieving done in connection with cold forming operations. The heat treated grades depend on either precipitation hardening or quenchining and tempering to develop specified mechanical properties.

It is estimated that of the nearly 800 Mt of steel produced in the world today about 12% could be defined as HSLA. Such steels are used in all major market sectors especially line-pipe and offshore (**Table 3.2**). They are used to different degrees in the various parts of the world. For example HSLA Steels are extensively used for both shipbuilding and pressure vessel purposes in Japan much more so than in Europe and North America. A growth opportunity for microalloyed steels is in the automotive sector as manufacturers strive to reduce the weight of vehicles. [40]

3.7 Applications of High Strength Steels

The requirements [5] of the user of the high strength steel, relate to the steel properties. The steel should have to be suitable for any given application. Dealing with the various applications for which high strength steel is used; the following may be included in the list, with perhaps many lesser known uses: aircraft undercarriages, bolts, pressure vessels, solid propellant rocket motor cases, and machine parts. It should be noted that the use of high strength steel is at present restricted almost entirely to those applications where strength/weight ratio of the item is of major importance. The extension of use to more general engineering may well depend upon the success of steel in these specialized fields.

The properties of high strength steel which are important to the user include strength at various temperatures, ductility and toughness, fatigue resistance, corrosion resistance, and weldability.

New high-strength steels are stronger, easier to form and have uniform mechanical properties which allow designers to create lighter, safer and more environmentally-responsible solutions. Steel is the material of choice for product manufactures that require their products to have strength, durability and value.

Table 3.2Proportion of HSLA steels produced world-wide (%) [40]

	Europe	N. America	Japan	
Linepipe	95	95	95	
Shipbuilding	40	20	75	
Offshore Steels				
Plates	90	30	70	
Sections	70	20	10	
Pressure Vessels	30	25	85	
Structural				
Sections	30	20	10	Annual World Tonnage ~800Mt HSLA Steels~12%
Section, automotive	80	80	80	
Section, ships	15—30	20	10	
Sheet pilling	25	15	100	
Rebar	100	5	10	
Plates	25	20	10—30	
Sheet and Coil (inc. Galv.)				
Automotive	30	20	30	
Building (not rebar)	95	80	70	

Steel is the most recycled material in the world. Almost half the world's steel is made from recycled material, two times more than all other materials added together steel can also be recycled from one product to other without any deterioration in quality.

3.7.1 Applications of HSLA steel

HSLA steels [5, 50, 51, 52] were originally developed in the 1960s for large-diameter oil and gas pipelines. The line pipe used in these projects required higher strength and toughness than mild carbon steel, and good weldability provided by a low carbon equivalent. The oil & gas sector is still market where the most important applications for HSLA steels are found, but the automotive and the offshore & onshore structural engineering sectors now consume significant quantities of these alloys. [50]

The HSLA steels are much stronger and tougher than ordinary carbon steels, ductile, highly formable, weldable, and highly resistant to corrosion. The increased strength of HSLA steel means that structures can be built that contain less steel and are therefore lighter than they otherwise would be. This is an important feature for cars and trucks because it leads to fuel economy. It is also important in the design of bridges since it means that the center spans can be longer and need fewer supporting beams. An advantage of HSLA steels is seen in the construction of tall television transmitter masts. The extra strength of the steel means that the sections making up the mast. They could be thinner and more stable because, they offer less resistance to the wind. HSLA steels are used also in pipelines, buildings, offshore structures, construction equipment and machinery, railroad equipment, and ships. For many applications, the most important factor in the steel selection process is the favorable strength-to-weight ratio of HSLA steels compared with conventional low-carbon steels. This characteristic of HSLA steels has led to their increased use in automobile components [5]. **Figure 3.16** shows the past and future use of high strength steels. However **Figure 3.17**shows some real applications of HSLA steels.

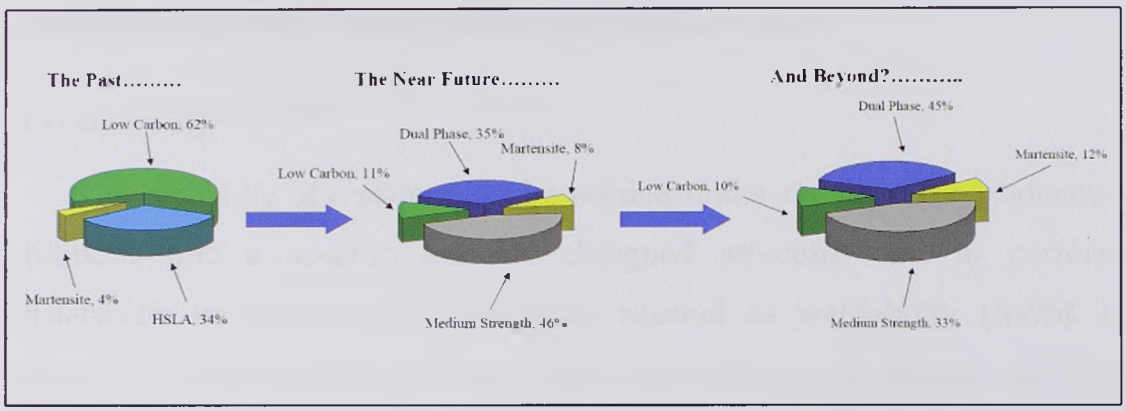

Figure3.16The past and future usage of high strength steels (automobile industry).[51]

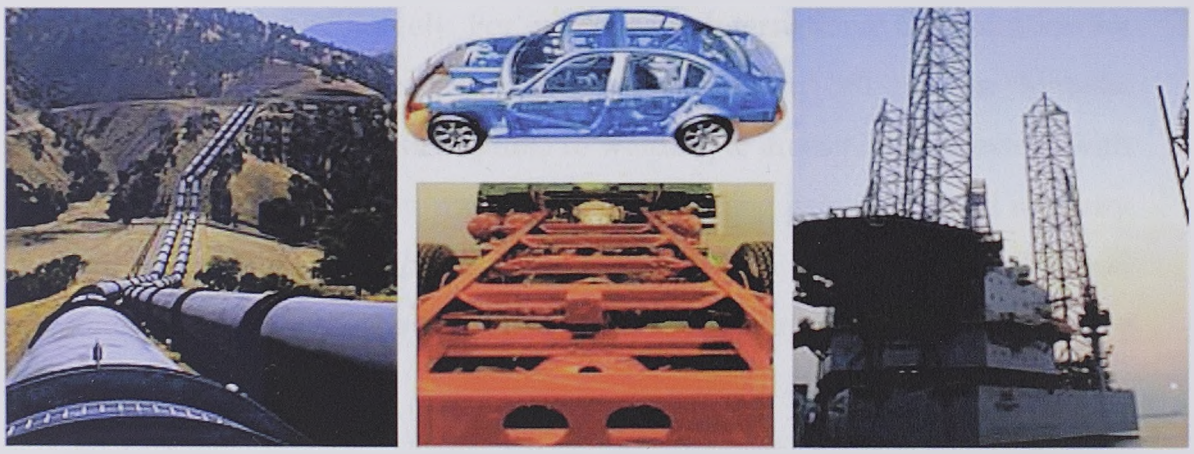

Figure3. 17 HSLA steel applications. [52]

4. Wedability and Welding Rules of HSLA Steels

4.1 Weldability[5, 53, 54, 55]

The capability of a material to be welded under the imposed fabrication conditions into a specific, suitably designed structure and to perform satisfactorily in the intended service is referred as weldability (AWS). It depends on various factors such as, nature of metals, weld designs, welding techniques, skills, etc. However it has been stated that all metals are weldable but some are more difficult than anther (**Figure 4.1**).[53]

However, weldability is often hard to define quantitatively, so most standards define it qualitatively. For instance the International Organization for Standardization (ISO) defines weldability in ISO standard 581-1980 as: "Metallic material is considered to be susceptible to welding to an established extent with given processes and for given purposes when welding provides metal integrity by a corresponding technological process for welded parts to meet technical requirements as to their own qualities as well as to their influence on a structure they form."[54]

Weldability could be divided into two general classes: (1) fabrication weldability and (2) service weldability. Fabrication weldability addresses the question, "can one join these materials without introducing detrimental discontinuities?" The acceptability of these discontinuities depends on the application requirements for the particular weldment. The fabrication weldability of steel may be adequate for noncritical application requirements for the particular weldment. The fabrication weldability of steel may be adequate for a noncritical application. Fabrication weldabilty deals primarily with discontinuities such as hydrogen-assisted cold cracks, hot cracks, reheat cracks, lamellar tearing, and porosity.

Service weldability addresses the question, "whether the finished weldmenthas adequate properties to serve the intended function or not?" An

important aspect of service weldability is the comparison of HAZ properties with those of the unaffected base metal. Again the acceptability of the service weldability depends on the intended application.

Service weldability involves the effect of the welding thermal cycle on the properties in the HAZ. Service weldability often determines the range of heat inputs allowable for particular steel. Low heat inputs may introduce unacceptable low-toughness microstructures, as well as fabrication- weldability problems associated with cold cracking.

High heat inputs can introduce coarse microstructure and HAZ properties, but the induced thermal cycle controls the microstructure and HAZ properties, but the induced thermal cycle controls the microstructure and properties. Therefore, both heat input and thickness should be considered.[55]

4.1.1 Effect of carbon content and alloying elements [5, 56, 57]

Traditionally, empirical equations have been developed experimentally to express weldability. Carbon equivalent (CE) is one such expression; it was developed to estimate the cracking susceptibility of steel during welding and to determine whether the steel needs preweld and postweld heat treatment to avoid cracking. Carbon equivalent equations do include the hardenability effect of the alloying elements by expressing the chemical compositions with different coefficients for the alloying elements have been reported. The International Institute of Welding (IIW) carbon equivalent equation is:

$$CE = C + \frac{Mn}{6} + \frac{Ni}{15} + \frac{Cu}{15} + \frac{Cr}{5} + \frac{Mo}{5} + \frac{V}{5} \qquad (4.1.1)$$

Where, the concentration of the alloying elements is given in weight percent. It can be seen in **Eq. 4.1.1** that carbon is the element that most affects weldability. Together with chemical elements, carbon may affect the solidification temperature range, hot tear susceptibility, hardenability, and cold-cracking behavior of steel weldment. **Figure 4.1** summarizes the CE and weldability description of some steel families. Because of the simplification and

generalization involved in (**Figure 4.1**) it should be used cautiously for actual welding situations.

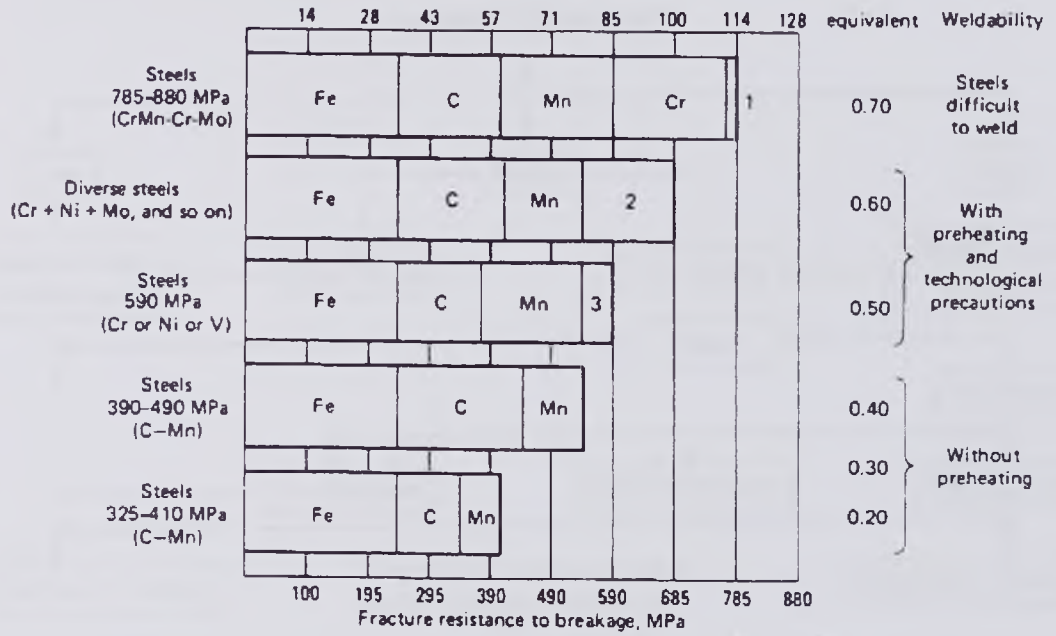

Figure 4.1Weldability of several families of steels as a function of carbon equivalent. [5]

Steels with lower CE values generally exhibit good weldability (**Table 4.1**). When the CE of steel is less than 0.45 %, weld cracking is unlikely, and no heat treatment is required. When CE is between 0.45 and 0.6 %, is likely, and preheat in the range of approximately 95 to 400 °C is generally recommended. When the CE of steel is greater than 0.6 %, there is a high probability that the weld will crack and that both preheat and post heat treatments will be required to obtain a sound weld. However **Figure 4.2** illustrates the effect of the CE variation on the low-high risk of cold crack.

Table 4.1Effect of CE on weldability. [56]

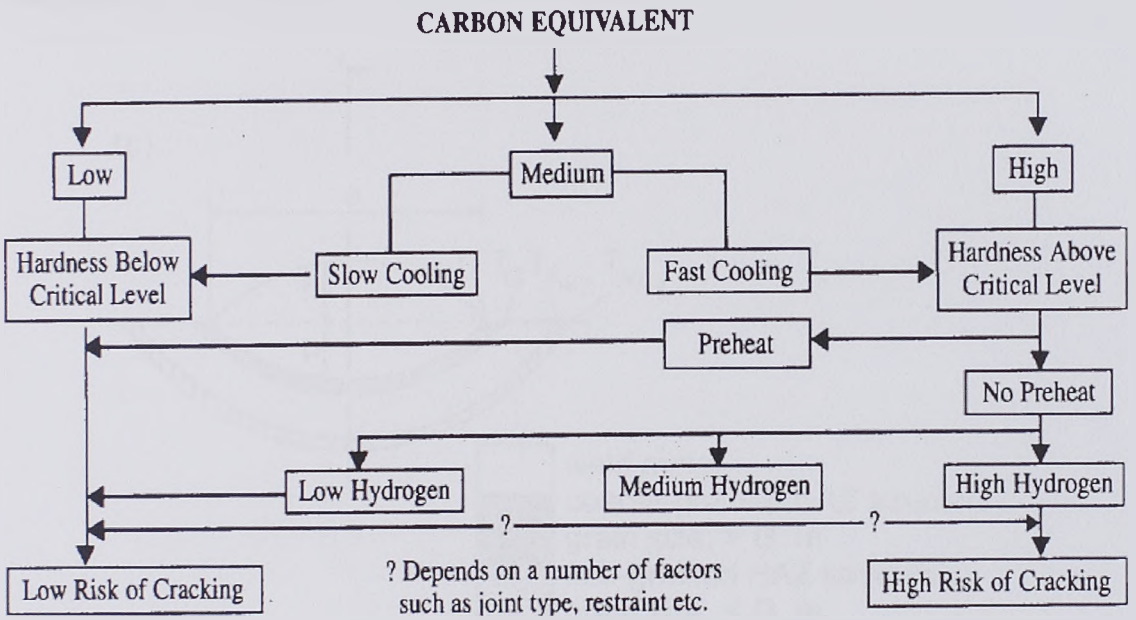

Figure 4.2 Flow chart of the effect of CE on low-high risk of cold cracking[57]

4.1.2 Characteristic Features of Welds [58,59]

Single-pass and multi pass weldments

In practical welding processes, particularly for welding of the thick plates, multi-pass welding is often required to fill up the joint gaps. Since the heat input is limited to avoid the coarse HAZ structure resulting from high heat input, the volume of deposited filler metal for each pass, which is proportion of the previous pass HAZ is reheated to a certain extent. Therefore, study of the reheated HAZ microstructure is important in investigating the whole HAZ weld joint. **Figure 4.3** Shows a schematic diagram of single and multi-run welds. However Figure 4.4 illustrates the various regions of a welded joint.

Except for a small part of the HAZ being subjected to the highest peak temperature during the second weld run, most of the reheat region experiences

a relatively low temperature in the second thermal cycle and is therefore subjected a relatively mild heat treatment. A major effect of reheating the HAZ is refining the structure.

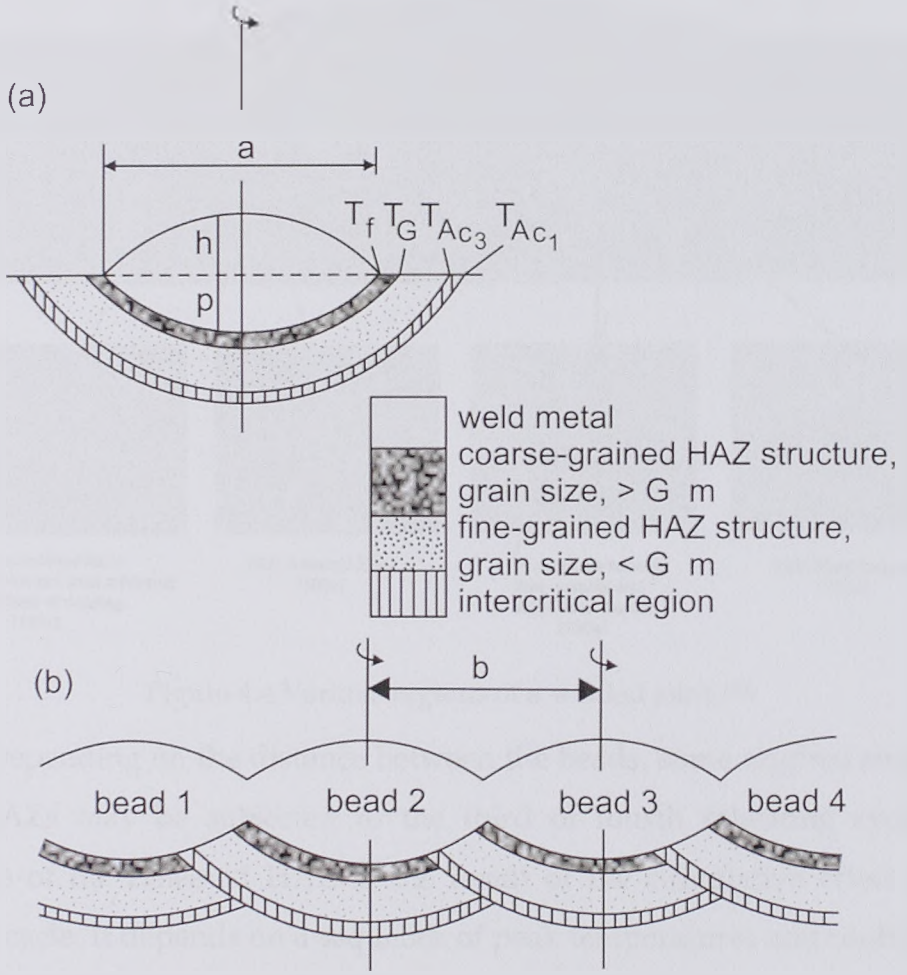

Figure 4.3 Schematic representation of structure distribution in HAZ of (a) single and (b) multi-pass weld deposits on flat plate. [58]

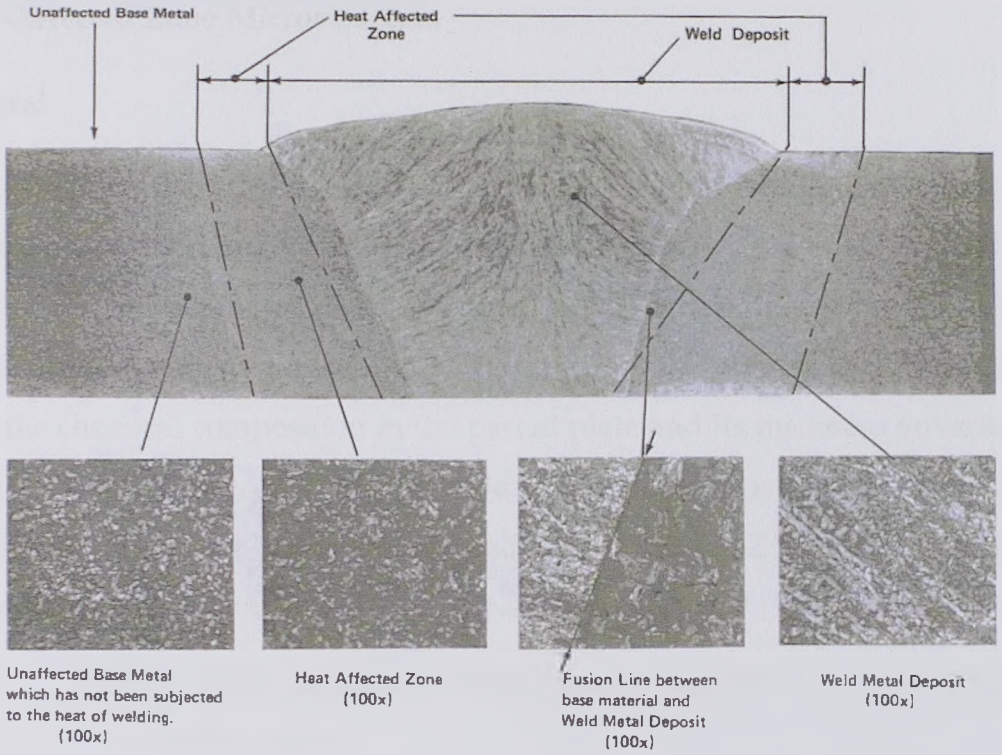

Figure 4.4 Various regions of a welded joint. [59]

Depending on the distance between the beads, some original single pass weld HAZs may be subjected to the third of fourth reheating cycles. The structure of the reheated HAZ is the result of the cumulative effect of each thermal cycle. It depends on a sequence of peak temperatures and cooling rates, and the precipitation behavior during each weld cycle, as well as on the composition and initial microstructure of the material. Since refinement of the HAZ structure leads to improvement of the mechanical properties of the HAZ, multi-layer welding is regarded as beneficial.

However, multi-pass welding with low heat input reduces the efficiency of the welding process. High heat input single pass welding is finding increasing application in the fabrication industry to increase welding productivity. Compared to multi-pass welding, single pass welding represents the most severe case with respect to the grain growth in the HAZ. [59]

4.1.3 Metallography of Welds [58, 60, 61, 62]

Heat-Affected Zone Microstructure

General

The heat affected zone, HAZ, is of great concern in a weldment since it can contain a large variety of microstructures (**Figure 4.5**), geometries, stresses and thereby have different properties depending on where in the HAZ a test is made. The time-temperature cycle during the weld process, in combination with the chemical composition in the parent plate and its thickness governs the HAZ properties. When judging the weldability of steel it is of great importance to consider the peak temperature reached in the HAZ which has a large influence on;

- The dissolution of microalloying precipitates in the grain-coarsened HAZ
- The austenite grain growth
- The cooling rate from the peak temperature. [60]

The microstructure in the true heat affected zone (HAZ) is largely dependent upon the heat input and its location or distance from the fusion boundary. As the distance from the fusion boundary increases, the peak temperature that the base metal microstructure is exposed to decreases. A high heat input increases the time that the base metal microstructure is exposed to the peak temperature. The peak temperature in the true HAZ does not reach the melting point of the C-Mn steel.

Generally, the true HAZ (**Figure 4.6**)is the base metal underlying the weld which has been heated to temperatures above the Fe-Fe Carbide metastable phase diagram A1 (723°C) temperature and below the solidus temperature, typically 1495°C. However, with higher heat input processes, such as submerged arc or electro slag welding, the true HAZ includes peak temperatures below the A1 temperature. This is because spheroidization of the

pearlite Fe carbide plates occurs as a result of tempering. The longer the base metal is exposed to temperatures just below the A1, the greater the spheroidization.

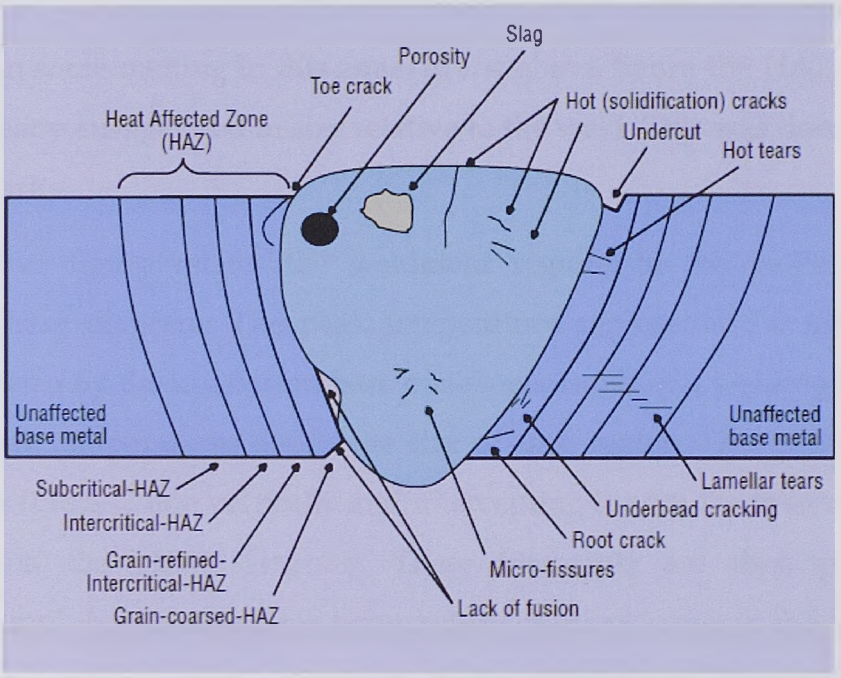

Figure 4.5 Drawing showing the various regions of the HAZ in a single-pass weld and the possible defects. [61]

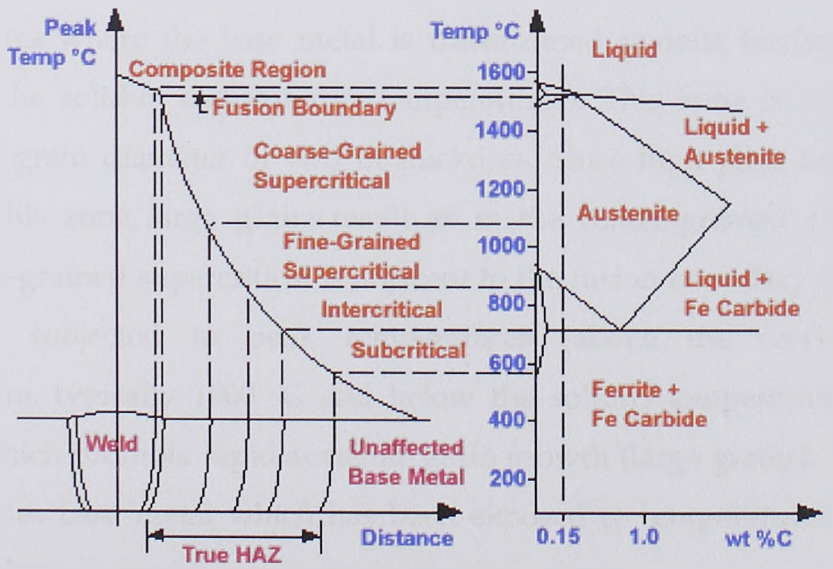

Figure 4.6True HAZ Regions and the Fe-Fe Carbide Metastable Phase Diagram.[62]

The true HAZ consists of four regions: coarse-grained supercritical, fine-grained supercritical, intercritical and the subcritical. **Figure 4.7** shows the microstructure for HSLA steel. The partially melted zone component of the fusion boundary is also considered part of the HAZ but not the true HAZ since there has been some melting in this zone. In the above figure the HAZ regions have been greatly exaggerated in size relative to the weld. This was done for the purpose of clarity.

The above figure relates the weldment regions to the Fe-Fe carbide metastable phase diagram. The peak temperature represents the maximum temperature seen by the unaffected base metal as a result of a welding thermal cycle. The peak temperatures define the size of each region. This is shown by extending the 0.15% C line vertically and intercepting it with the lines dividing the phases on the phase diagram. These intercepts are then projected horizontally until they intersect the temperature gradient curve in the figure to the left. This second intercept is then extended vertically and downward to the weldment to reveal the "relative" width of each HAZ region. In practice the HAZ width is very small. In practice, the HAZ size is very small in relation to the weld size. The partially melted zone has been subjected to peak temperatures where the base metal is transformed to delta ferrite and liquid (between the solidus and liquidus temperatures). This zone is very narrow, perhaps a grain diameter or two in thickness. Since high peak temperatures occur in this zone, large grains result as in the coarse-grained supercritical. The coarse-grained supercritical is adjacent to the fusion boundary of weld and has been subjected to peak temperatures (above the recrystallization temperature, typically 1000 ◦C and below the solidus temperature, typically 1495◦C) which promote rapid austenite grain growth (large grains). This region also includes base metal which has been exposed to temperatures below the solidus, where austenite and delta ferrite both exist. In practice, this region is rarely seen because of the very narrow temperature zone in which austenite

and delta ferrite exist. In practical terms, the thickness of this region is usually less than a grain diameter.

The fine-grained supercritical is adjacent to the coarse-grained supercritical and has been subjected to peak temperatures below the recrystallization temperature but above the A3 temperature (the equilibrium cooling temperature at which some of the austenite transforms to ferrite). Since the peak temperature is below the recrystallization temperature, rapid austenite grain growth does not occur. In practice, aluminum killed carbon steels which have been agitated with nitrogen during steel making, precipitate Al nitrides in this temperature zone. The Al nitrides are extremely small and precipitate at the base metal grain boundaries. Their presence at the grain boundaries helps prevent the grain boundaries from moving; hence, the high peak temperatures do not result in large grain growth.

The intercritical is adjacent to the fine-grained supercritical and has been subjected to peak temperatures between A3 and A1, where the base metal ferrite and carbides begin to transform to austenite. Grain refinement occurs at these peak temperatures. A normalizing heat treatment of the base metal occurs in this region. The subcritical is between the intercritical and unaffected base metal and has been subjected to peak temperatures below the A1. At temperatures just below the A1, the pearlite carbide plates begin to spheroidize. A tempering heat treatment of the base metal occurs in this region, however, the pearlite does not completely spheroidize since the weld thermal cycle is too short for this to happen.[62]

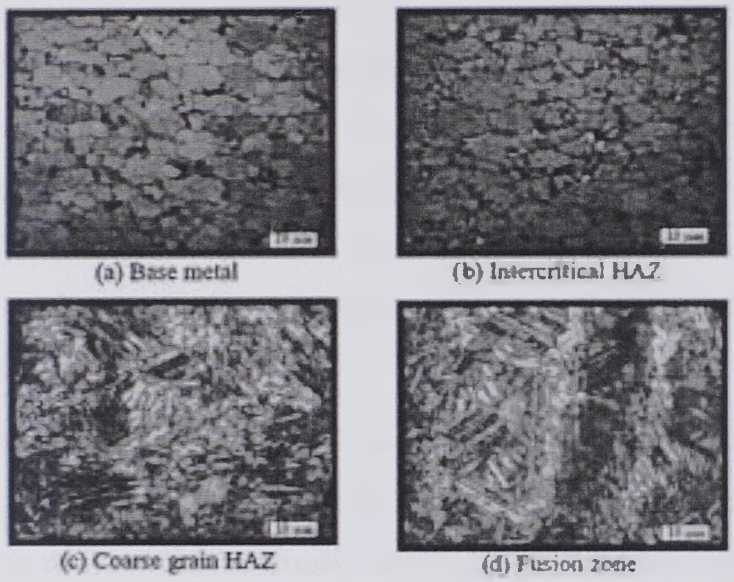

Figure 4.7Microstructure for HSLA steel. [58]

4.1.4 Weld Cracks [5, 63, 64]

There are a variety of physical defects such as undercut, insufficient fusion, excessive deformation, porosity, and cracks that can affect weld quality. Of those defects, cracks are considered to be the worst since even a small crack can grow and lead to failure. All welding standards show zero tolerance for cracks whereas the other defects are tolerated within certain limits. There are three requirements for cracks to form and grow: a stress raising defect, tensile stress, and material with low fracture toughness. Microscopic defect locations are available in practically all welds including geometric features and weld chemistry that can raise the local stress enough to induce a crack. That leaves the engineer to work with the stress environment and toughness: if either of the two can be effectively controlled then cracks can be prevented from initiating and growing. Toughness is a measure of resistance to crack growth; resistance can be provided by blunting of the crack tip in ductile materials. However, if applied strain rate is very high (as would be the case when a spot weld cools at the end of the pulse) and the stress field is multi-axial, even ductile materials exhibit poor toughness and produce rapid crack growth.

Hard materials, such as martensite formed during cooling of steels, are brittle and have poor toughness. Toughness can be improved by controlling alloy chemistry and post-weld heat treatment. Stresses can be reduced by changing the joint design to ensure that the weld is under very low tensile load, and preferably, have a compressive load at possible crack locations. Joint deigns and fillet shapes can be controlled to minimize stress concentrators that assist in initiation of cracks.

Cracks that form in and around the weld can be distinguished into two main categories, hot cracks and cold cracks. Cracks can also form in and near the weld during use and can be caused due to fatigue or corrosion. Cracks that form during the cooling process are referred to as hot cracks and cracks whose formation is delayed are called cold cracks. To identify how and why a particular crack formed, we need to dig deeper into weld design, identify crack locations, and evaluate related metallurgy. Once the root cause or causes are identified, appropriated action can be taken to avoid crack formation. [63]

In general, carbon and low-alloy steels are among the most weldable of materials. However, they are susceptible, to one degree or another, to:

- Hydrogen-induced cracking (Cold cracking)
- Hot cracking
- Lamellar tearing
- Stress-relief cracking
- Hydrogen-Induced Cracking (Cold cracking)

Hydrogen-induced cracking (also referred to as cold cracking, delayed cracking, or under bead cracking) is the most serious problem affecting weldability. Any hardenable carbon or alloy steel is susceptible. This type of cracking results from the combined effects of four factors:

- A susceptible (brittle) microstructure
- The presence of hydrogen in the weld metal
- Tensile stresses in the weld areas

Hydrogen-induced cracking occurs after weld cooling (hence the term cold cracking) and is often delayed for many hours while atomic hydrogen diffuses to areas of high tensile stress. At microstructural flaws in a tensile stress field, the hydrogen changes to its molecular form, causing cracking. Cracking may occur in the HAZ or weld metal, and it may be longitudinal or transverse. Toe cracks and root cracks start in areas of high stress concentration (**Figure 4.8**). Cracking may therefore occur in less susceptible microstructures or at relatively low hydrogen levels. This type of cracking is often delayed while the necessary hydrogen diffuses to the area.

One of the serious problems with hydrogen induced cracking is difficulty in detecting the presence of a crack. The delayed nature of some of the cracks demands that inspection not be carried out too soon, especially in welds that will have external stresses applied when put in service.[5]

As indicated in **Figure 4.9**, zone I steels have low carbon and low hardenability and are not very susceptible to cracking. Zone III steels have both high carbon and high hardenability, and all welding conditions will produce crack-sensitive microstructures. Therefore, to avoid hydrogen-induced cold cracking in zone III steels, the user must apply low-hydrogen procedures, including preheat and PWHT. Zone II steels have higher carbon levels with lower hardenability. It is possible to avoid crack-sensitive microstructures in zone II steels by restricting HAZ cooling rates through control of heat input and, to a minor extent, with preheat. **Figure 4.9** also shows that HTLA steels, squarely in zone III, require special considerations for welding. Chromium-molybdenum steels and quenched and tempered steels also require some attention, as do some HSLA steels. Low carbon steels are readily welded except in thick sections, for which some precautions may be necessary. The TMCP steels have been specifically developed to lie in zone I, and so their weldability and resistance to cold cracking is excellent.[5]

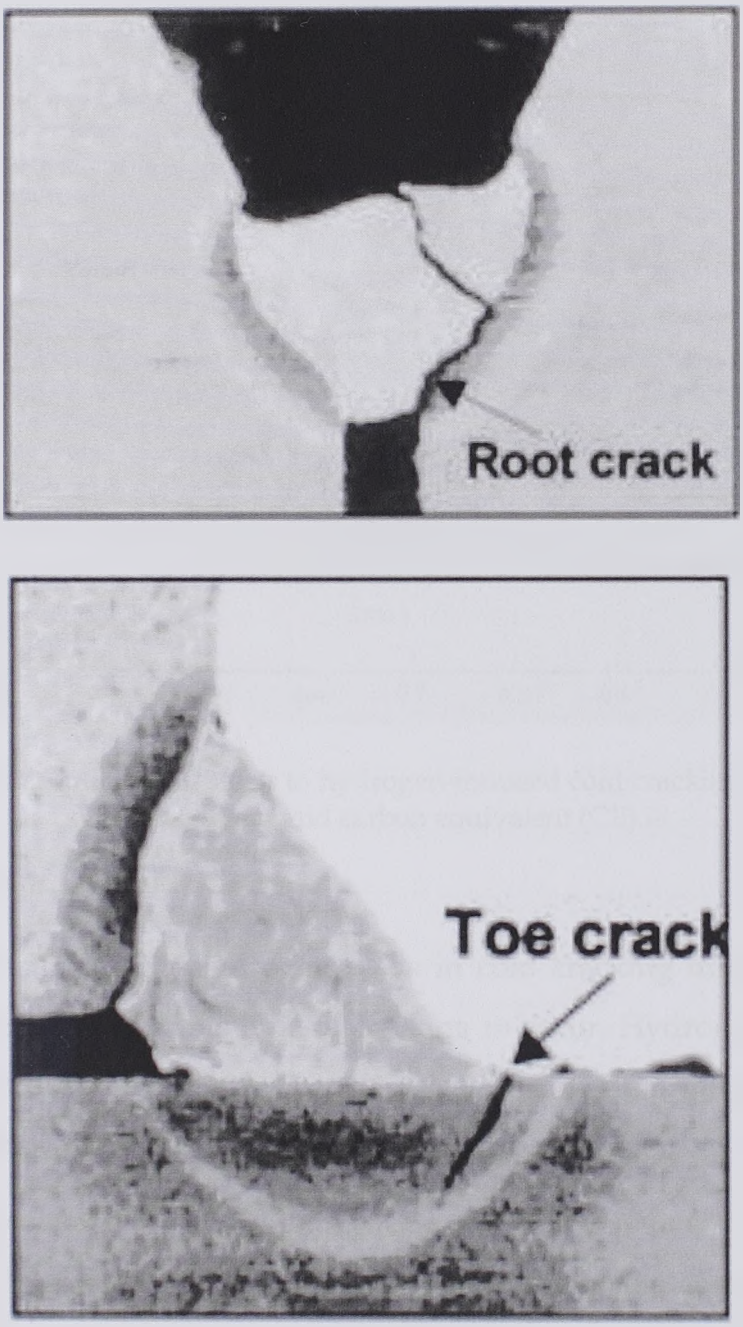

Figure 4.8Hydrogen-induced cracking in the HAZ of shielded metal-arc weld in low carbon steel (18x).[64]

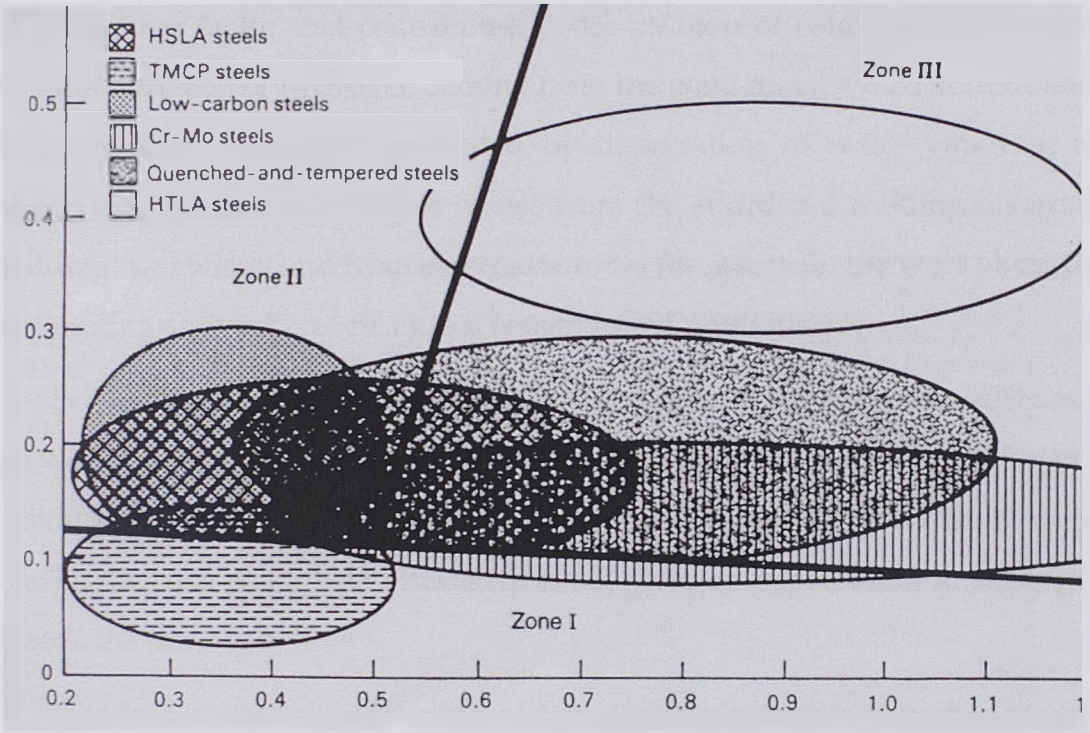

Figure 4.9 Susceptibility of steels to hydrogen-induced cold cracking relative to carbon content and carbon equivalent (CE).[5]

The influence of Hydrogen

The exact role that hydrogen plays in cold cracking unknown, but its presence is necessary for this type of cracking to occur. Hydrogen is generally introduced into the weld area during welding. The principal source of hydrogen is the welding consumable. Other sources include:

- Moisture in the flux coating of shielded metal arc welding electrodes, in submerged arc fluxes, or in the core of flux-cored electrodes.
- Hydrogen-containing lubricants left on the surface of wire electrodes or in the seams of cored electrodes
- Hydrogen-containing compounds or residues left on the plate surface (these include grease, oil, paint, rust, and so on).
- Leaking water-cooled torches, broken gas lines, or high moisture in the shielding gas.
- Aspiration of moisture-laden air into the weld are

Another factor that contributes to the creation of cold cracking in steel weld the diffusion of hydrogen coming from the weld metal which accumulates during welding. Hydrogen generated by dissociation of water vapor in an electric arc, and the water vapor comes from the additional welding materials (cladding, wet wires) and from external sources (moisture on the workpiece, the surrounding atmosphere, etc...) as it is mentioned previously.

For all types of steel, an increase of hydrogen content in the weld, as a rule, contributes to increased susceptibility to creation of cold cracking. Since it is shown that the most dangerous hydrogen diffusion from the weld metal exceeds the base metal heat affected zone, it gives an explanation to hydrogen exceeds the time. [65, 66, 67, 68]

It is known that the solubility of hydrogen in austenite is higher than in ferrite, while the diffusion coefficient of hydrogen in ferrite higher than in austenite (**Figure 4.10**). These two characteristics have an important role in the movement of hydrogen in the HAZ. Hydrogen, formed in the welding zone, intensely dissolves in the weld metal, and from it diffuses into the base metal which will later undergo martensitic transformation.

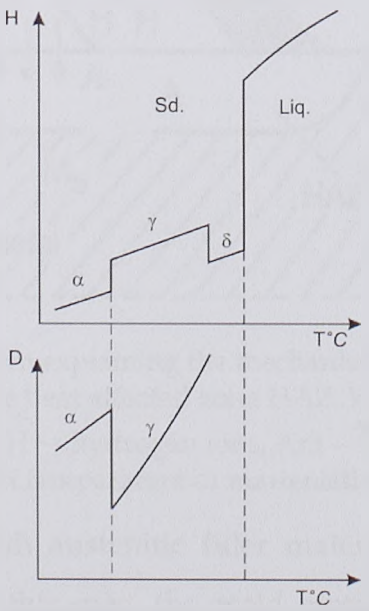

Figure 4.10 The dependence of solubility (H) and hydrogen diffusion coefficient (D) of the steel temperature.

In front of the isotherm weld metal in the austenitic condition, is saturated with hydrogen. Pearlitic transformation of weld metal hydrogen solubility decreases rapidly as the diffusion coefficient increases rapidly, so hydrogen passes into the base material (along the line A-B in **Figure 4.11**), which is still in the austenitic condition and has a higher solubility of hydrogen.

Since the diffusion coefficient of hydrogen in austenite small, it will remain hydrogen near the welded joints, and creates the hydrogen-rich front-line blending. Beyond point B appears to martensitic transformation, which moves inward and met with the hydrogen diffusion front, so that the austenite, which transforms into martensite, near the weld, but rich in hydrogen. This captured hydrogen near the fusion line passing from atomic to molecular state, which causes enormous pressure and the stresses caused by welding and transformation leads to the creation of splashes. [65, 66]

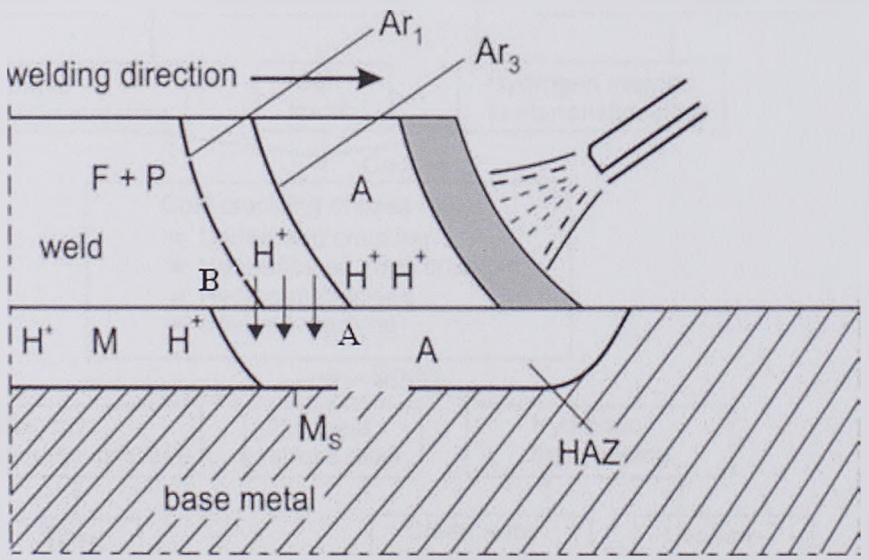

Figure 4.11Schematic diagram explaining the mechanism of atomic hydrogen penetration from the weld to the heat affected zone HAZ: F – ferrite, P – pearlite, A – austenite, M – martensite, H+ - hydrogen ions, Ar3 – $\gamma \rightarrow \alpha$ transformation temperature, Ms – start temperature of martensitic transformation

When welding steel with austenitic filler material practically does not occur cracks in the HAZ. In this case, the weld metal that cannot transform retains all the hydrogen. In addition austenitic weld metal is very flexible and

easily deformed, and is able to undertake the transformation of the grid voltage occurred in the HAZ, which leads to reduced stress in the HAZ and reduced probability of occurrence of cold cracking in it.

Prevention of Hydrogen-Induced Cracking

The major causes and cures to avoid cold cracking in both base and weld metal are illustrated in the **Figures 4.12 & 4.13** respectively.

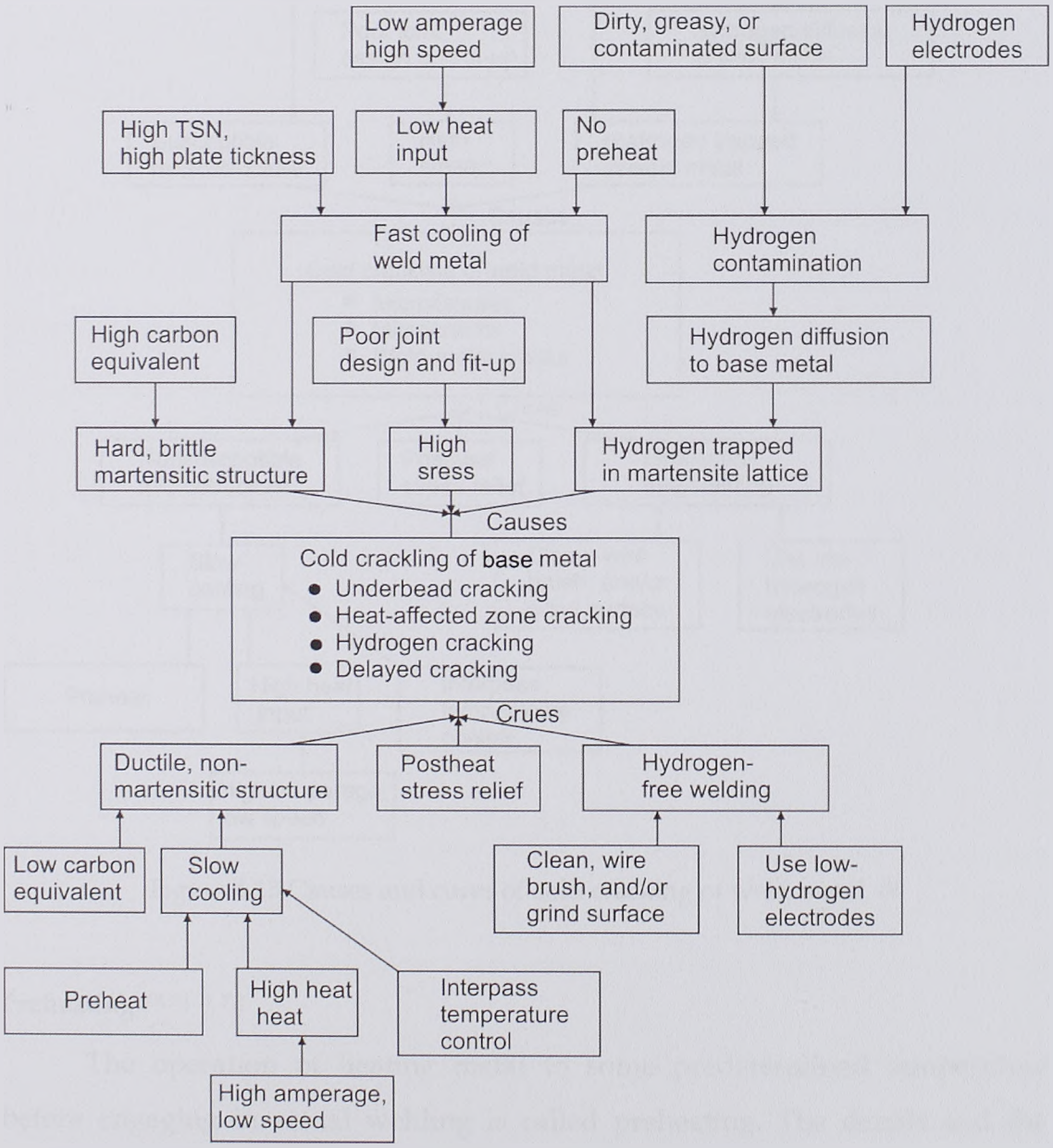

Figure 4.12 Causes and cruses of cold cracking of base metal.[5]

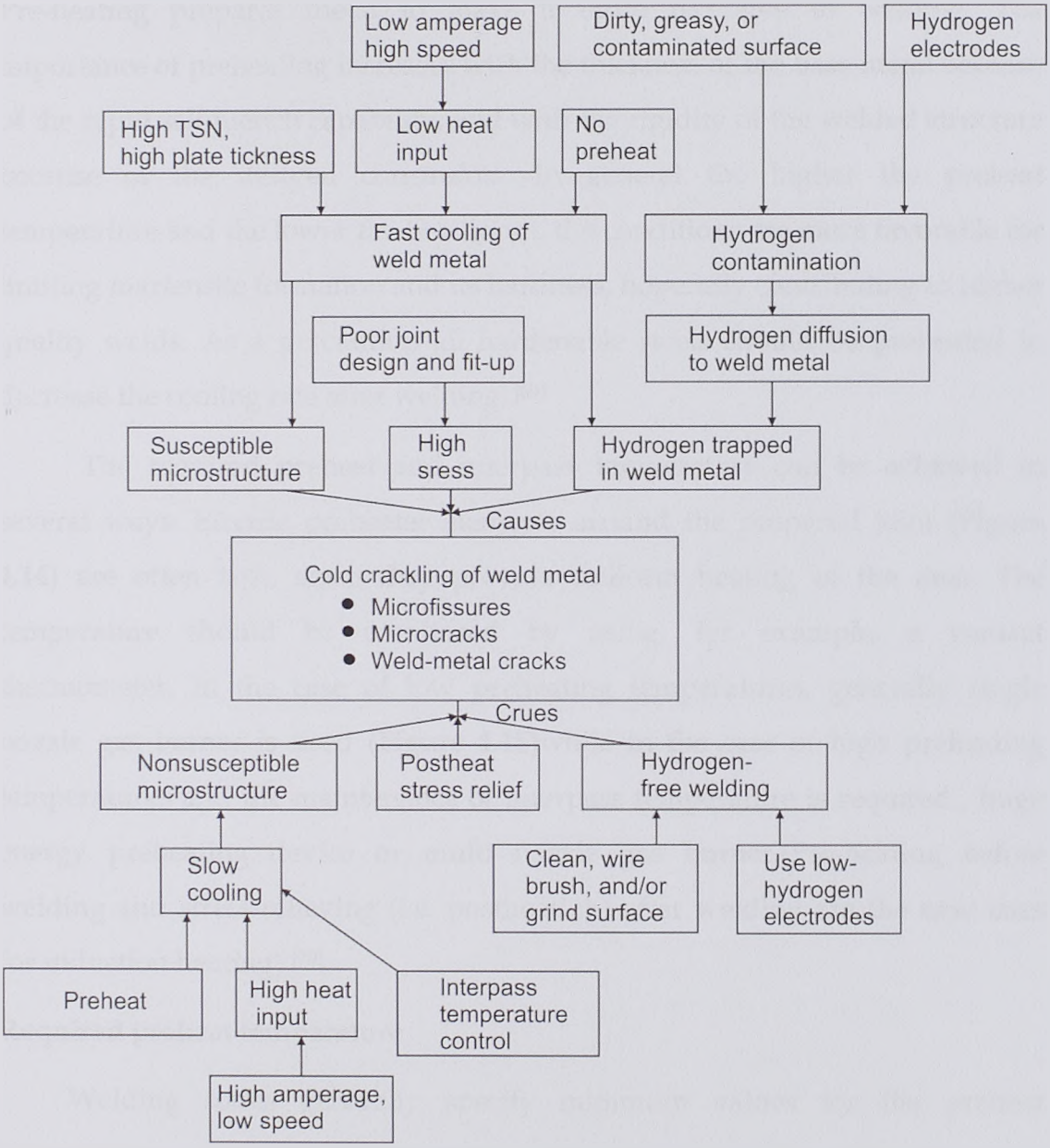

Figure 4.13 Causes and cures of cold cracking of weld metal. [5]

Preheating [69, 70, 71, 72]

The operation of heating metal to some predetermined temperature before engaging in actual welding is called preheating. The details and the modes may be different in various situations but in general the purpose is to influence the cooling behavior after welding so that shrinkage stresses will be

lower (relative to welding without preheating) and cooling rate will be milder. Pre-heating prepares metal to make it more receptive to welding. The importance of preheating increases with the thickness of the base metal because of the rapid selfquench capability, and with the rigidity of the welded structure because of the derived constraints. In general the higher the preheat temperature and the lower the heat input, the conditions are more favorable for limiting martensite formation and its hardness, hopefully contributing to higher quality welds. As a precaution all hardenable steels should be preheated to decrease the cooling rate after welding. [69]

The required preheat and interpass temperature can be achieved in several ways. Electric preheater elements around the prepared joint (**Figure 4.14**) are often best, since they provide uniform heating of the area. The temperature should be monitored by using, for example, a contact thermometer. In the case of low preheating temperatures, generally single nozzle gas burner is used (**Figure 4.15**)while in the case of high preheating temperatures and the maintenance of interpass temperature is required , huge energy preheating device or multi nozzle gas burner.(Pre-heating before welding and stress-relieving (i.e. postheating) after welding are the new uses for induction heating).[70]

Required preheat temperature

Welding codes generally specify minimum values for the preheat temperature, which may or may not be adequate to prohibit cracking in every application. For example, if a beam-to-column connection made of ASTM A572-Gr50 jumbo sections (thicknesses minimum prequalified preheat of (107°C) is required (AWS D1.1-96, Table 3.2).

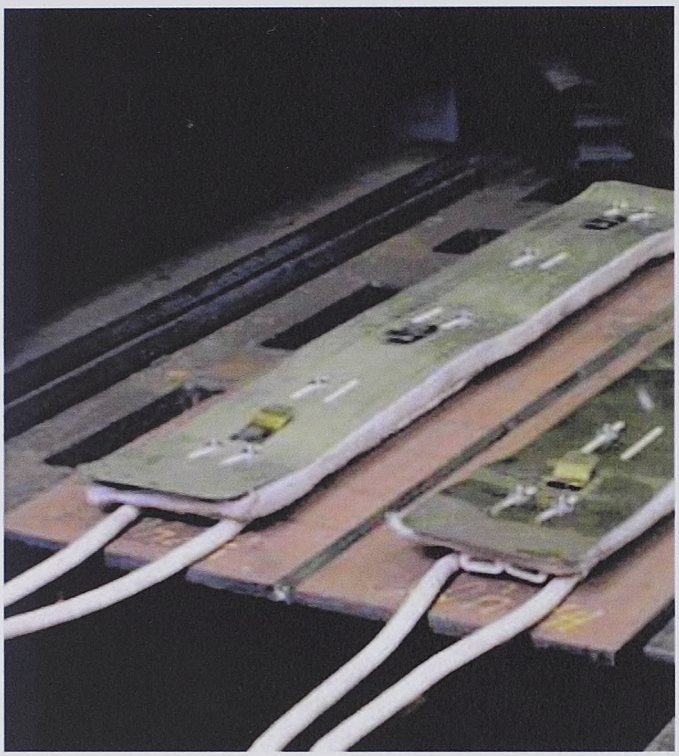

Figure 4.14 Electric preheater elements aroundthe prepared joint. [70]

Figure 4.15 Single nozzle gas burner preheating of longseam pipe.[71]

When no welding code is specified, and the need for preheat has been established, how does one determine an appropriate preheat temperature?

Consider an approach outlined in the American Welding Society's Structural Welding Code, AWS D1.1, Annex XI: "Guideline on Alternative Methods for Determining Preheat." Two procedures are presented for establishing a preheat temperature. These techniques, developed primarily from laboratory cracking tests, are beneficial when the risk of cracking is increased due to the chemical composition, a greater degree of restraint, higher levels of hydrogen or lower welding heat input. [72]

However, beside those methods suggested by the AWS there are many other methods to estimate the necessary minimum preheating temperatures. For instance the chart method developed by Nippon Steel [73] for selecting the critical preheat temperature for specific steels and called the master curve method by the authors is described below.

The first issue is what to select as carbon equivalent. The CEN was adopted in this method. In **Figure 4.16**, the critical preheat temperature determined for various steels in the y-groove weld cracking test are compared with the carbon equivalents calculated by Nippon Steel authors. Among the three carbon equivalents (CE(IIW), P_{cm} and CEN), the CEN is shown to have the best correlation with the critical preheat temperature. This is the reason for adopting the CEN.

The second issue is what preheat temperature to select. Nippon Steel Corporation authors, made it possible to predict the critical preheat temperature by the y-groove weld cracking test specified in JIS Z 3158. The reason is that steel manufacturers and many steel users often refer to the results of the y-groove weld cracking test when determining the critical preheat temperature in their actual welding operations. Of course, the critical preheat temperature determined by the y-groove weld cracking test depends on welding heat input and hydrogen content. The experimental procedure first predicted the critical preheat temperature under the standard conditions of 1.7 KJ/mm heat input and 5mm/100g hydrogen content. **Figure 4.17** Shows the

relationship between the CEN calculated from the experimental data of various steels and the critical preheat temperature determined by the y-groove weld cracking test. The critical preheat temperature varies with the plate thickness, because the restraint intensity of the specimen varies with the plate thickness. **Figure 4.17** Shows curves that constitute the base of this selection procedure. In that sense, these curves are named the master curves.

The effect of the heat input and hydrogen content is expressed as a change in the CEN (ΔCEN). This method is similar to BS 5135. When the actual heat input and hydrogen content are different from the standard conditions, this method determines which standard condition they correspond to **Figures. 4.18** and **4.19** show the curves to determine the ΔCEN when the heat input and hydrogen content are different from the standard conditions. The cold cracking susceptibility of the HAZ is strongly influenced by its hardness and hardnenability. When high-hardnenability steel is welded, the HAZ microstructure becomes predominantly martensitic even if the heat input changes to some extent. When lower-hardenability steel is welded, the heat input has important bearings as it changes the bainite volume fraction. In **Figure 4.19**, the X-axis is a logarithmic plot. This is because the effect of hydrogen on cold cracking susceptibility is logarithmic. When **Figure 4.19** was prepared, this fact confirmed from experimental results. **Figures 4.17 to 4.19** can be used to predict the critical preheat temperature in the y-groove weld cracking test.

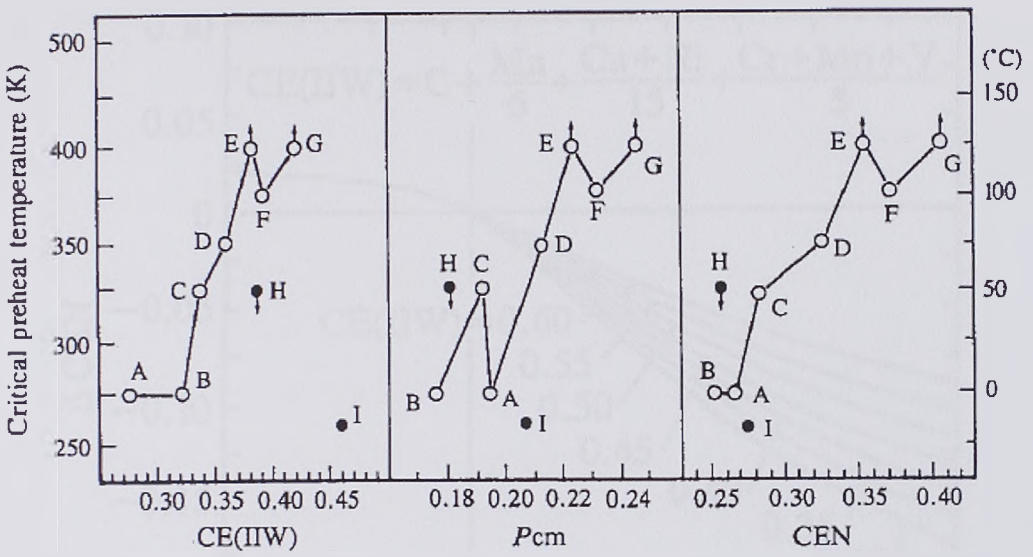

Figure 4.16Relationship between carbon equivalents and critical preheat temperature (y-groove weld cracking test).[73]

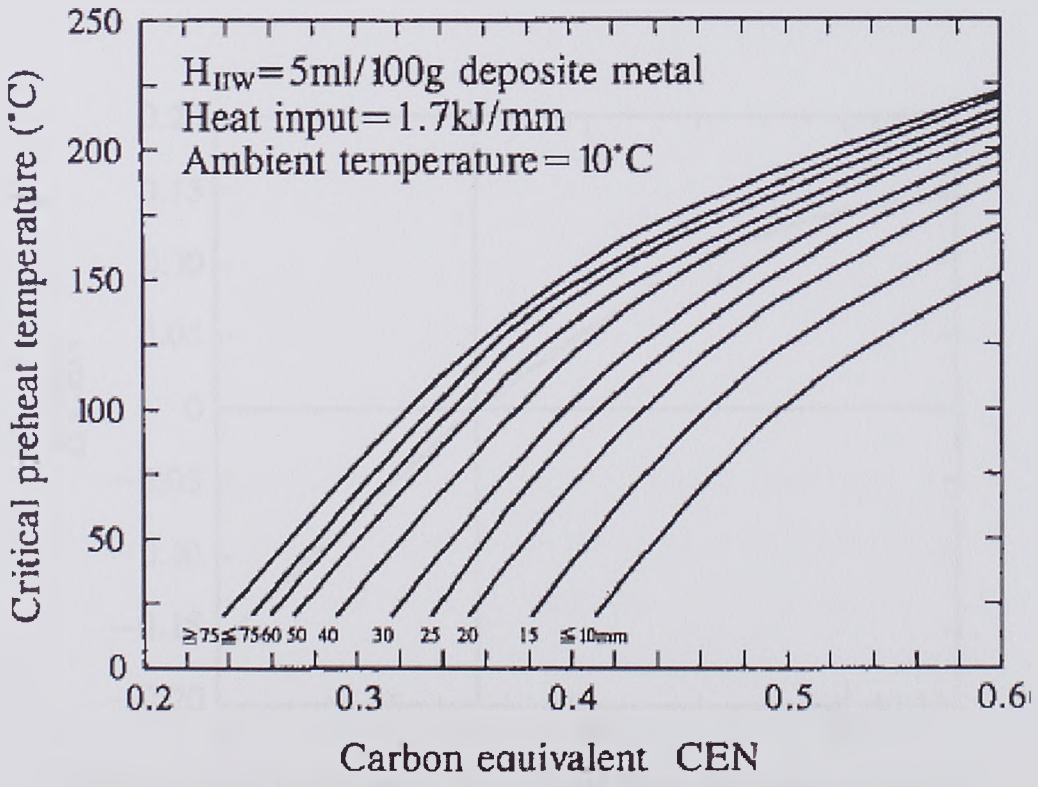

Figure 4.17Relationship between weld metal hydrogen content and ΔCEN.[73]

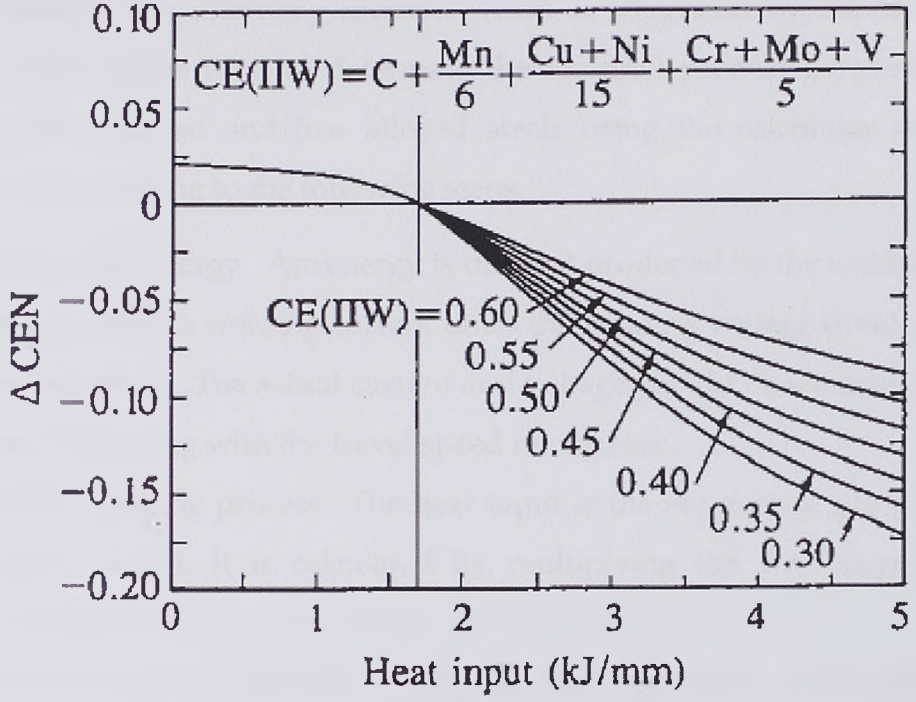

Figure 4.18 Relationship between heat input and ΔCEN.[73]

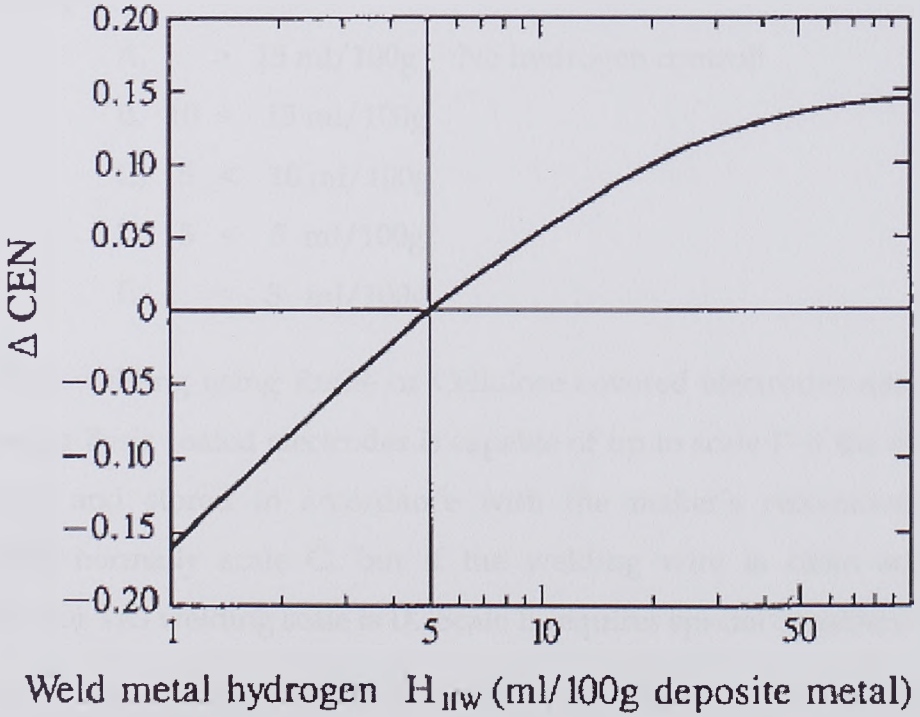

Figure 4.19 Master curves in preheat temperature prediction method.[73]

However the following method which is suggested by the mentioned reference [74] can be used to determine the required preheat temperature for welding non alloyed and low alloyed steels using the calculator shown in **Figure 4.20** according to the following steps:

1. Enter Arc Energy. Arc energy is the heat produced by the welding arc; it is equal to the welding current times the welding voltage divided by the travel speed. The actual current and voltage should be measured during welding along with the travel speed in mm/sec.
2. Select welding process. The heat input is the arc energy going into the parent metal. It is calculated by multiplying the Arc energy by an efficiency factor specific to the welding process.
3. Enter Carbon Equivalent. The CE must be based on the IIW. The program will calculate it for you if the base metal composition is known.
4. Select Hydrogen Scale. Diffusible hydrogen content is split into 5 groups:

   A, > 15 ml/100g No hydrogen control!
   B, 10 < 15 ml/100g
   C, 5 < 10 ml/100g
   D, 3 < 5 ml/100g
   E, < 3 ml/100g

MMA welding using Rutile or Cellulose covered electrodes use scale A. MMA using Basic coated electrodes is capable of up to scale D if the electrodes are baked and stored in accordance with the maker's recommendations. MIG/MAG normally scale C, but if the welding wire is clean scale D is possible. For TIG welding scale is D. Scale E requires special consideration.

5. Enter the combined thickness of the joint. Consider the thickness of all paths taking heat from the weld. For example: The combined thickness for a butt weld between two plates of the same thickness will be twice the base metal thickness, for a T fillet weld three times the thickness.

6. When all data has been correctly entered click the calculate preheat button.

Figure 4.20 Preheat temperature calculator[74]

4.1.5 Testing of Cold Cracking Sensitivity[5, 75, 76, 77, 78]

A range of mechanical tests is available to measure the HIC susceptibility of weldments produced by a given process or consumable. Each test has a bias toward producing either HAZ or weld metal cracking and will affect the orientation of cracking. This is due to the geometry of the test and the resulting stresses imposed on the weldment. [75]

Y-Groove (Tekken test)[76]

Specimens

Test assembly configuration is shown in **Figure 4.21**. All weld joint surfaces shall be machined to 4 micrometers R3 minimum. When it is possible to identify the rolling direction of the material being tested, the parts should be cut and assembled with the rolling direction perpendicular to the weld groove, unless otherwise specified.

The test assembly is fabricated by depositing welds on each end of the weld groove to provide the necessary restraint, as shown if **Figure 4.21**. Section A-A. Low-hydrogen type mild steel filler metal is normally used. Welds shall be deposited by a suitable welding process, using a deep penetrating arc and a weave-bead technique to fill the joints with a minimum number of weld beads. Care shall be taken to minimize angular distortion during welding. Weld reinforcement should be approximately 2 mm. Maximum inter pass temperature should be in accordance with steel manufacturers recommendations as applicable to the steel type being joined.

Each test assembly shall be dimensionally inspected after cooling to ensure the proper configuration as shown in **Figure 4.21**, section B-B. The groove root opening dimension shall be within tolerance.

Fabricate a minimum of three test assemblies per set.

Procedure

1. All welding shall be performed in the flat position.

2. Test assemblies shall be uniformly heated in an oven, to a temperature slightly higher than the desired preheat temperature. The test assembly is removed from the oven and the surface temperature near the bevel area shall be monitored. Welding shall begin when the desired preheat temperature is reheated.

3. The single-pass test weld shall be deposited as shown in **Figure 4.22**. Welding technique which promote good fusion and crater fill shall be employed. Following welding, the assembly shall be allowed to cool in still air. It shall be left at ambient temperature for a minimum period of 48 hours before examination for cracks.

4. The test weld area shall be examined for surface cracks. If surface cracks are visible, no further examination is required. If cracking is not visible, the weld shall be sectioned and examined microscopically.5. When sectioning is required, the test should be sectioned at the one-fourth length positions. Water-cooled mechanical means shall be used to section the test welds. Assemblies shall be securely clamped in such a manner that the cutting process does not contribute to weld root cracking. Sectioned specimens shall be polished, etched and examined at 20X for cracks.

6. When the test is used to evaluate susceptibility to hydrogen cracking, a diffusible hydrogen determination shall be performed for each welding process and consumable in accordance with AWS A4.3. The diffusible hydrogen determination shall be performed under the same conditions as the test weld. However the test data should be recorded as a report on a Test Result Sheet similar to **Table 4.2**.

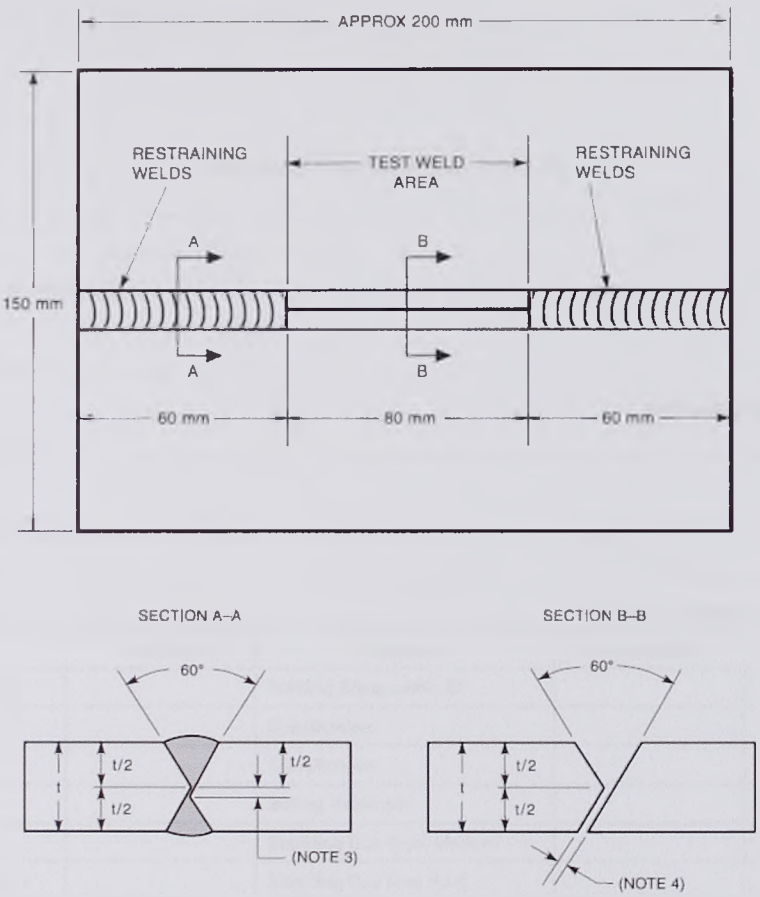

Figure 4.21Oblique Y-groove test assembly. [76]

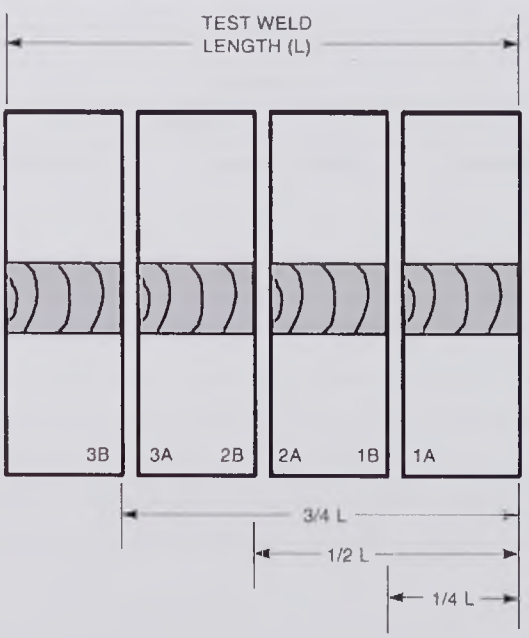

Figure 4.22Sectioning of test plat.[76]

Table 4.2Oblique Y-groove test results.[76]

AWS B4.0M:2000

OBLIQUE Y-GROOVE TEST RESULTS

Company Name _____ Date _____

Job/Test No. _____ Sheet _____ of _____

Description of Investigation _____

Material Identification _____

Material Thickness _____ Rolling Direction Indicated Y / N

Material Heat Treatment _____

Applicable Welding Procedure No. _____

Welding Details _____ Process _____

Date of Welding _____ Time Lapse—Welding to Testing (hrs) _____

Parameters	Test Weld	Parameters	Anchor Weld	Test Weld
Electrode/Wire Dia.		Welding Consumable ID		
Amperage		Specification		
Voltage		Classification		
Polarity		Baking Treatment		
Travel Speed		Shielding Gas Type, Medium		
Preheat Temperature		Shielding Gas Dew Point		
Heat Input		Max. Interpass Temp.		
Humidity (RH)		Measuring Method		
Ambient Temp.				
Hydrogen Determination Method		Date	Result	
EXAMINATION				
	Surface		Section	
Assembly No.	Inspection Method	Results (C or NC)	Inspection Method	Results (C or NC)

No. of Test Assemblies Inspected _____ Total % Cracking _____

Remarks _____

Tested By _____

Signature _____ Date _____

Gapped bead on plate test

The GBOP test piece is made up of two blocks, one of which has machined recess on one face (**Figure 4.23**). The blocks are clamped together (**Figure 4.24**) so that the machined recess forms a slot between the two blocks. It provides a good measure of the resistance to transverse weld metal cracking. However Figure 4.25 shows the GBOP test sectioning. [75]

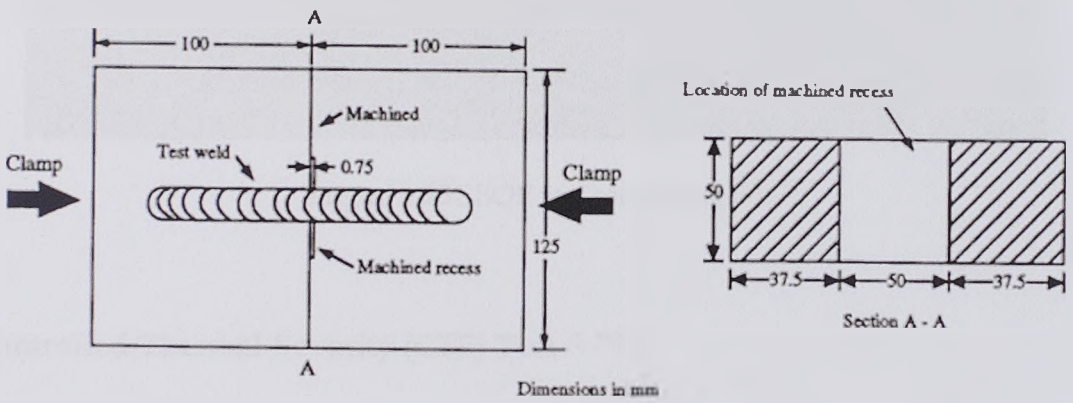

Figure 4.23Schematic of the GBOP test specimen.[75]

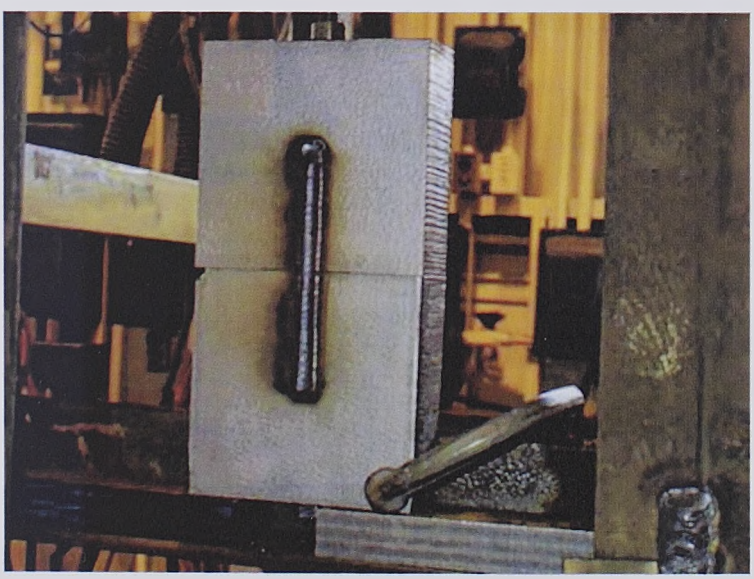

Figure 4.24 GBOP clamped blocks.[77]

Figure 4.25GBOP test sectioning.[77]

Controlled-Thermal-Severity (CTS) Test [5, 78]

The CTS[5] test (Controlled Thermal Severity BS 7363 1990) is based on the principle of the fillet joint and serves for a selection of optimum welding parameters and also as a test of quality of the base material (e.g. for admissible hardness value). The test plate (**Figure 4.26**), 35 mm thick is made up of two asymmetrically screwed sections mechanically shaped straight. An auxiliary weld is made from two or three sides on several layers. When it cools and the screw is tightened, the test weld itself is made in one or two sides, 4-6 mm in thickness and 75 mm in length. Susceptibility to cracking grows with the increasing gap between the plates; therefore a backing strip is often placed between the two plates whereby the gap in the fillet weld is enlarged. With this test, occur in the underbead zone or in the weld metal. The test weld can be sectioned into samples minimally 72 h after completion. Each specimen is assigned a thermal severity number (TSN) according to plate thickness-using equations (4.1.2) & (4.1.3). For bithermal welds:

$$TSN = 4(t + b) \qquad (4.1.2)$$

Where: t and b are the thickness of the top and bottom plates, respectively. For trithermal welds

$$TSN = 4(t + 2b) \qquad (4.1.3)$$

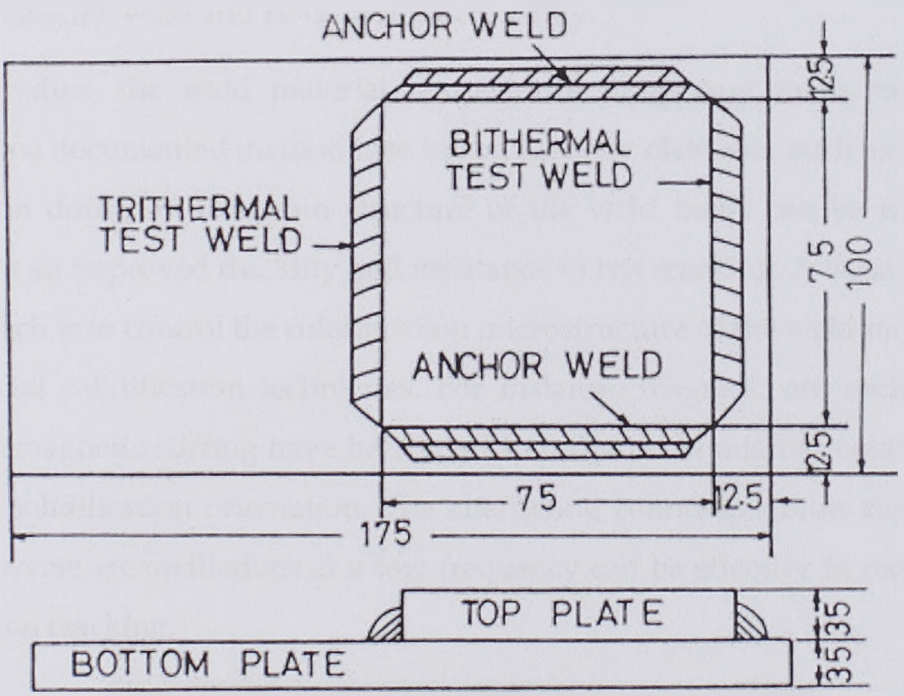

Figure 4.26CTS test assembly (dimensions in mm).[78]

A series of plate thickness, which provide varying cooling rates, are tested. The crack susceptibility of the base-metal filler material (welding wire or electrode) combination is determined by the minimum TSN that produces cracking. Controlled-thermal-severity testing is used to measure the cold crack sensitivity of steels under cooling rates controlled by the thickness of the plates and the differences in cooling rates between bithermal and trithermal welds. This test is primarily used to evaluate the crack sensitivity hardenable steels. [5]

Hot Cracking [79, 80]

Hot cracking (**Figure 4.27**) has been a subject of intensive studies over the last few decades. Hot cracking occurs during the solidification process due to a combination of metallurgical behavior on cooling and the surrounding thermomechanical conditions. In general, two basic approaches are usually taken: 1) improving the weld and heat-affected zone (HAZ) material ductility and 2) improving the thermomechanical conditions during welding. Historically, the majority of the research work has been focused on the former, i.e., improving the weld and HAZ material ductility.

To reduce the weld material temperature range and to increase its ductility, one documented method is to introduce alloy elements, such as Ti, Zr, V and B. In doing so, the grain structure of the weld metal can be refined, resulting in an improved ductility and resistance to hot cracking. A variation of this approach is to control the solidification microstructure of the weld metal by using special solidification techniques. For instance, magnetic arc oscillation and electromagnetic stirring have been used to refine weld microstructure and to change solidification orientation. The alternating columnar grains resulting from transverse arc oscillations at a low frequency can be effective in reducing solidification cracking.

Figure 4.27 Hot crack in welded joint.[80]

Lamellar Tearing [5, 81]

Lamellar tearing can occur beneath the weld especially in rolled steel plate which has poor through-thickness ductility. Lamellar tearing was observed in the construction of buildings, metal structure bridges, in the manufacture of pressure vessels, ships and nuclear equipment. Typically, the cracks appear in solders of several passes in the joints angle in T or L and they are always associated with points high stress concentration (**Figure 4.28**). The surface of the fracture is fibrous with long parallel sections which are indicative of low parent metal ductility in the through-thickness direction, (**Figure 4.29**)

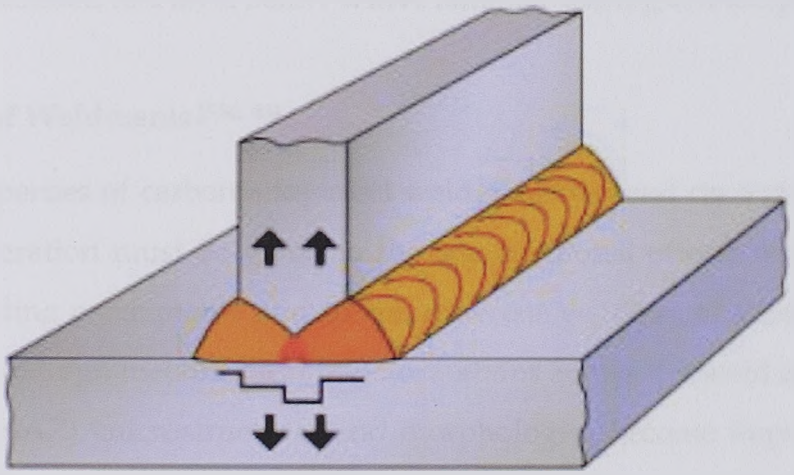

Figure 4.28lamellar tearing in T butt weld. [81]

Figure 4.29Appearance of fracture face. [81]

To avoid lamellar tearing the following steps should be taking in consideration:

- Use plate material with improved through-thickness properties. A reduction in oxygen content or a reduction in sulfur content will reduce the amount of inclusions in the steel.
- Change the joint design to minimize through-thickness contraction stresses.
- Use lower-strength welding consumables. This will absorb and reduce some of the through-thickness stress.
- In extreme cases, the surface of the plate may be ground or machined to a level below where lamellar tearing is anticipated. [5]

4.2 Properties of Weldments [5,82, 83]

The properties of carbon alloy steel weldments depend on a number of factors. Consideration must be given to the compositional effects of the base metal and welding consumable and to the different welding processes used. Because steels undergo metallurgical transformations across the weld and heat-affected zone (HAZ), microstructures and morphologies become important. A wide range of microstructures depend on energy input, preheat, metal thickness, weld bead size, and reheating effects due to multipass welding. As a result of their different chemical compositions and weld inclusions (oxides and sulfides), weld metal microstructures are usually significantly different from those of HAZ and base metal. Similarity, properties across the weld zone can also vary. The influences of welding processes, welding consumables, and welding parameters on the weldment properties are emphasized. The service properties of weldments in corrosive environments and subjected to cyclic loading are also considered. [5]

4.2.1 Effect of Alloying Elements [83]

About twenty different elements are used in various proportions and combinations in the manufacture of both carbon and low alloy structural steels. Some are used because they impart specific properties to the steel when they alloy with it (i.e. dissolve in the iron), or when they combine with carbon, wholly or in part, to form compounds known as carbides. Others are used because they are beneficial in ridding the steel of impurities or rendering the impurities harmless. Still another group is used to counteract harmful oxides or gases in the steel. The elements of this last group act only as fluxes or scavengers and do not remain in the steel to any extent after solidification occurs. Some elements fall into more than one of the above groups. However the effects of some of the more common alloying elements are as follows:

Aluminum is often used to promote nitriding but its major use in steel making is as a deoxidizer. It may be used alone, as in low carbon steels where exceptional drawability is desired, or more commonly in conjunction with other deoxidizers. It effectively restricts grain growth and its use as a deoxidizer to control grain size is widely practiced in the steel industry.

Carbonalthough not generally considered an alloying element, is by far the most important element in steel. As carbon, is added to steel up to about 90 percent, its response to heat treatment and its depth of hardening increase. In the "as- rolled" condition, increasing the carbon content increases the hardness, strength and abrasion resistance of steel but ductility, toughness, impact properties and machinability decrease.

Chromium contributes to the heat treatment of steel by increasing its strength and hardness. Its carbides are very stable and chromium may be added to high carbon steels subject to prolong anneals to prevent graphitization. Chromium increases resistance to both corrosion and abrasion. Chromium steels maintain strength at elevated temperatures.

Columbiumis used in carbon steels to develop higher tensile properties. It also combines with carbon to provide improved corrosion resistance, and is often used for this purpose in stainless steels.

Iron is the principal element and makes up the body of steel. In commercial production iron always contains quantities of other elements. Production of pure iron is accomplished with difficulty and generally in small quantities. Iron does not have great strength, is soft, ductile and can be appreciably hardened only by cold work.

Manganeseby its chemical interaction with sulphur and oxygen makes it possible to roll hot steel. It is next in importance to carbon as an alloying element. it has a strengthening effect upon iron and also a beneficial effect upon steel by increasing its response to heat treatment. It increases the machinability of free machining steels but tends to decrease the ductility of low carbon drawing steels.

Molybdenum has a pronounced effect in promotion of hardenability. It raises the coarsening temperature of steel, increases the high temperature strength, improves the resistance to creep and enhances the corrosion resistance of stainless steels.

Nickel is soluble in iron and, in combination with other elements, improves the hardenability of steel and toughness after tempering. It is especially effective in strengthening unhardened steels and improving impact strength at low temperatures. It is used in conjunction with chromium in stainless steels.

Phosphorus strengthens steel but reduces its ductility. It improves the machinability of high sulphur steels and under some conditions may confer some increase in corrosion resistance. Silicon is one of the principal steel deoxidizers and is commonly added to steel for this purpose. In amounts up to about 2.5% it increases the hardenability of steels. Specified coarse grain steels

are silicon killed. In lower carbon electrical steels, silicon is used to promote the crystal structure desired in annealed sheets.

Sulphur added to steel increases machinability. Because of its tendency to segregate, sulphur may decrease the ductility of low carbon drawing steel. Its detrimental effect in hot rolling is offset by manganese.

Titaniumis an extremely effective carbide former and is used in stainless steels to stabilize the steel by holding carbon in combination. Titanium is used for special single coat enameling steels. In low alloy structural steels its use in combination with other alloys promotes fine grain structure and improves the strength of the steel in the "as-rolled" condition.

Vanadiumis a mild deoxidizer and its addition to steel results in a fine grain structure which is maintained at high temperature. It has very strong carbide forming tendencies and very effectively promotes strength at high temperatures; vanadium steels have improved fatigue values and excellent response to heat treatment. In unhardened steels it is particularly beneficial in strengthening the metal.

4.2.2 Controlling Toughness in the HAZ [5]

Unlike face-centered cubic metals, which are ductile at all temperatures, body-centered cubic metals such as steel undergo a ductile-to-brittle transition at a temperature that is substantially influenced by metallurgical factors, including microstructure, grain size, carbon and alloy content, and inclusion content. Unexpected brittle behavior in an engineering structure because of this transition could cause a catastrophic failure.

Microstructure, Excellent toughness can be achieved in steel weld metal if the microstructure is essentially acicular ferrite with only a trace of grain-boundary ferrite, minimal bainite, and no martensite. Unless the carbon content is extremely low, fully bainitic and/or martesitic structures must be avoided.

The grain size and oxide inclusion content should be as minimal as welding conditions permit.

Welding process, The prior-austenite and acicular ferrite grain sizes are small and the inclusion content is negligible in welds deposited by the gas-tungsten arc, shielded metal arc, and gas-metal arc welding processes. Therefore, these methods are the best means of obtaining welds with excellent toughness in the as-welded condition (**Figure 4.30**). The HAZ toughness values of the resulting welds are generally good because of the fine HAZ grain size, characteristic of low-heat-input welding methods.

Hardness, levels are lowest for high heat inputs, such as those produced by submerged arc weldments, and are highest for low-energy weldments (with faster cooling rates) made by the shielded metal arc process. Depending on the welding conditions, weld metal microstructures generally tend to be fine grained with basic flux and somewhat coarser with acid or rutile (TiO_2) flux compositions.

4.2.3 Filler Metal - Low hydrogen [5, 67, 84]

When selecting filler metalsthe specifier may elect to require "low hydrogen electrodes." Such electrodes may be required to minimize the possibility of hydrogen related cracking. In some cases the engineer may specify low hydrogen electrodes because he believes these electrodes will also provide weld deposits exhibiting a high minimum level of notch toughness. While this may be true, it cannot be assumed.

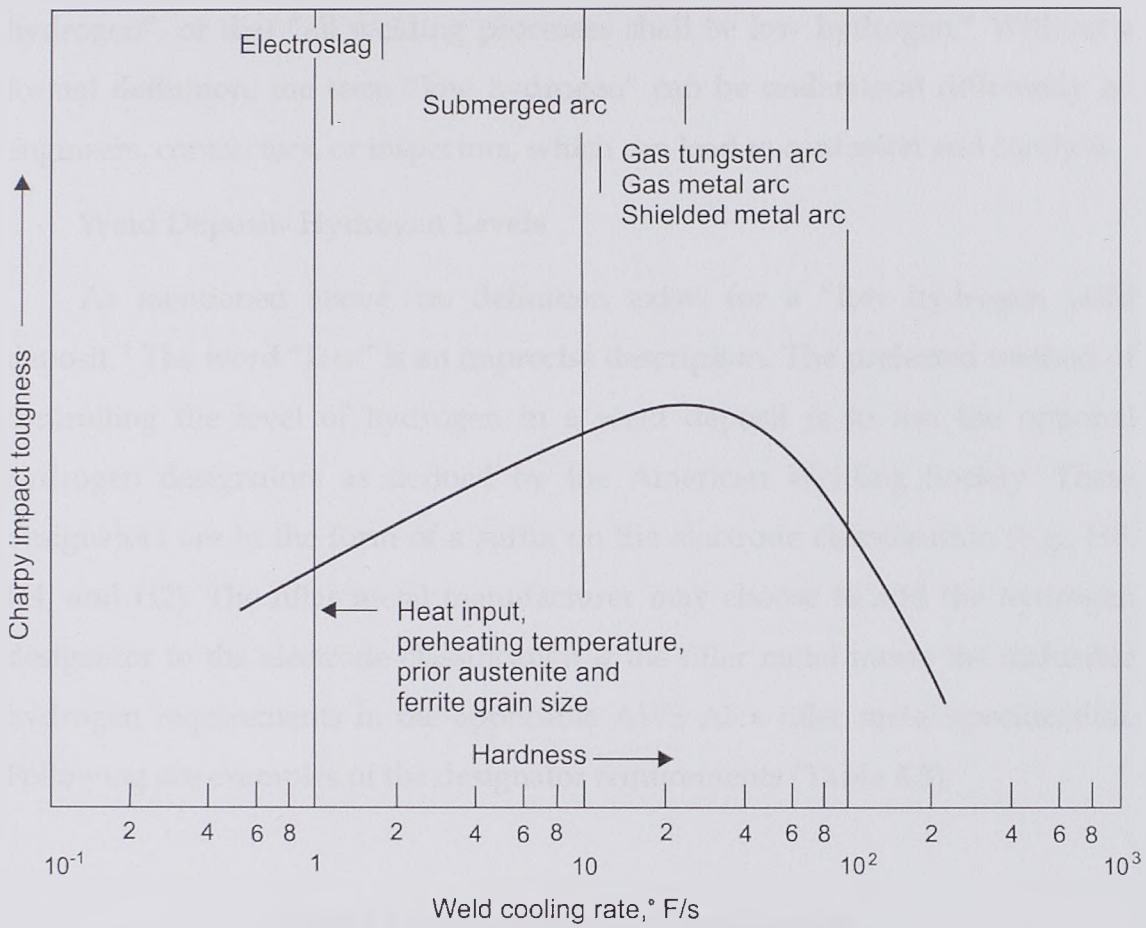

Figure 4.30Effect of welding process on weld metal toughness for low-alloy steels.[5]

However, the term "low hydrogen" has been around for about 60 years. It was first introduced to differentiate this classification of shielded metal arc welding (SMAW) electrode (e.g., E7018) from other non-low hydrogen SMAW electrodes (e.g., E6010). They were created to avoid hydrogen cracking on high strength steels, such as armor plate.

Although so-called "low hydrogen electrodes" have been around for many years, there is some confusion about what is meant by the term. Many codes and specifications use the designation, however, neither "low hydrogen" nor "low hydrogen electrodes" are listed in the American Welding Society's (AWS) Standard Welding Terms & Definitions (AWS A3.0-94)2.This may come as a surprise to some, especially to engineers that have been specifying that "only low hydrogen electrodes shall be permitted," or "all welds shall be low

hydrogen", or that "all welding processes shall be low hydrogen." Without a formal definition, the term "low hydrogen" can be understood differently by engineers, contractors, or inspectors, which can lead to confusion and conflicts.

Weld Deposit- Hydrogen Levels

As mentioned above, no definition exists for a "low hydrogen weld deposit." The word "low" is an imprecise description. The preferred method of controlling the level of hydrogen in a weld deposit is to use the optional hydrogen designators as defined by the American Welding Society. These designators are in the form of a suffix on the electrode classification (e.g., H8, H4, and H2). The filler metal manufacturer may choose to add the hydrogen designator to the electrode classification if the filler metal meets the diffusible hydrogen requirements in the applicable AWS A5.x filler metal specification. Following are examples of the designator requirements (**Table 4.3**):

Table 4.3 Optional Hydrogen Designators [84]

	Diffusible Hydrogen, mL/100g
H8	8
H4	4
H2	2

The use of a filler metal is common in many fusion welding processes. To select the proper filler metal/electrode, the primary considerations are whether the weld metal can be produced defect-free and whether the weld metals are compatible with the base metal and can provide satisfactory properties. These characteristics are determined by the:

- Chemistry of the electrodes
- Dilution of the base metal

- Flux system or shielding gas
- Weld-pool solidification and subsequent cooling and transformation [5]

The strength of the weld metal is improved not by increasing the carbon content, but by adding the alloying elements that provide solid-solution or precipitation strengthening and modification of the microstructures.

The selection of the proper filler metal is based not on the chemistry of the base metal, but rather on matching the weld metal and base metal service properties. Using a filler metal with chemistry identical to that of the base metal may not provide the desired results, because the microstructures of the weld metal are entirely different from those of the base metal. For most carbon and low-alloy steels, the solidification and rapid cooling rate involved in fusion welding result in a weld metal that has higher strength and lower toughness than that has higher strength and lower toughness than the base metal when they are of the same chemistry. Consequently, the filler metal often contains a lower carbon. The weld metal microstructure in carbon and low-alloy steels contains a variety of constituents, ranging from blocky ferrite to acicular ferrite to bainite to martensite.

The considerations governing the choice of filler metals for welding HSLA steels are often very similar to those for welding structural carbon steels, except that it is necessary to use low-hydrogen welding practices with HSLA steel. The amount of hydrogen carried by the filler metal to the weld pool should be evaluated with reference to the carbon equivalent (CE) and composition parameter (P_{cm}). Additional consideration must be given to choose an arc electrode and procedure that will provide adequate levels of notch toughness in both the weld metal and the (HAZ). For all of the commonly used arc welding processes, filler metals are available that can produce weld metal with various levels of notch toughness. Suggested electrodes for arc welding several HSLA

steels for structural and pressure-vessel applications are available (examples of consumables are given in **Table 4.4**).[5]

Table 4.4Examples of welding consumables, AWS class. [67]

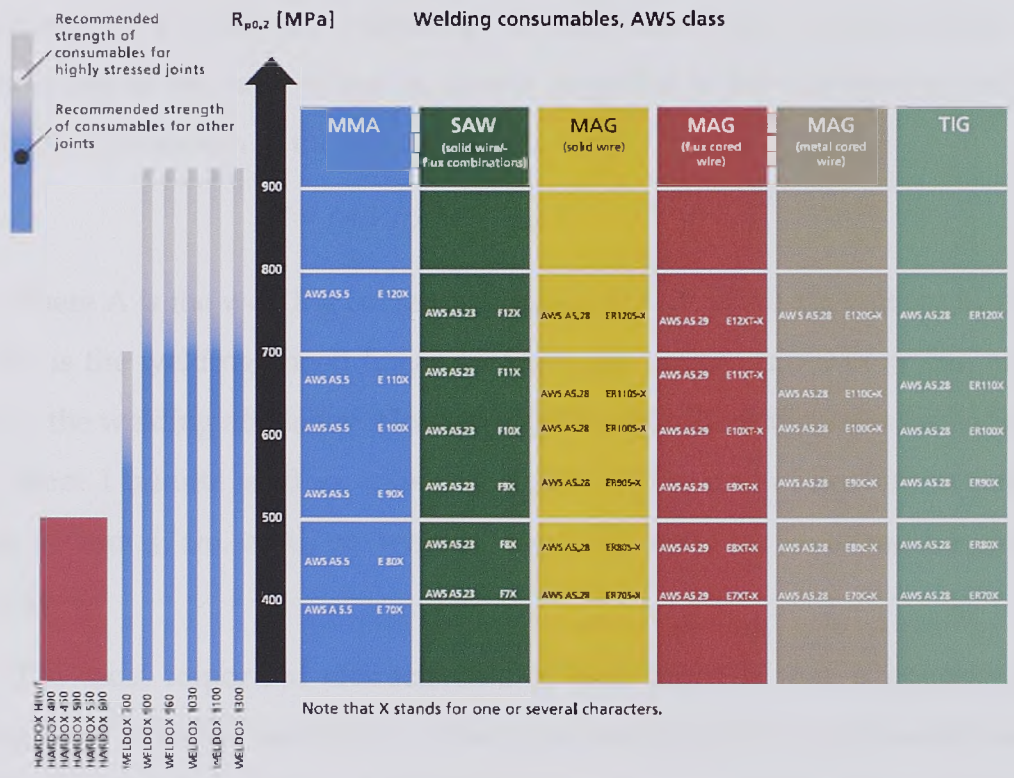

However, the hydrogen content should be lower than or equal to 5 ml of hydrogen per 100 g of weld metal when welding with unalloyed or low alloyed welding consumables. Solid wires used in MAG and TIG welding can produce these low hydrogen contents in the weld metal. The hydrogen content for other types of welding consumables can best be obtained from the respective manufacturer. If consumables are stored in accordance with the manufacturer's recommendations, the hydrogen content will be maintained at the intended level. This applies, above all, to coated consumables and fluxes. [67]

Heat Input [85]

Heat input can be referred to as "the electrical energy supplied by the welding arc to the workpiece." In practice, however, heat input can approximately (if the arc efficiency is not taken into consideration) be characterized as the ratio of the arc power supplied to the electrode to the arc travel speed, as shown in the following equation:

$$HI = (A.V.\eta)/WS \quad (4.2.1)$$

Where A is the welding current in amperes (A),V is the arc voltage in volts (V), WS is the welding speed linear measure per minute (m/min or cm/min), and η is the welding efficiency. However "60" standardizes the units for "A" and "WS," since 1 minute is 60 seconds). . In this way, the unit of heat input can be J/mm, kJ/mm, J/cm, or kJ/cm where "J" and "kJ" stand for Joule and kilo-Joule respectively.

The most important characteristic of heat input is that it governs the cooling rates in welds and thereby affects the microstructure of the weld metal and the heat affected zone. A change in microstructure directly affects the mechanical properties of welds. Therefore, the control of heat input is very important in arc welding in terms of quality control. **Figure 4.31** shows how heat input affects the cooling rates in welds. This figure suggests that the effect of heat input on the cooling rate is more significant in lower heat input ranges at every preheating temperature when the plate thickness is kept constant.

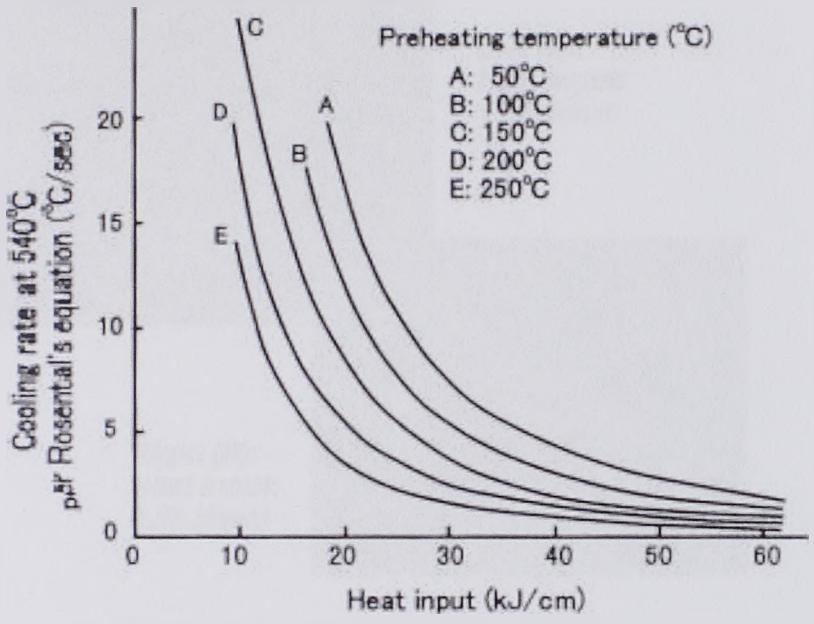

Figure 4.31The effect of heat input on cooling rates in welds as a function of preheating temperatures (Plate thickness: 19mm). [85]

However **Figure 4.32** shows the use of higher heat input (A: 2.5kJ/mm) causes more coarse microstructure when compared with lower heat input (B: 1.0kJ/mm). This marked difference in microstructure results in significant effect on the strength of welds as shown in **Figure 4.33**.

4.3 Welding of HSLA Steel [5, 61]

High strength low alloy steels can be welded by the entire commonly used arc welding processes (**Figure 4.34**). Shielded metal arc, gas metal arc, flux cored arc, and submerged arc welding are used for most applications. Low hydrogen practices should be employed with all processes when carbon equivalents values indicate susceptibility towards cracking. High heat- input welding processes such as electroslag, and multiple-wire-submerged arc can be used to weld these steels. However, the advantage of their use warrants careful evaluation where notch toughness in the weld metal and HAZ is a requirement. Resistance spot seam, projection, upset, or flash welding also can join the HSLA steels. [5]

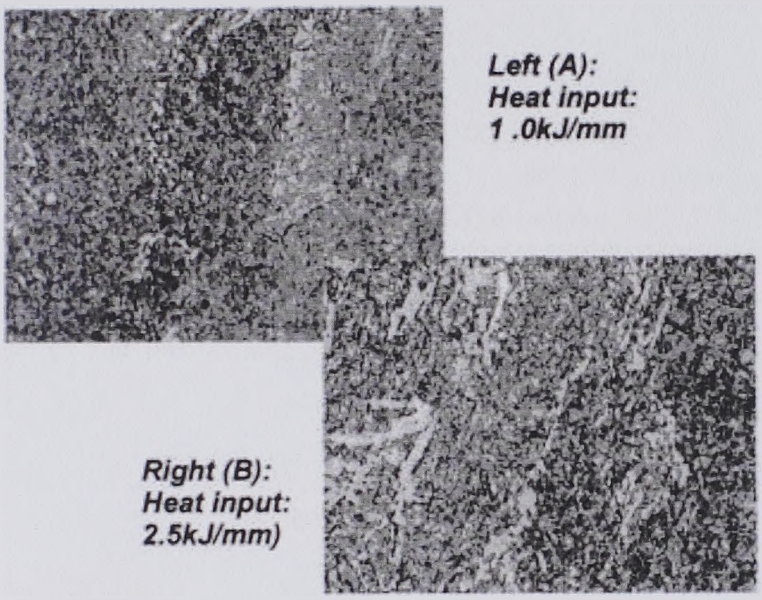

Figure 4.32A comparison of microstructures of gas metal arc welded all-deposited metals of an ER80S-G trial wire, using two different amounts of heat input (×400) (Source c. XII-1647-00, 2000).[85]

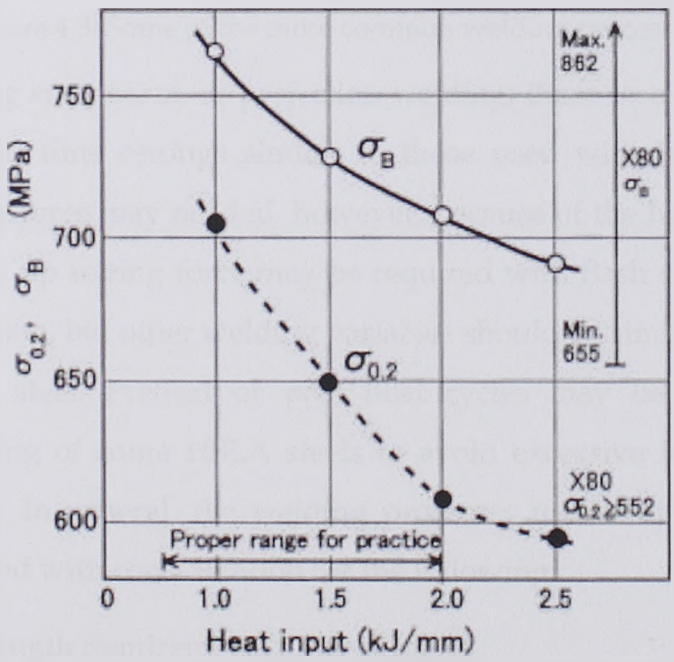

Figure 4.33The effect of heat input on strength of all - deposited metals of an ER80S-G trial wire in gas metal arc welding (Source: IIW Doc. XII-1647-00, 2000).[85]

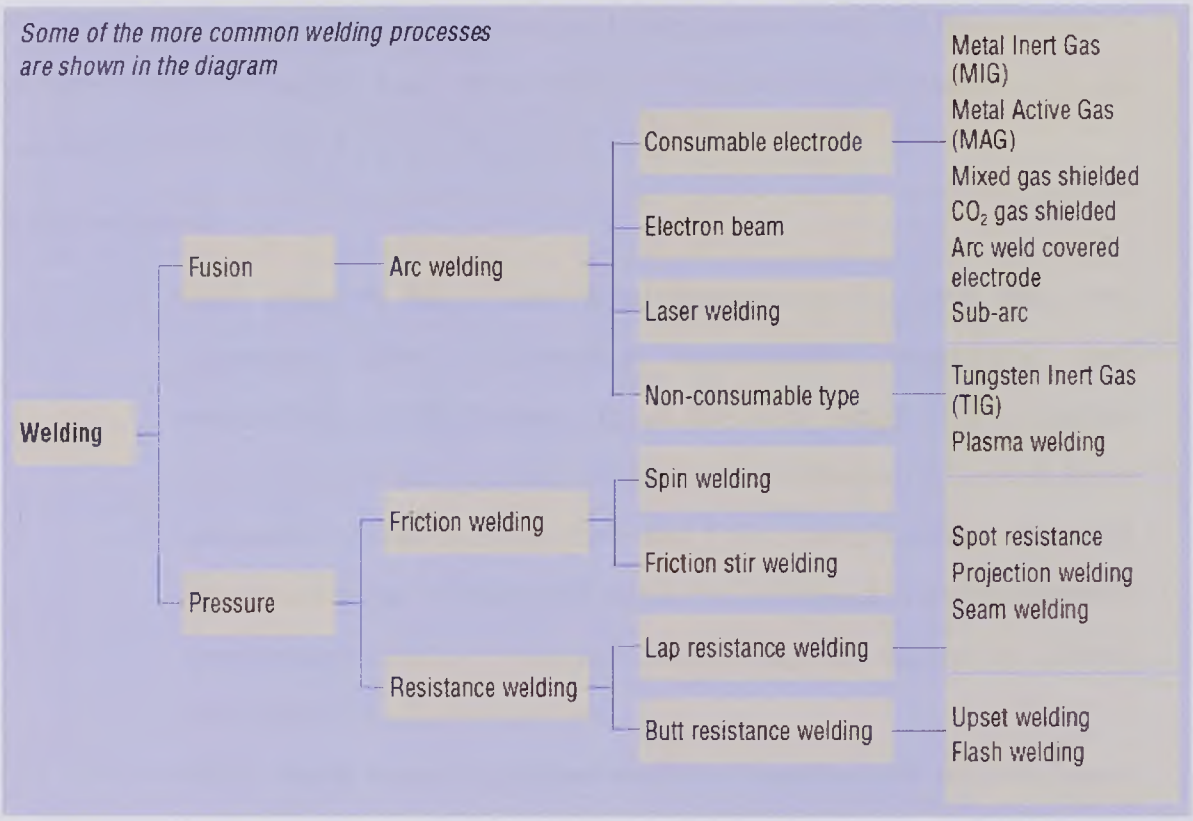

Figure 4.34Some of the more common welding process.[61]

When using spot, seam, or projection welding, these steels can be welded with current and time settings similar to those used with low-carbon steel, Higher electrode force may needed, however, because of the higher strength of the steel. Higher up setting force may be required with flash or upset welding for the same reason, but other welding variables should be similar to those used for low-carbon steel. Preheat or post heat cycles may be helpful during resistance welding of some HSLA steels to avoid excessive hardening of the weld and HAZ. In general, the welding processes used to join HSLA steels should be selected with consideration for the following:

- Strength requirements of weld metal.
- Weld metal behavior during multipass welding.
- Toughness requirements.
- Propensity for weld-metal and HAZ cracking.

However the welding processes and parameters used in this work for welding high strength low alloy (HSLA) NIONIKRAL70 steel will be mentioned in the second part of the thesis.

4.4 Conclusion

- Both chapters 3& 4 have been constructed to cover the most important issues concerning applications, properties, and weldability of HSLA steel. From the wide range of information source used which exceeds 90 different references of the last three decades, it could be concluded that HSLA steel is one of the most important types of structural steels and still used in many different applications such as, pressure vessels, bridges, cars, trucks, cranes, platforms and other structures.
- HSLA steels vary from other steels in that they are made to meet all requirements for ductility, weldability and toughness. These steels have yield strengths which can be anywhere between 250-590 MPa with an increased strength-to-weight ratio over standard steels.
- However, studying the evaluation of weldability of this type of steel in particular avoidance of cold cracking phenomenon leads through these two chapters to many important factors which could minimize the risk of having such a serious problem in the welded joints of HSLA steel.
- In brief it could be said that the previous part of this thesis is a near theoretical back ground of the experimental work, and for more details one could refer to the mentioned references.

5. Weldability Testing-Experimental Procedure

5.1 Measures to avoid cold cracking phenomenon

Bearing in mind that the three main factors responsible for the creation of cold crack sensitive microstructure, diffusion of hydrogen and stress, it is clear that the measures taken to avoid cold cracking phenomenon can be divided into three groups: measures to regulate the structure of the weld, measures to reduce the amount of hydrogen in the weld or weld zone and measures to reduce the stresses caused by welding.

It is known that the probability of formation of cold crack grow larger as the higher the carbon content and alloying elements that increase the tendency toward hardening increase.

However from the standpoint of the most sensitive structure annealing could reduce the risk of cold cracks. It is necessary to take measures to reduce the amount of low temperature transformation products of austenite - martensite and lower bainite , to reduce tetragonal martensite , to reduce the austenite grain size , to reduce segregation at austenite grain boundaries (especially in multi-layer welding) and to provide a second order stress relaxation at the grain boundaries.

These requirements are achieved by:

-Selection of alloying base metal and weld metal, which can provide a homogeneous chemical, and structural composition. This implies the presence of slag and orientation of layers that act as stress concentrators.

-Reduction of hydrogen content in base metal and weld metal in particular.

-Using special additional wires and powders, multi-layer welding electrodes in the swinging movement of automatic welding, the pulsed current

welding regime (at small thickness of metal) and the selection of optimum welding regimes allow to obtain a uniform grain structure of weld metal.

Finally, it should be noted that modern metallurgy and welding technology, and modern thermal treatment may with great probability to prevent occurrence of cold cracking even in high strength steel.

5.2 Investigating of susceptibility of NIONIKRAL-70 steel to cold cracking

Recognizing that knowledge of cold cracks in steel formed as a result of three factors (microstructure, content of hydrogen diffusion and charge) access to the calculation of the sensitivity of NIONIKRAL-70 steel to cold cracking , using the empirical formula, which itself includes the influential factors. The influence of chemical composition, i.e. Alloying elements on the occurrence of cold cracking is determined by the value of carbon equivalent.

Of the many expressions to calculate the carbon equivalent, while investigating susceptibility of NIONIKRAL-70 steel to cold cracking, used the terms recommended by the International Institute of Welding (IIW) and the expression for this class of steel developed by Ito and Bessy.

$$CE = C + Mn/6 + (Cr + Mo + V)/5 + (Ni + Cu)/5 \ (IIW) \quad (5.1)$$

$$Ce = C + \frac{Si}{30} + \frac{Mn + Cr + Cu}{20} + \frac{Ni}{60} + \frac{Mo}{15} + \frac{V}{10} + 5B(Ito\ and\ Bessy) \quad (5.2)$$

The same authors (Ito and Bessy) introduced anther parameter (Pp), which encompasses the influence of chemical composition (by Ce value), the content of hydrogen diffusion and the coefficient of rigidity of the welded joint.

Pp parameter expression is as follows:

$$Pp = Ce + H/60 + K/40 * 10^{3} \quad (5.3)$$

Where: Ce - the carbon equivalent of Ito and Bessy formula H - Hydrogen content (ml/100g)

K- Stiffness coefficient with but joints K= 66S (5.4)

S- Thickness (mm)

Table 5.1 contains data on the carbon equivalent and Pp parameter for all batches made of NIONIKRAL-70 steel.

Table 5.1Details of carbon equivalent and Pp parameter for the NIONIKRAL-70 steel

Batch No.	CE (IIW)	Ce (Ito &Bessy)	P_P
180079	0.67	0.25	0.38
180080	0.66	0.25	0.38
180226	0.63	0.25	0.38
180227	0.67	0.28	0.41
NN-70	0.74	0.30	0.4(0.43)

For calculations the parameters calculated with hydrogen diffusion content of 6 ml/100g, and the stiffness coefficient is taken for sheet of 18mm except for the last value of (NN-70) where the parameter is calculated for the worst case, i.e. the thickness of 30 mm.

However the values of Pp parameter indicated that it is steel in which may be expected to cold cracking and the diagram given in **Figure 5.1** will be required to provide preheating to a temperature about 200 °C.

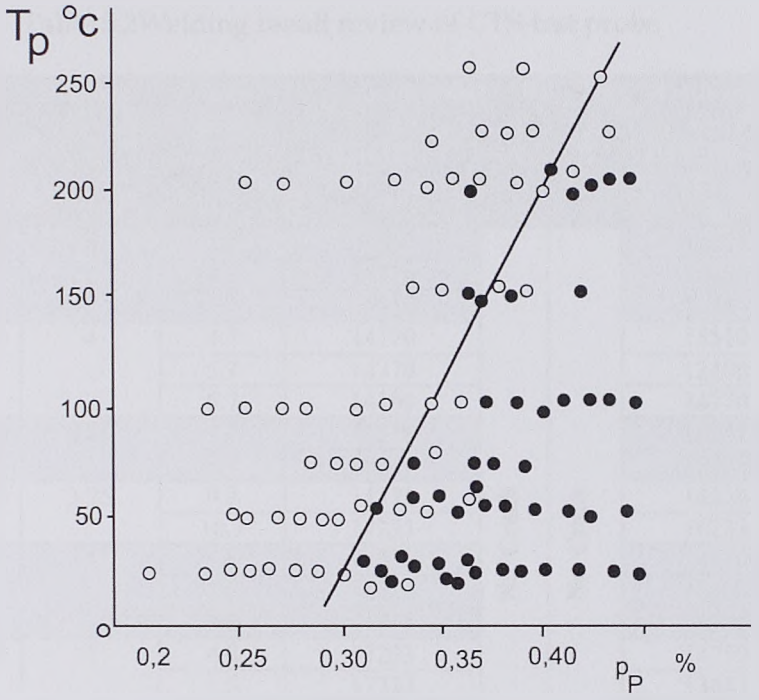

Figure 5.1Influence of preheating temperature on welded steel
(•with crack, ○ without crack)

5.2.1 CTS (Controlled Thermal Severity) test

The method details already explained in chapter 4. In this study to test the sensitivity of steel NIONIKRAL-70 to cold cracking through CTS probe 18 mm thickness sheets were used from both 180079 and 180080 batches. It was experimented with electrodes (TENACITO 75 - TENACITO 80) and electrodes diameters of 3.25 and 4.0 mm. **Table 5.2** provides an overview of CTS welding test with calculated welding heat input in (J/cm) for each seam.

Table 5.2Welding result review of CTS-test probe

Batch No.	Electrode	Diameter (mm)	Sample code	Brithermal (2D)			Trithermal (3D)		
				Heat Input (J/cm)	A	B	Heat Energy (J/cm)	C	D
180079	TENACITO 75	4	1.7	9124	No Crack	No Crack	13487	No Crack	No Crack
			2.7	14770			13487		
			3.7	15510			13487		
	TENACITO 80	4	4.7	14770			15510		
			5.7	14770			12480		
			6.7	14100			14770		
	TENACITO 75	3,25	7.7	15510			18247		
			8.7	18247			16326		
	TENACITO 80	3,25	9.7	14770			16326		
			10.7	17233			16233		
180080	TENACITO 75	4	1.8	16326			14770		
			2.8	16326			16326		
			3.8	15510			16326		
	TENACITO 80	4	4.8	17233			14770		
			5.8	17233			13487		
			6.8	15510			14770		
	TENACITO 75	3,25	7.8	13235			13235		
			8.8	13235			13235		
	TENACITO 80	3,25	9.8	8653			10714		
			10.8	13235			13235		

Preparations for microscopic examination were done after seven days from welding. Two from brithermal weld (A and B) and two from trithermal weld (C and D). Samples were prepared by grinding, polishing and etched 5% solution of nitric acid in alcohol. At the optical microscope of 80 preparations were examined with magnification up to 500 times.

However for both batches of NIONIKRAL-70 steel welded with the two different diameter electrodes, no cold cracks were found. **Figure 5.2** and **Figure 5.3,** show a few characteristic structures of the two welds brithermal and trithermal. For a number of products hardness was measured and change characteristic diagrams are given in **Figure 5.4, Figure 5.5, Figure 5.6** and **Figure 5.7** respectively. However hardness distributions comparison between the batches (180079 and 180080) is illustrated in **Figure 5.8, Figure 5.9, Figure 5.10** and **Figure 5.11** respectively.

100X

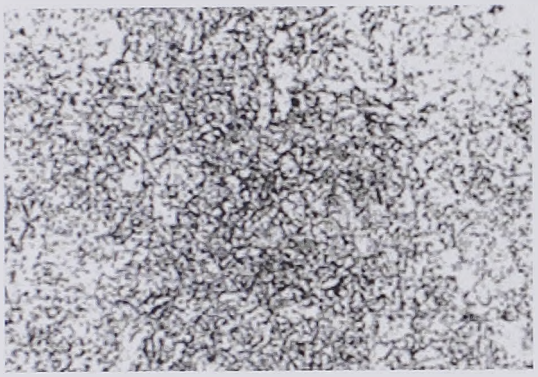

Base material

200X

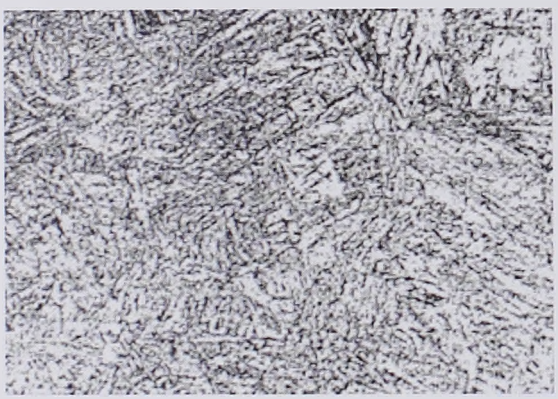

HAZ

200X

HAZ

Figure 5.2Microscopic images of CTS test brithermal sample (8.8)

200X

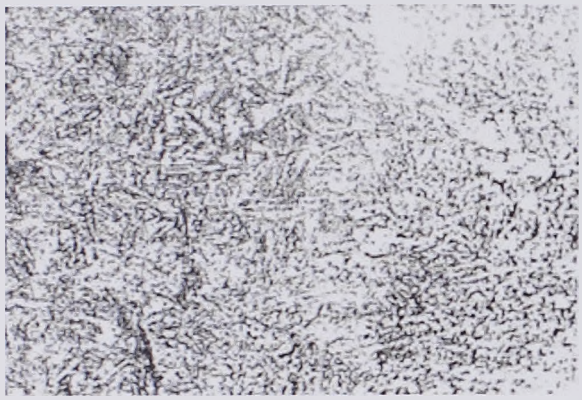

Base material

200X

Base material

200X

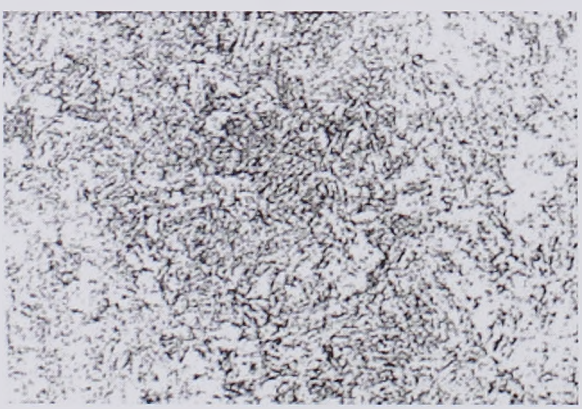

HAZ

Figure 5.3Microscopic images of CTS test trithermal sample (2.7)

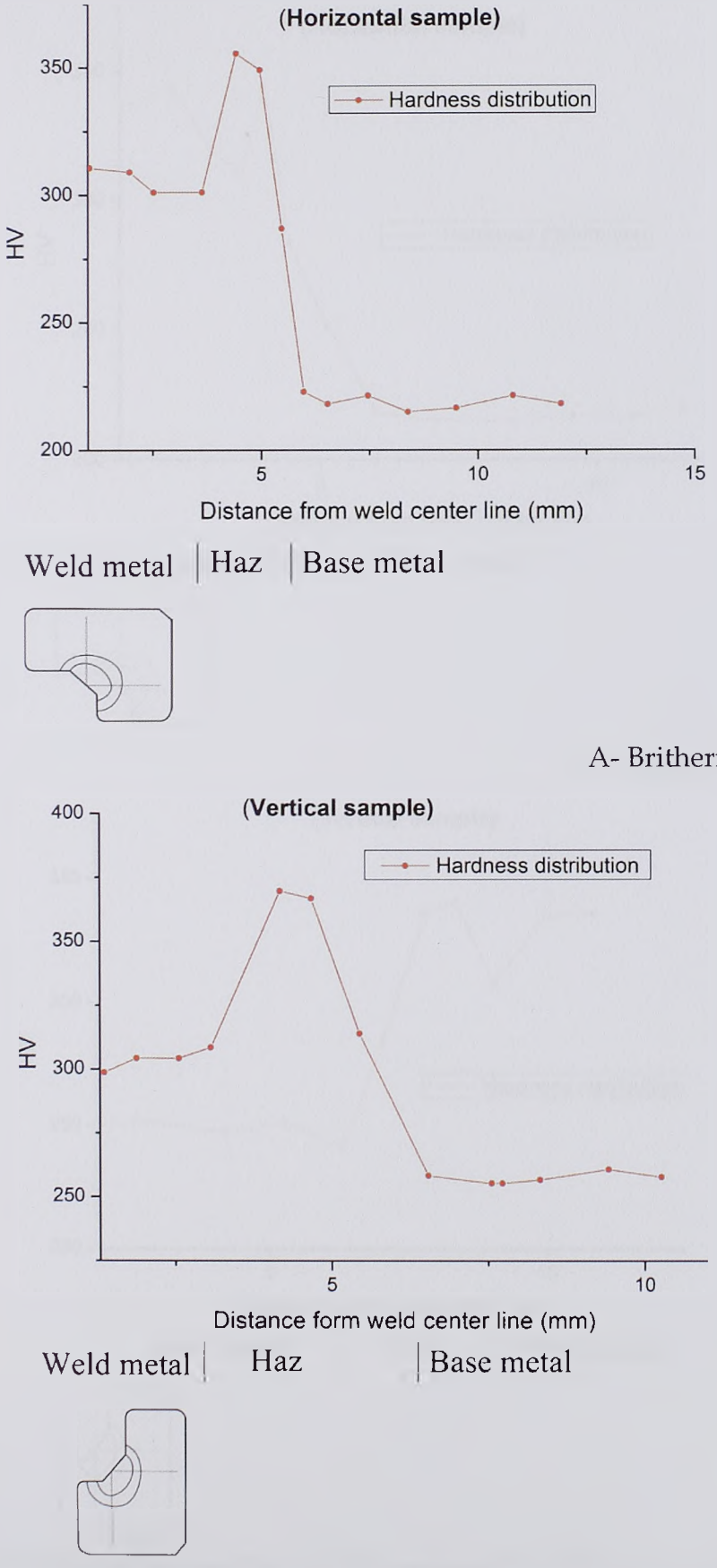

Figure 5.4Change of hardness through the section of the CTS probe sample (9.7)

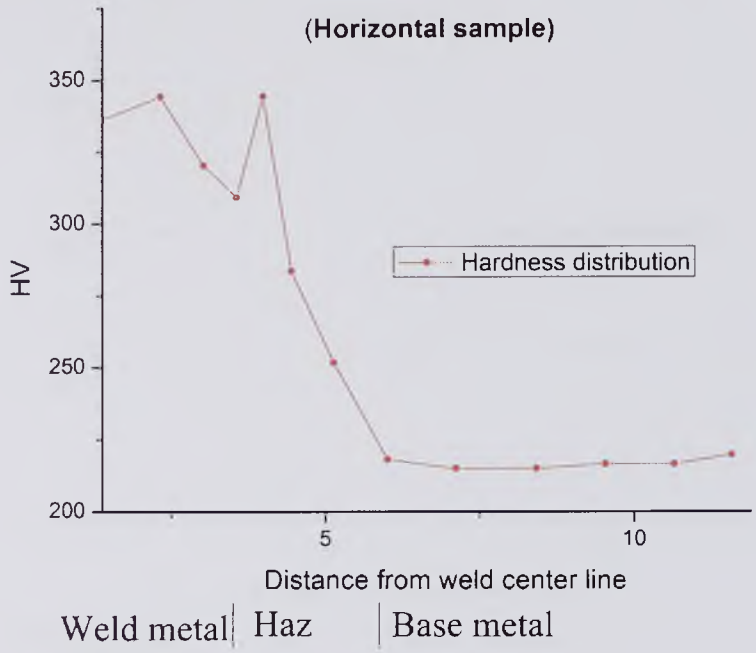

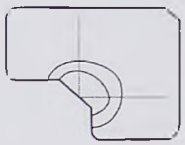

C- Trithermal Sample

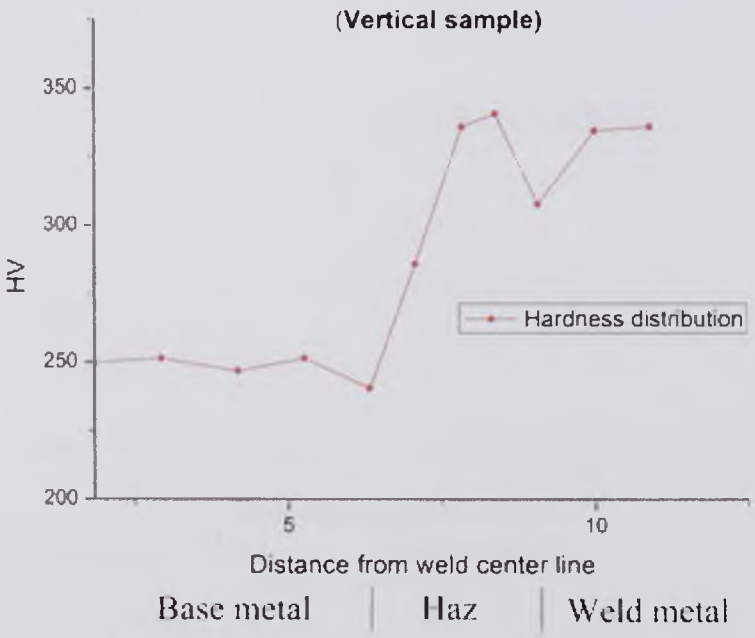

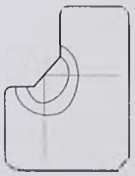

Figure 5.5Change of hardness through the section of the CTS probe sample (9.7)

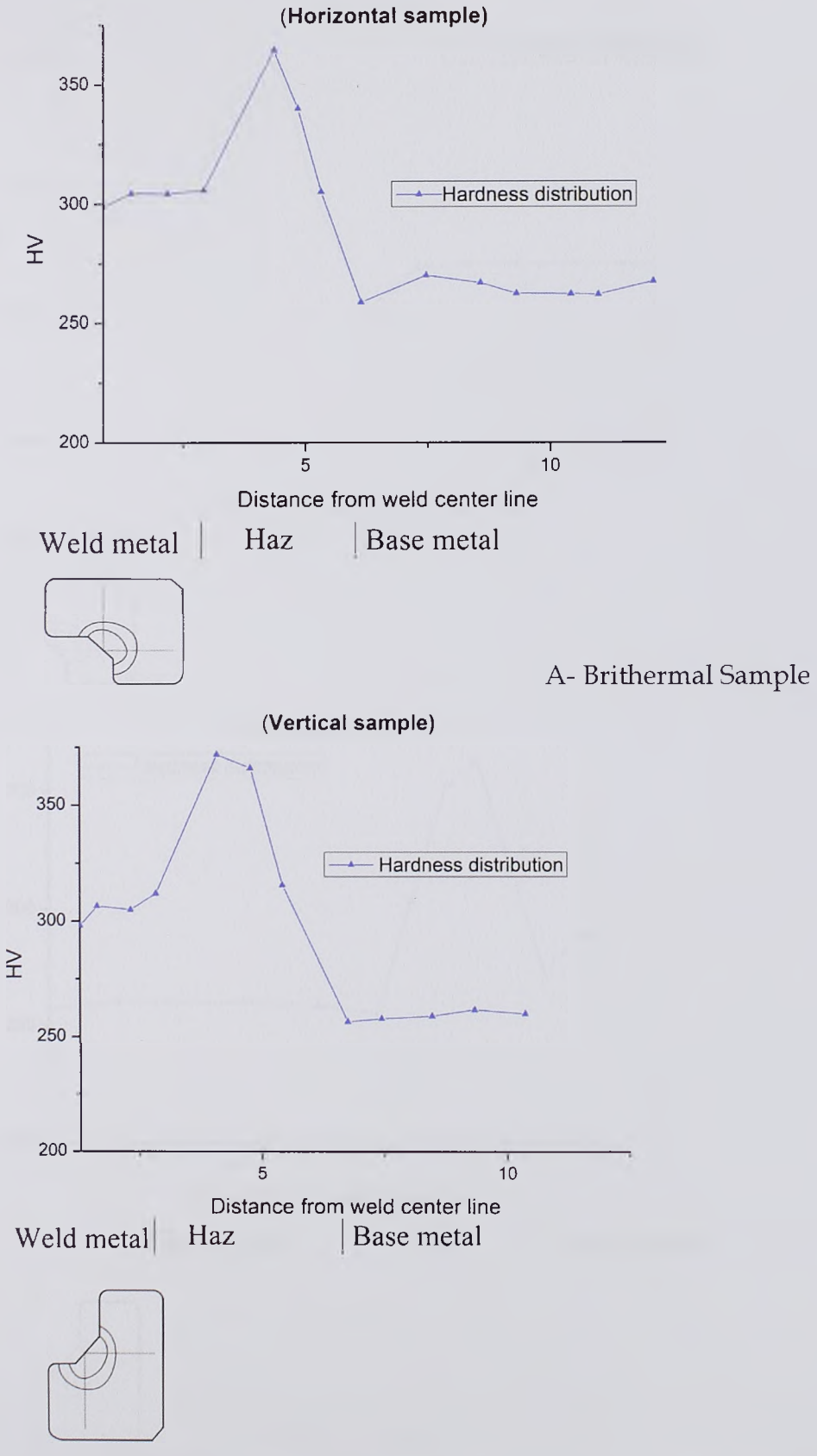

Figure 5.6 Change of hardness through the section of the CTS probe sample (9.8)

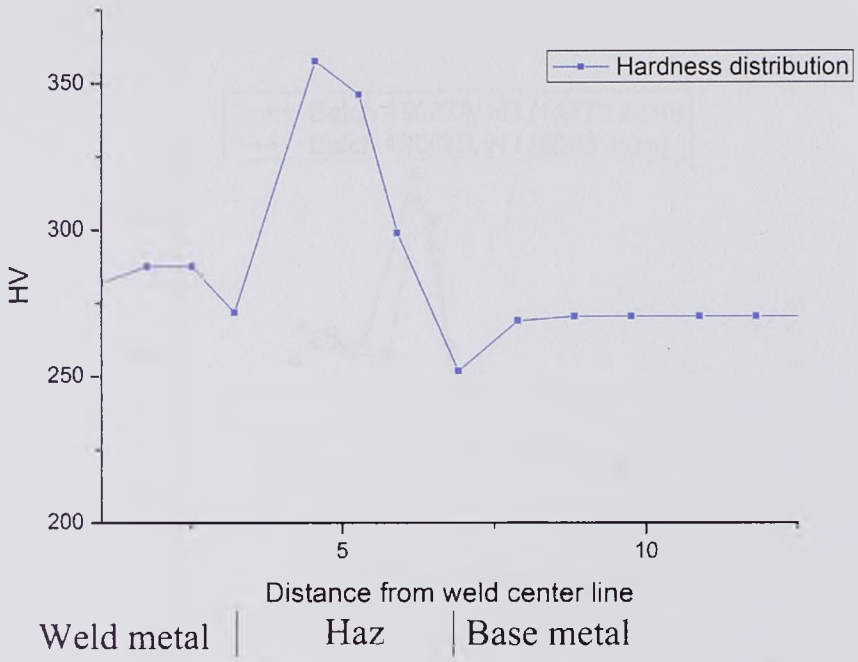

Weld metal | Haz | Base metal

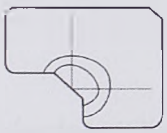

C- Trithermal Sample

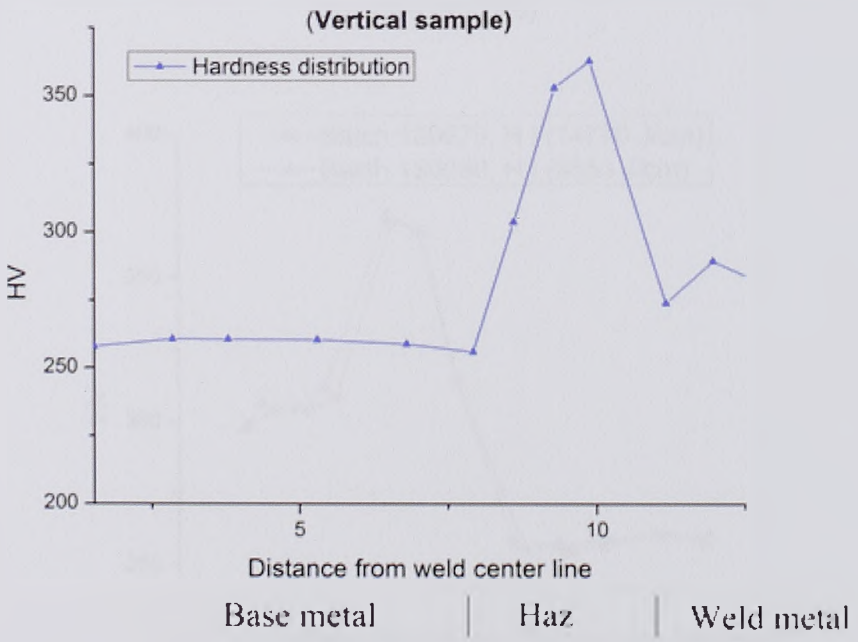

Base metal | Haz | Weld metal

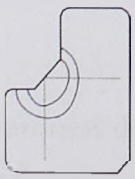

Figure 5.7 Change of hardness through the section of the CTS probe sample (9.8)

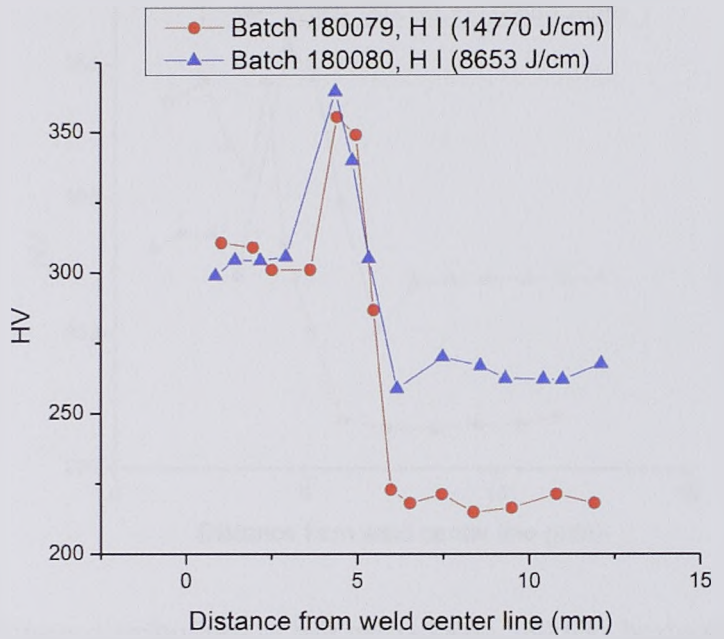

Figure 5. 8 Hardness distributions of batches (180080, 180079), horizontal brithermal samples (9.7, 9.8)

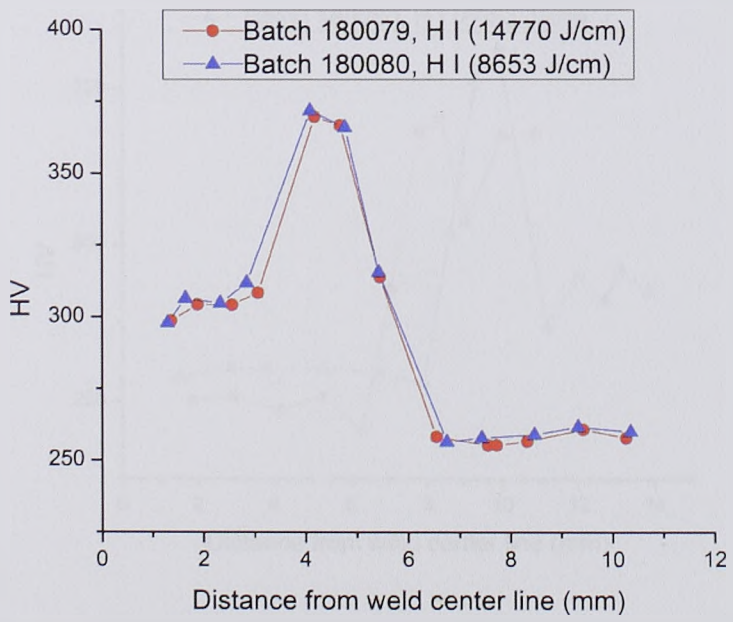

Figure 5. 9 Hardness distributions of batches (180080, 180079), vertical brithermal samples (9.7, 9.8)

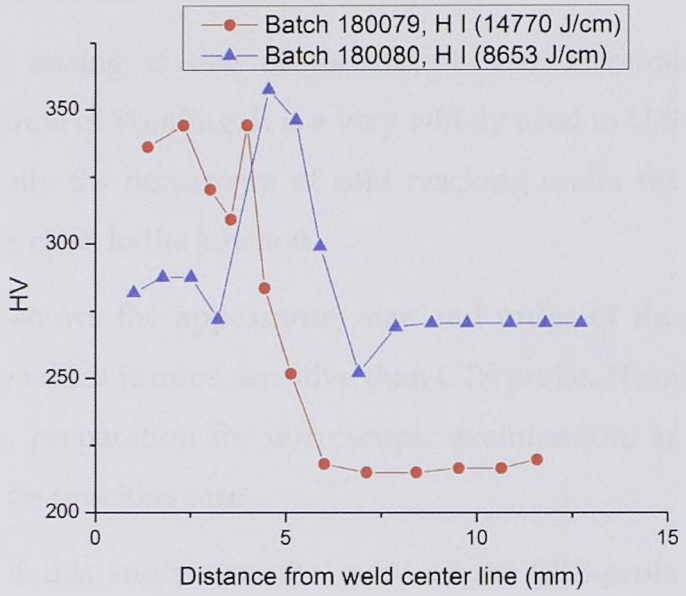

Figure 5. 10 Hardness distributions of batches (180080, 180079), horizontal trithermal samples (9.7, 9.8)

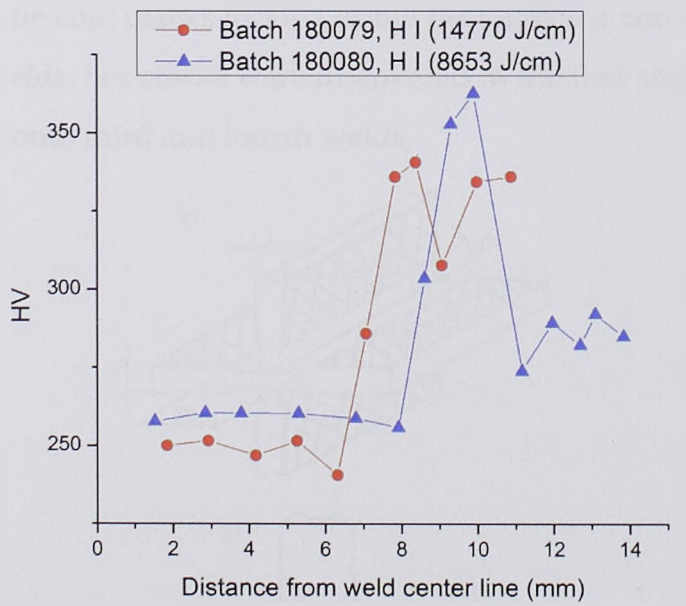

Figure 5. 11 Hardness distributions of batches (180080, 180079), vertical trithermal samples (9.7, 9.8)

5.2.2 Intersection test-method and extent of testing

Intersection testing is one of the oldest tests recommended by the International Institute of Welding. It is a very widely used in U.S laboratories. It is intended to verify the occurrence of cold cracking under the trail or in the heat affected zone, close to the junction.

Figure 5.12 shows the appearance, size and order of the application of intersection probe which is more sensitive than CTS probe. However the testing (eye examination, preparation for microscopic examination, and hardness) is similar to that of the previous case.

The scope of this study was the same as the CTS-probe, and detailed information about the experiment is given in **Table 5.3**. For a number of products on the microscope examination revealed the existence of crack. Analysis of the spatial position and direction indicated the appearance of warm (HC) and cold cracks (CC). Warm crack extended through additional metal (HC-AM), while the cold cracks located in the heat affected zone (CC-HAZ). In the experiment welds, hot cracks were discovered in the first and second, while the cold in the second, third and fourth welds.

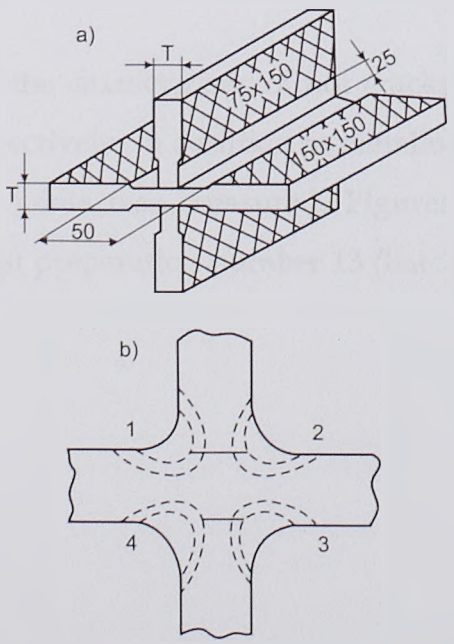

Figure 5. 12 a) Intersection testing b) microscopic preparation

Table 5.3Review of welded samples of the cross-test probe

Batch No.	Electrode	Diameter (mm)	Sam. code	Heat Input (J/cm)				Welds metallographic			
				1	2	3	4	1	2	3	4
180079	TENACITO 75	4	15	17935	16418	19075	15865				
			16	16583	15789	19527	17098				
			17	17742	16837	19412	17742				
	TENACITO 80	4	12	16583	16019	18033	18232				
			13	16256	15865	18644	17098				
			14	17935	17010	19075	18232			CC-HAZ	
	TENACITO 75	3,25	3	10548	8562	9482	9766		HC-AM		
			4	9482	9294	9615	10000				
	TENACITO 80		5	10000	10548	8928	9294		HC-AM		
			6	10593	10548	10822	10204	HC-AM			CC-HAZ
180080	TENACITO 75	4	18	17098	16836	19075	17553		CC-HAZ		
			19	17188	17010	18232	18232		HC-AM	CC-HAZ	
			20	18132	17935	18232	17935				
	TENACITO 80	4	9	17010	14224	16500	18436				
			10	16019	16500	17098	17742				
			11	16019	16176	18857	19412				
	TENACITO 75	3,25	1	11062	9842	9652	9294		CC-HAZ		
			2	10730	10000	8928	9842		HC-AM		
	TENACITO 80	3,25	7	10373	8772	9652	9470	HC-AM			
			8	10548	10373	9804	10000	HC-AM			

Noted that in the above table 5.3:

- CC-Cold Crack
- HC- Hot Crack and
- AM - Additional Material

Figure 5.13 shows the characteristic of hot cracks and **Figure 5.14** shows those of cold cracks respectively. In addition to metallographic analysis, change in hardness of welded joints was measured. **Figures 5.15** shows change of hardness through the test preparation number 13 (batch 180079, electrode T-80, Ø4mm).

100X

a) Sample 6.7 weld metal crack

100X

b) Sample 6.7 weld metal crack

200X

c) Sample 7.8 weld metal crack

Figure 5. 13 Cracks in cross-probe samples a) weld metal crack b) weld metal crack and c) weld metal crack

200X

a) Sample 12.7 crack at the junction

200X

b) Sample 1.8 crack in the HAZ

Figure 5. 14 Cold cracks (cross-shaped probe). a) Sample 12.7 crack at the junction and b) Sample 1.8 crack in the HAZ

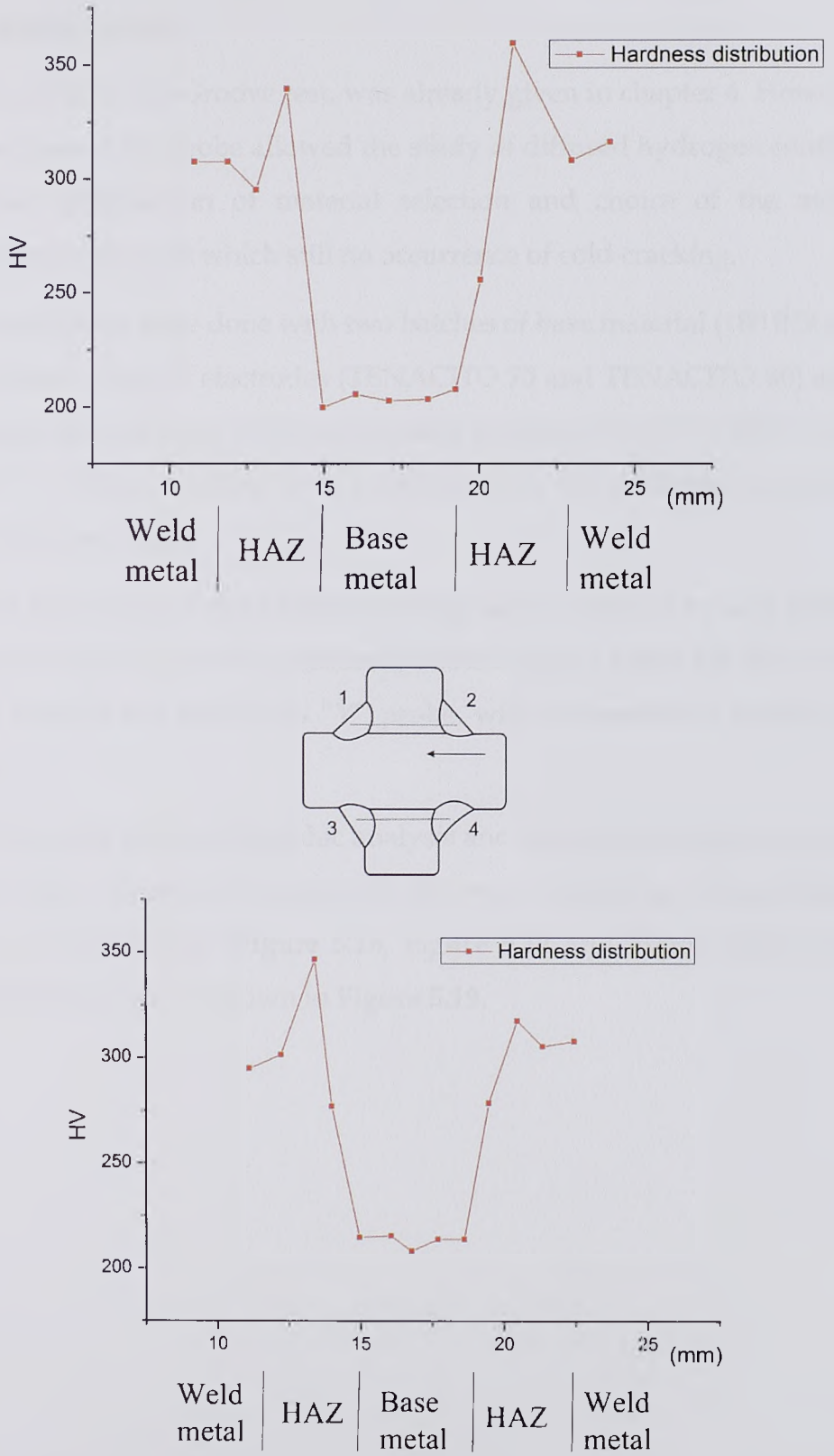

Figure 5. 15 Change of hardness through the test preparation number 13(batch 180 079, additional material T-80, Ø4mm)

5.2.3 Y-Probe method

The details of Y-Groove test, was already given in chapter 4. However the main purpose of the probe allowed the study of diffused hydrogen content and additional optimization of material selection and choice of the minimum preheat temperature at which still no occurrence of cold cracking.

Experiments were done with two batches of base material (180 079 and 180 080) with two kinds of electrodes (TENACITO 75 and TENACITO 80) and four preheating temperatures. The samples were preheated at 20 ° C, 100 ° C, 150 ° C and 200 ° C. Before welding as in previous cases, the electrodes were dried at 350 ° C for three hours.

The heat input of the applied welding was calculated by and preheating temperatures were precisely measured. **Tables 5.4** and **Table 5.5** show the basic data on welded test specimens "Y" probe, with the results of metallographic analysis.

The results of metallographic analysis and hardness changes diagrams the welded joints through Y-probe for different preheating temperatures are obtained and shown in (**Figure 5.16, Figure 5.17 and Figure 5.18**) while the detected cold cracks are shown in **Figure 5.19.**

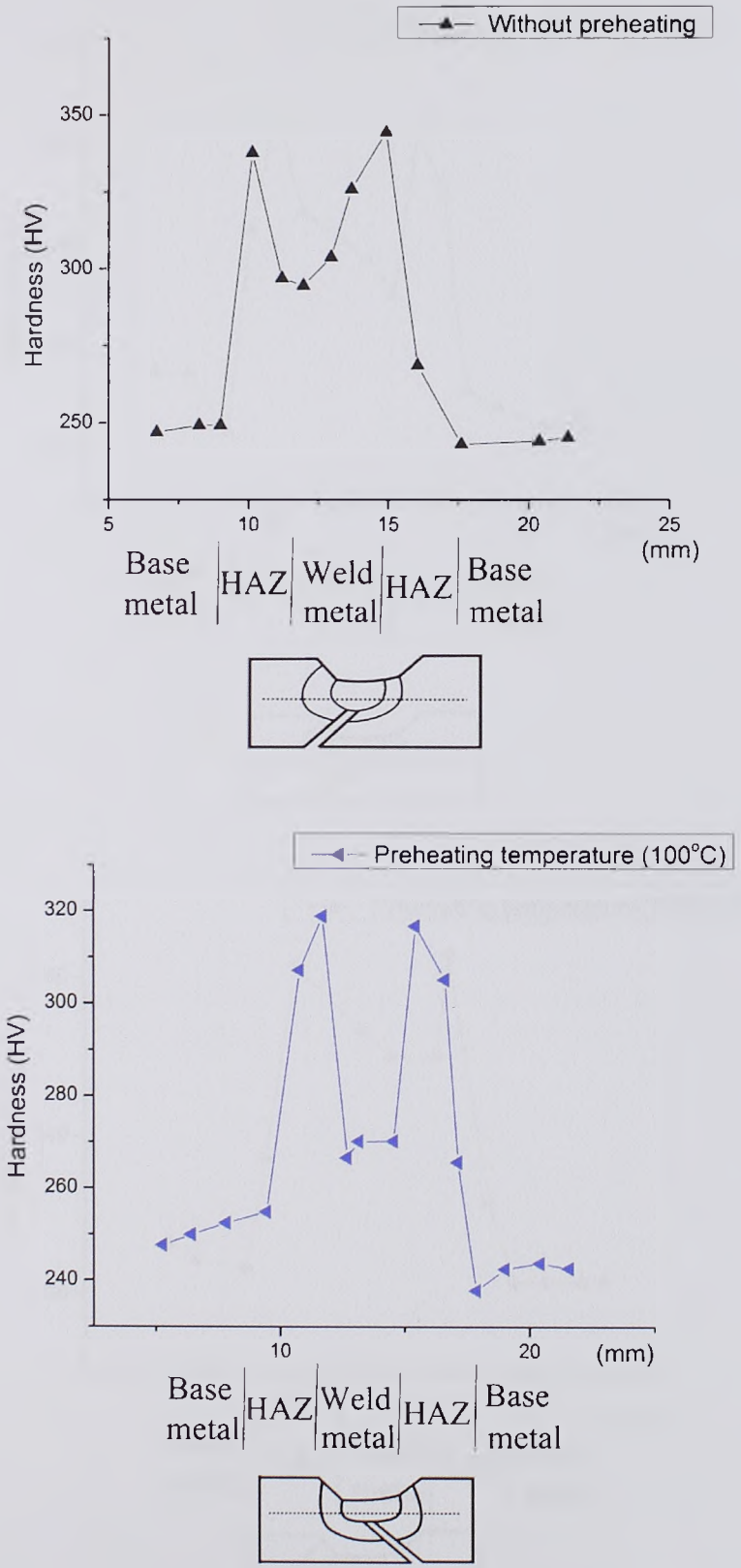

Figure 5. 16 Influence of preheating temperature on hardness change through welded compound Y-probe (batch 180079 electrode T-80, Ø4 mm)

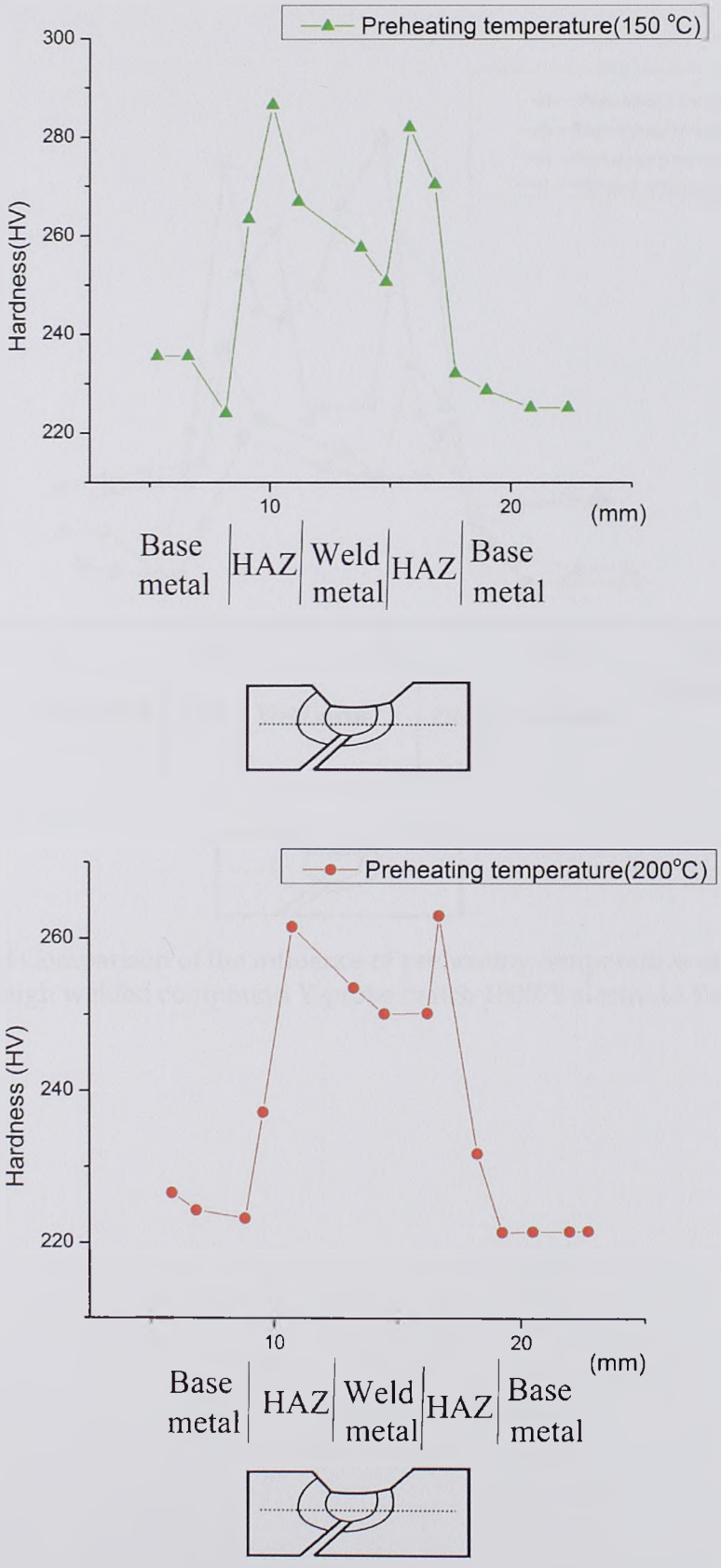

Figure 5. 17 Influence of preheating temperature on hardness change through welded compound Y-probe (batch 180079 electrode T-80, Ø4 mm)

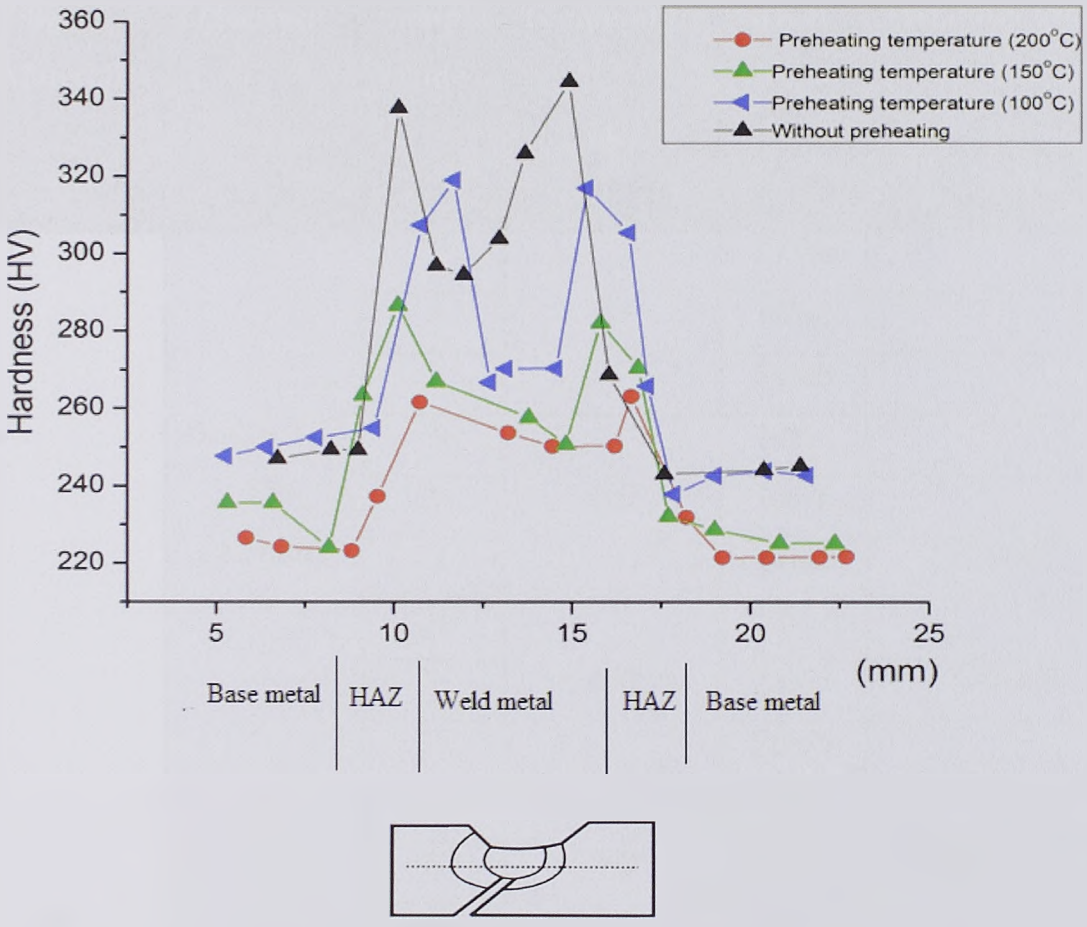

Figure 5. 18 Comparison of the influence of preheating temperature on hardness change through welded compound Y-probe (batch 180079 electrode T-80, ∅4 mm)

Table 5.4Review and surveyed of welded samples of Y-probe batch 180079

Basic Material	Electrode	Sample code	Temperature (°C)	Heat input (J/cm)	Metallographic Finding
180079	TENACITO 75 (Ø4 mm)	7	20	14348	
		8		14348	
		9		14348	
		19	100	19412	
		20		20625	
		21		19412	CC-HAZ
		34	150	2062 5	
		35		23571	CC-HAZ
		36		20625	
		46	200	22000	
		47		23571	CC-HAZ
		48		19412	
	TENACITO 80 (Ø 4mm)	10	20	15000	
		11		15000	
		12		13750	
		22	100	18333	
		23		19412	CC-HAZ
		24		20625	
		31	150	22000	
		32		22000	
		33		23571	
		43	200	25385	
		44		23571	
		45		23571	

Table 5.5Review and surveyed of welded samples of Y-probe batch 180080

Batch No.	Electrode	Sam. code	Temperature (^{0}C)	Heat input (J/cm)	Metallographic Finding
180080	TENACITO 75 (Ø4 mm)	4	20	15000	
		5		14348	CC-HAZ
		6		13750	CC-HAZ
		16	100	17368	
		17		18333	
		18		`9412	
		28	150	23571	
		29		20625	
		30		25385	CC-HAZ
		40	200	20625	
		41		22000	CC-HAZ
		42		23571	
	TENACITO 80 (Ø 4mm)	1	20	14348	CC,Longitudinal
		2		15744	"
		3		16500	"
		13	100	18333	"
		14		18333	
		15		18333	
		25	150	18333	
		26		20625	
		27		23571	CC-HAZ
		37	200	17368	
		38		19412	
		39		20625	
		49	20	17368	CC,Longitudinal
		50		16500	"
		51		20625	"

500X

a) Sample 5 cracks in HAZ

200X

b) Sample 48 cracks in HAZ

200X

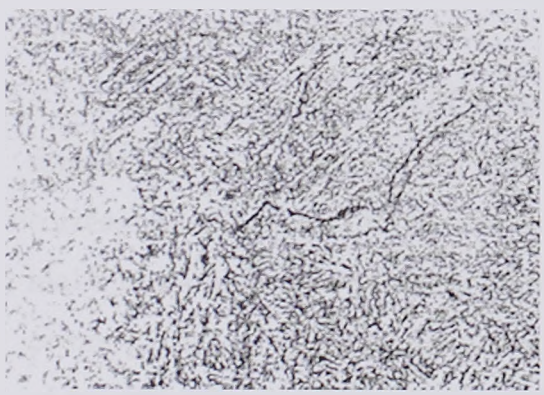

c) Sample 21 cracks in HAZ

200X

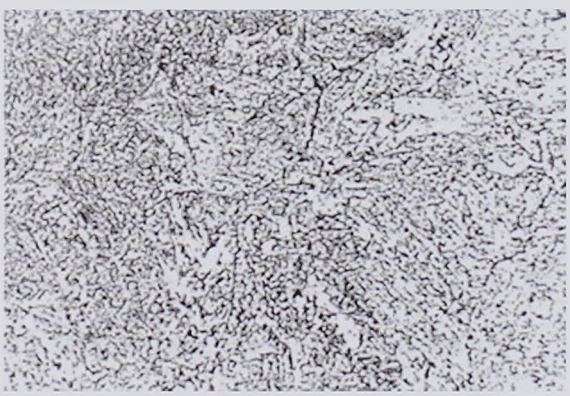

d) Sample 23 cracks in HAZ

Figure 5. 19 Detected cold cracks in Y-probe testing

5.2.4 Cabelka-Million probe, description and scope of testing

This test is used to evaluate the tendency of steel to the specific type of cold crack, so called (late-breaking crack). In welded joints of high strength steel cracks occur late in roughly kernel martensite, obtained by cooling from the highest temperature austenite. However another important cause of delayed crack the acting tensile force component normal to the direction of propagation of the crack. The incubation period of delayed cracking depends on the direction and size of the local stress.

In order to investigate the sensitivity of NIONIKRAL-70 steel to delayed cracking experimented with samples from batches 180079, 180080. The used electrodes are TENACITO-75 and TENACITO-80, with a diameter of (Ø3, 25mm). The main welding parameters were: intensity of current 120-140 A and welding voltage 20-40 V.

To calculate sensitivity of steel to the phenomenon of delayed cracking requires two parts: a thorn (**Figure 5.20 a**) and conical ring (**Figure 5.20 b**) which are made of a material to be tested. The construction of these elements is so constructed that it can be welded mandrel head with the upper edge of the ring. Welding is performed to make a separate double chamber which is cooled by water (**Figure 5.21**).

However the function of these devices is to prevent strong heating of the samples so as to reduce the rate of cooling of the sample, which would correspond to real conditions of welding. Welding pins and rings in the display make it simulate real welding conditions. After welding, specimens shall be promptly placed in the tool where the rupture strains (**Figure 5.22**). In a series of ten test tubes load is reduced until the test tube does not shoot enough and long-time loads (more than 104 min).Test results according to the method Cabelka-Millio are shown in **Table 5.6** and the tighten-time diagram is illustrated in **Figure 5.23**.

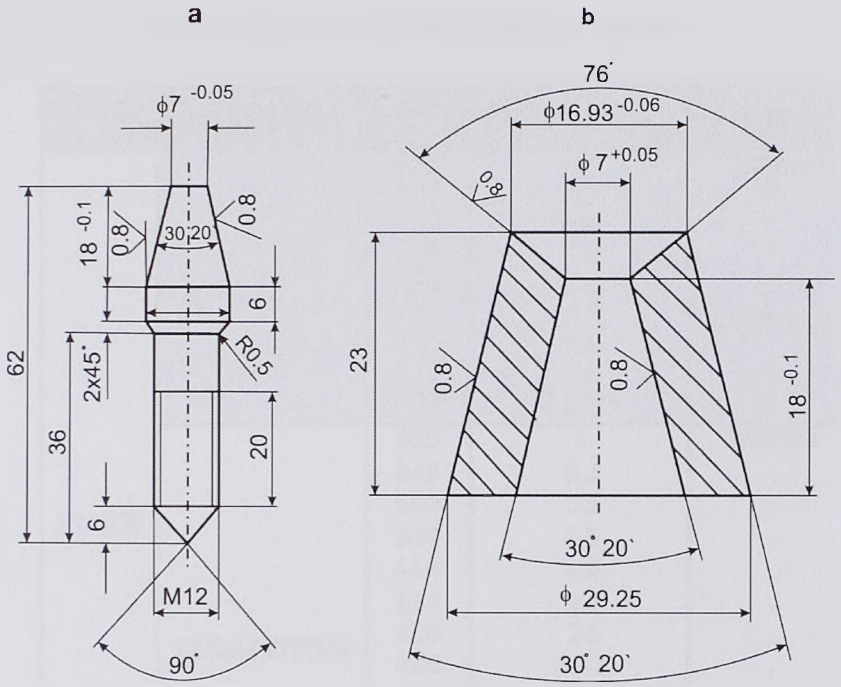

Figure 5. 20Cabelka-Million probe for testing delayed cracking

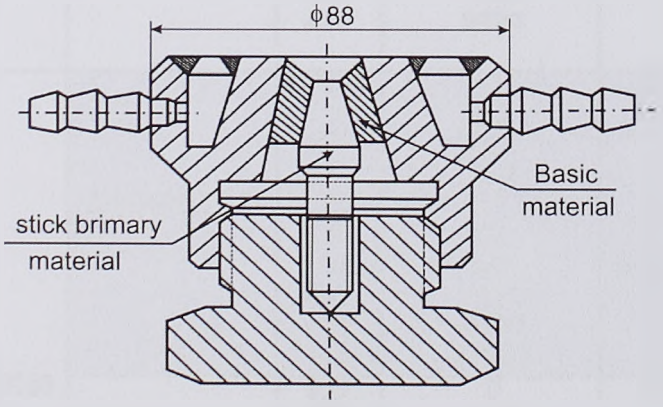

Figure 5.21 Gadget for welding tubes

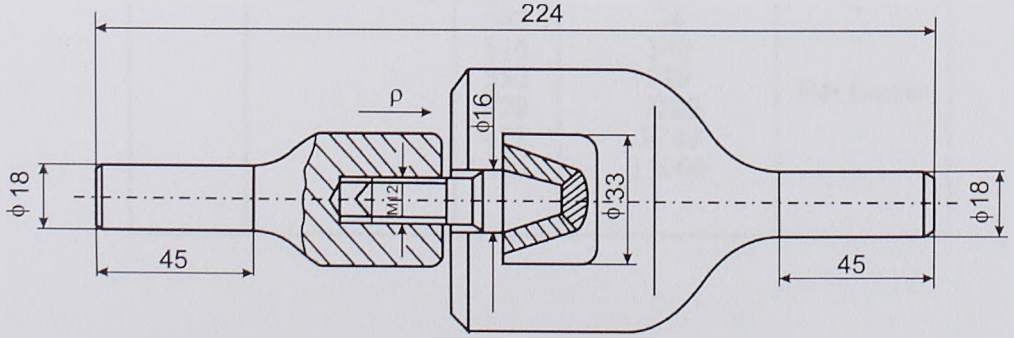

Figure 5. 22 Cabelka-Million probe tool for testing

Table 5.6Results of Cabelka-Million method

Batch N0.	Filling material	σ (MPa)	Tightening time (min)	Remark
180079	TENACITO -75	699	0	Broken
		617	0.3	"
		620	3.35	"
		555	6.7	"
		539	52.5	"
		423	65	Not broken
		497	73	
		411	4380	"
		385	16500	"
	TENACOTO-80	855	0	Broken
		845	0.1	"
		698	1.5	"
		649	1.5	"
		418	8.8	"
		626	9.7	"
		420	24	"
		440	33.3	"
		410	54	"
		533	56	"
		357	76	"
		317	5200	Not broken
		338	7300	"
		418	9720	"
180080	TENACITO -75	782	0	Broken
		720	3.5	"
		695	10.6	"
		677	12.2	"
		596	17	"
		530	53	"
		501	643	"
		441	2160	Not broken
		465	4700	"
		466	25920	"
	TENACOTO-80	929	0	Broken
		894	0.75	"
		732	1	"
		742	11.1	"
		629	15.75	"
		613	31	"
		508	76	"
		510	140	"
		552	229	"
		429	7200	Not broken
		473	8700	"
		475	12900	"

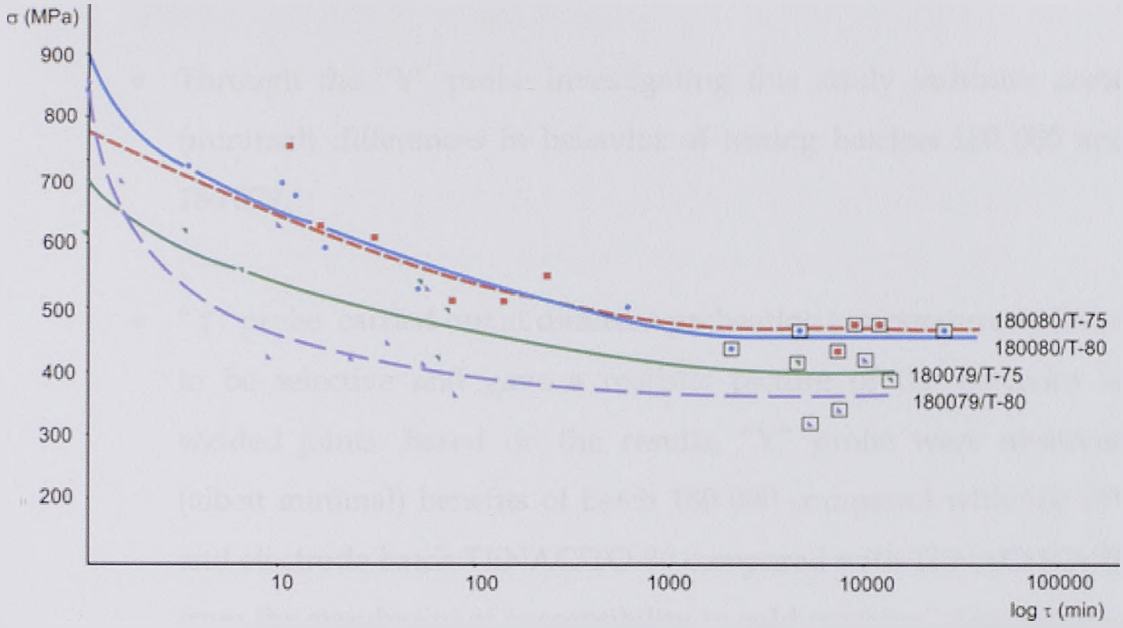

Figure 5. 23 Results of Cabelka-Million test probe

5.3 Conclusion

- Based on the susceptibility testing of NIONIKRAL-70 steel to cold cracking it could be concluded that for this HSLA steel there is a risk of cold cracking.

- Although CTS testing probe did not indicate such a conclusion, further investigations of intersection probe showed that it is more sensitive than CTS probe and the occurrence of cold cracking in welded joints of NIONIKRAL-70 steel can occur.

- The increased preheating temperature of 200 ° C in Y-Groove test causes a clear reduction in the hardness distribution which was in the range (250-270 HV) in both weld metal and HAZ of the welded joints of (batch 180079 electrode Tinacito-80, ⌀4 mm) which could reduce the probability of having such a crack.

- Through the "Y" probe investigating this study indicates some (minimal) differences in behavior of testing batches 180 080 and 180 079.

- "Y" probe, carried out at different preheating temperatures proved to be selective and gave a realistic picture of the behavior of welded joints. Based on the results, "Y" probe were observed (albeit minimal) benefits of batch 180 080 compared with 180 079 and electrode batch TENACITO-80 compared with TENACITO-75, from the standpoint of susceptibility to cold cracking. According to the values of carbon equivalents (CE, Ce and Pp) and the results obtained by various technological tests; we can say that there is a risk of cold cracking.

- From the comparisons between the two steel batches (180079&180080) of the CTS test it could be concluded that for the case of brithermal (2D) the hardness distribution was almost the same for both batches despite the heat input increasing. However for the case of trithermal (3D) the WM hardness was higher in the batch 180079 with heat input of (14770 J/cm) whereas its HAZ hardness was a bit lower than that of batch 180080 with heat input of (8653 J/cm).

- Cabelka-Million test probe results unequivocally demonstrated that batch of 180 079 more sensitive to the phenomenon of delayed cracking than batch 180 080. In any case, the fact remains that when welding NIONIKRAL-70 steel should take precautions to reduce the risk of occurrence of cold cracking.

- Finally analysis of results shows that the NIONIKRAL -70 steel within the limits of chemical composition and thickness up to 30 mm with other mechanical and technological characteristics puts the newly conquered steel the most promising high-strength steel meant for shipbuilding and manufacture of pressure vessels.

6. Evaluation of HSLA Steel Wedability using Taguchi Method for DOE

6.1 Introduction

Design of Experiment (DOE) is a powerful statistical technique for improving product/process designs and solving production problems. A standardized version of the DOE, as forwarded by Dr.Genichi Taguchi, allows one to easily learn and apply the technique product design optimization and production problem investigation. Since its introduction in the U.S.A. in early 1980's, the Taguchi approach of DOE has been the popular product and process improvement tool in the hands of the engineering and scientific professionals.[86]

6.2 Taguchi method for the optimization of process parameters

Optimization [87] of process parameters is the key step in the Taguchi method for achieving high quality without increasing cost. This is because optimization of process parameters can improve quality characteristics and the optimal process parameters obtained from the Taguchi method are insensitive to the variation of environmental conditions and other noise factors. Basically, classical process parameter design is complex and not easy to use. However the flowchart of the Taguchi method for DOE is illustrated in **Figure 6.1**, and its main general steps [88] could be summarized as the following:

- Define the process objective, or more specifically, a target value for a performance measure of the process.
- Determine the design parameters affecting the process.
- The number of levels that the parameters should be varied at must be specified.
- Create orthogonal arrays for the parameter design indicating the number of and conditions for each experiment.

- The selection of orthogonal arrays is based on the number of parameters and the levels of variation for each parameter, and will be expounded below.
- Conduct the experiments indicated in the completed array to collect data on the effect on the performance measure.
- Complete data analysis to determine the effect of the different parameters on the performance measure.

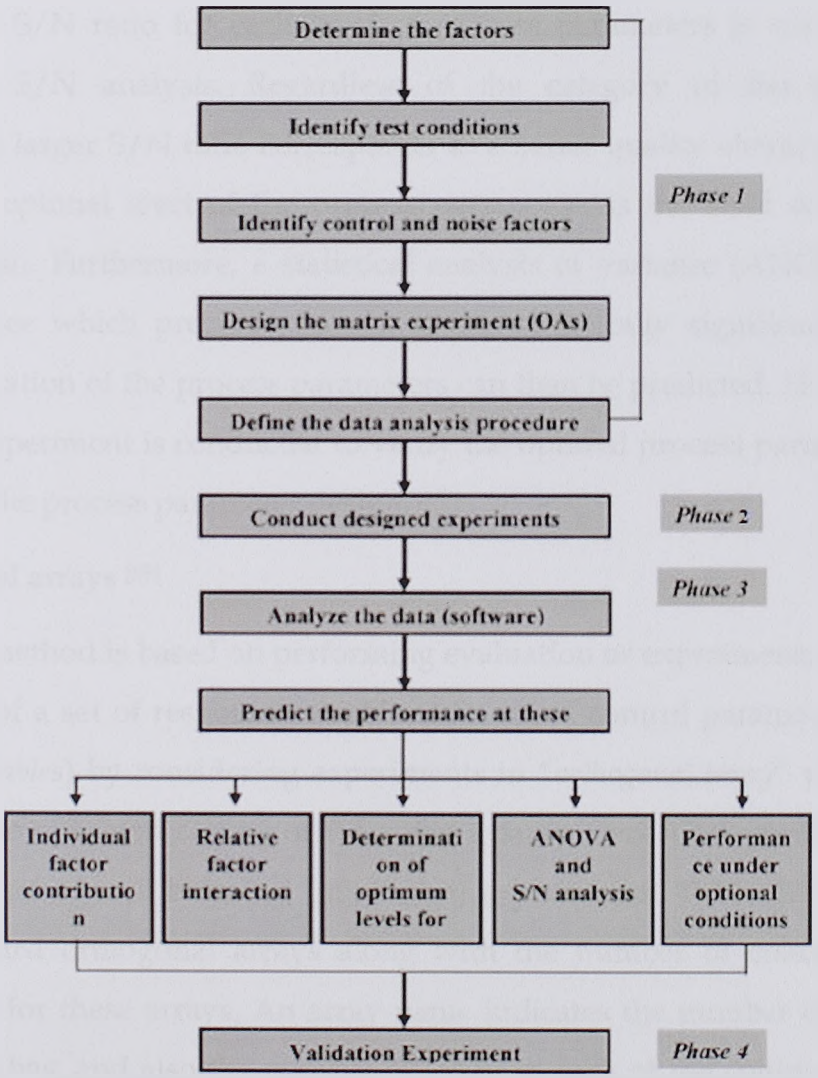

Figure 6. 1Taguchi method for DOE flowchart [88]

A large number of experiments have to be carried out when the number of process parameters increases. To solve this task, the Taguchi method uses a special design of orthogonal arrays to study the entire process parameter space

with a small number of experiments only. A loss function is then defined to calculate the deviation between the experimental value and the desired value. Taguchi recommends the use of the loss function to measure the deviation of the quality characteristic from the desired value. The value of the loss function is further transformed into signal-to-noise (S/N) ratio.

Usually, there are three categories of the quality characteristic in the analysis of the S/N ratio, i.e. lower-the better, higher-the-better and nominal-the better. The S/N ratio for each level of process parameters is computed based on the S/N analysis. Regardless of the category of the quality characteristic, a larger S/N ratio corresponds to a better quality characteristic. Therefore, the optimal level of the process parameters is the level with the higher S/N ratio. Furthermore, a statistical analysis of variance (ANOVA) is performed to see which process parameters are statistically significant. The optimal combination of the process parameters can then be predicted. Finally, a confirmation experiment is conducted to verify the optimal process parameters obtained from the process parameter design.

6.2.1 Orthogonal arrays [89]

Taguchi method is based on performing evaluation or experiments to test the sensitivity of a set of response variables to a set of control parameters (or *independent variables*) by considering experiments in "*orthogonal array*" with an aim to attain the optimum setting of the control parameters. *Orthogonal arrays* provide a best set of well balanced (minimum) experiments. **Table 6.1** shows eighteen standard orthogonal arrays along with the number of columns at different levels for these arrays. An array name indicates the number of rows and columns it has, and also the number of levels in each of the columns. For example array L_4 (2^3) has four rows and three "*2 level*" columns. Similarly the array L_{18} ($2^1 3^7$) has 18 rows; one "*2 level*" column; and seven "*3 level*" columns. Thus, there are eight columns in the array L_{18}. The number of rows of an *orthogonal array* represents the requisite number of experiments. The number of

rows must be at least equal to the degrees of the freedom associated with the factors i.e. the *control variables*. In general, the number of degrees of freedom associated with a factor (*control variable*) is equal to the *number of levels for that factor minus one*. For example, a case study has one factor (A) with "*2 levels*" (A), and five factors (B, C, D, E, F) each with "3 *levels*". **Table 6.2** depicts the degrees of freedom calculated for this case. The number of columns of an array represents the maximum number of factors that can be studied using that array.

Table 6.1 Standard orthogonal arrays [89]

Orthogonal array	Number of rows	Maximum Number of factors	Maximum number of columns at these levels			
			2	3	4	5
L4	4	3	3	-	-	-
L8	8	7	7	-	-	-
L9	9	4	-	4	-	-
L12	12	11	11	-	-	-
L16	16	15	15	-	-	-
L16	16	5	-	-	5	-
L18	18	8	1	7	-	-
L25	25	6	-	-	-	6
L27	27	13	-	13	-	-
L32	32	31	31	-	-	-
L32	32	10	1	-	9	-
L36	36	23	11	12	-	-
L36	36	16	3	13	-	-
L50	50	12	1	-	-	11
L54	54	26	1	25	-	-
L64	64	63	63	-	-	-
L64	64	21	-	-	21	-
L81	81	40	-	40	-	-

Table 6.2The degrees of freedom for one factor (A) in "*2 levels*" and five factors (B, C, D, E, F) in "*3 levels*" [88]

Factors	Degrees of freedom
Overall mean	1
A	2-1=1
B,C,D,E,F	5×(3-1) = 10
Total	12

6.2.2 Static problems

Generally, a process to be optimized has several control factors (process parameters) which directly decide the target or desired value of the output. The optimization then involves determining the best levels of the control factor so that the output is at the target value. Such a problem is called as a "STATIC PROBLEM". This can be best explained using a P-Diagram **Figure 6.1** which is shown below ("P" stands for Process or Product). The noise is shown to be present in the process but should have no effect on the output. This is the primary aim of the Taguchi experiments - to minimize the variations in output even though noise is present in the process. The process is then said to have become ROBUST.

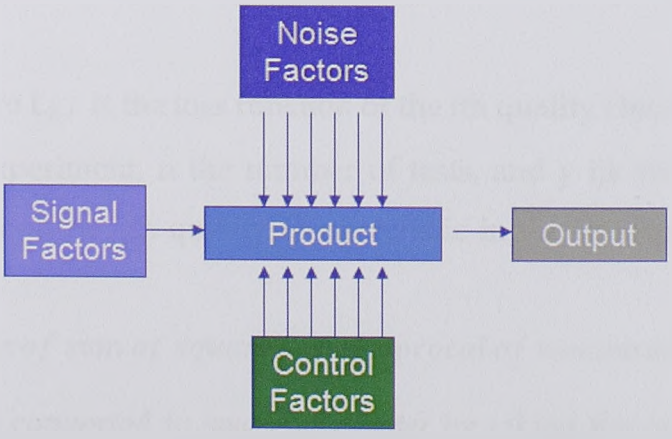

Figure 6.2 Diagram for static problems [90]

6.2.3 Signal to noise (S/N) ratio

There are three forms of *signal to noise* (S/N) ratio that are of common interest for optimization of static problems.

- Smaller-the-better, this is expressed as

$$n_j = -10\ Log_{10}\ [mean\ of\ sum\ of\ squares\ of\ measured\ data] \qquad (6.1)$$

This is usually the chosen S/N ratio for all the undesirable characteristics like "*defects*" for which the ideal value is zero. When an ideal value is finite and it's maximum or minimum value is defined (like the maximum purity is 100% or the maximum temperature is 92 °C or the minimum time for making a telephone connection is 1 sec), then the difference between the measured data and the ideal value is expected to be as small as possible. Thus, the generic form of S/N ratio becomes,

$$n_j = -10\ Log_{10}\ [mean\ of\ sum\ of\ squares\ of\ \{measured\text{-}ideal\}] \qquad (6.2)$$

- Larger-the-better

  The loss function of the higher the better quality characteristic can be expressed as:

$$L_{ij} = \frac{1}{n}\sum_{i=1}^{n}\frac{1}{y_{ijk}^2} \qquad (6.3)$$

  Where L_{ij}, is the loss function of the ith quality characteristic in the jth experiment, n the number of tests, and y ijk the experimental value of the ijth quality characteristic in the jth experiment at kth test.

$$n_j = -10\log_{10}[mean\ of\ sum\ of\ squares\ of\ reciprocal\ of\ measured\ data] \quad (6.4)$$

This is often converted to *smaller-the-better* by taking the reciprocal of the measured data and next, taking the S/N ratio as in the *smaller-the-better* case.

- Nominal-the-best

This is expressed as

$$n_j = -10\, log_{10}[\frac{square\ of\ mean}{variance}] \qquad (6.5)$$

This case arises when a specified value is the most desired, meaning that neither a smaller nor a larger value is desired.

6.2.4 Analysis of Variance ANOVA

The purpose of ANOVA [87] is to investigate which welding process parameters significantly affect the quality characteristics. This is accomplished by separating the total variability of the S/N ratios, which is measured by the sum of squared deviations from the total mean of the S/N ratio, into contribution by each of the welding process parameter and the error. The percentage contribution by each of the welding process parameters in the total sum of the squared deviations can be used to evaluate the importance of the process parameter change on the quality characteristic.

For the analysis of variance ANOVA of the orthogonal array L4 (2^3) which used in this work:

Mean of sum of main characteristic (y_{ijk}),

$$m = \sum (y_{ijk1} + y_{ijk2} + \cdots + y_{ijkn}) \qquad (6.6)$$

$$m_{A1} = \frac{1}{2}(y_{ijk1} + y_{ijk2}) \quad (6.7)$$

$$m_{A2} = \frac{1}{2}(y_{ijk3} + y_{ijk4}) \quad (6.8)$$

$$m_{B1} = \frac{1}{2}(y_{ijk1} + y_{ijk3}) \quad (6.9)$$

$$m_{B2} = \frac{1}{2}(y_{ijk2} + y_{ijk4}) \quad (6.10)$$

$$m_{C1} = \frac{1}{2}(y_{ijk1} + y_{ijk4}) \quad (6.11)$$

$$m_{C2} = \frac{1}{2}(y_{ijk2} + y_{ijk3}) \quad (6.12)$$

Grand total sum of squares: $\sum_{i=1}^{4} n_j^2$ (6.13)

Sum of squares due to mean: $\sum_{l=1}^{4} m^2$ (6.14)

Total sum of squares: $\sum_{i=1}^{4}(n_j - m)^2$ (6.15)

Sum of squares due to A: $2\sum_{i=1}^{4}(m_{Ai} - m)^2$ (6.16)

Sum of squares due to error: $\sum_{i=1}^{4} e_i^2$ (6.17)

6.3 Optimal selection of process parameters using Taguchi method

Optimization of process parameters [91] is the key step in the Taguchi's method to achieve high quality without increasing cost. This is because, optimization of process parameters can improve quality characteristic and optimal process parameters obtained from Taguchi method are insensitive to the variation of environment conditions and other noise factors.

6.3.1 Fracture toughness quality characteristic case

In metallurgy, fracture toughness [92] refers to a property which describes the ability of a material containing a crack to resist further fracture. It is a quantitative way of expressing a material's resistance to brittle fracture when a crack is present.

Fracture toughness is an indication of the amount of stress required to propagate a pre-existing flaw.

Flaws may appear as:

- Cracks
- Voids
- Metallurgical inclusions
- Weld defects
- Design discontinuities

A parameter called the stress-intensity factor (K) is used to determine the fracture toughness of most materials. The stress intensity factor is a function of:

- Loading
- Crack size
- Structural geometry

However in the present study manual metal arc (MMA) welding process, two electrodes TENACITO 75 and TENACITO 80 have been used to strike an electrical arc with base metal. The welding process is used to weld the base metal of NIONIKRAL-70 steel through four trials of Y-Groove test. The chemical composition and mechanical properties of the base metal steel are given in **Table 6.3** and **Table 6.4** respectively.

Table 6. 3 Chemical composition of the selected NIONIKRAL -70 steel in Wt%

Mtrl	**C**	**Si**	**Mn**	**P**	**S**	**Cr**	**Ni**	**Cu**	**Al**
%	0.106	0.209	0.220	0.005	0.0172	1.2575	2.361	0.246	0.007
Mo	**Ti**	**As**	**V**	**Nb**	**Sn**	**Ca**	**B**	**Pb**	**W**
0.305	0.002	0.017	0.052	0.007	0.014	0.0003	0	0.0009	0.0109
Sb	**Ta**	**Co**	**N**						
0.007	0.009	0.0189	0.0096						

Table 6. 4 Mechanical properties of the NIONIKRAL-70 steel

Specimen orientation		Yield stress	Tensile strength
		$R_{p0.2}$, MPa	R_m, MPa
Parallel to rolling	BM	780	820
	WM	718	791
	HAZ	750	800

6.3.2 Orthogonal array experiment

In the present study, two- levels process parameters i.e. preheating temperature, heat input and electrode strength are considered. The values of the welding process parameters are listed in **Table 6.5**. The total degrees of freedom of all process parameters are 3. The degrees of freedom of the orthogonal array should be greater than or at least equal to the degrees of freedom of all process parameters. Hence, L4 (2^3) orthogonal array was chosen

which has 3 degrees of freedom. This is shown in **Table 6.6**. However four experiments are conducted based on the orthogonal array, instead of 8 possibilities.

Table 6. 5Welding parameters and their levels (MMAW process)

Symbol	Process Parameter	Level 1	Level 2
A	Preheating Temperature (°C)	Room Temp. (20°C)	200°C
B	Heat Input (KJ/cm)	10	15
C	Electrode strength(N/mm^2)	Tenacito80 850	Tenacito75 720

Table 6. 6Orthogonal array type L4 (2^3)

Experiment number	A	B	C
1	1	1	1
2	1	2	2
3	2	1	2
4	2	2	1

As discussed earlier, the weld fracture toughness belongs to the higher-the-better quality characteristic (Eq. 6.3 and Eq. 6.4). The fracture toughness of the welded joints is measured for each experiment trial and the results are shown in **Table 6.7**. The corresponding S/N ratio for the four experiments is shown in **Table 6.8** and the mean S/N ratios for the three parameters two levels are calculated as shown in **Table 6.9**.

Table 6. 7 Experimental observations of fracture toughness

Trial number	Fracture toughness (MPa√m)	Average values of fracture toughness (MPa√m)
1	36, 33, 32	33.666
2	56, 63, 58	59
3	68, 75, 74	72.333
4	88, 77, 92	85.666

Table 6. 8 S/N ratio of experimental fracture toughness results

Trial number	S/N (db)
1	30.5438
2	35.4170
3	37.1867
4	38.6561

Table 6. 9 Mean S/N ratio for the parameters

Level	Factor A	Factor B	Factor C
1	32.9804	33.8652	34.5999
2	37.9214	37.0365	36.3018

6.3.3 Analysis of Variance (ANOVA)

The purpose of ANOVA in Taguchi method as mentioned previously is to investigate which welding process parameters significantly affect the quality characteristics (Eq. 6.6 - Eq. 6.17). The results of the ANOVA of this study are shown in **Table 6.10**. Both of percentage contribution and S/N ratio charts have been plotted as illustrated in **Figure 6.3** and **Figure 6.4** respectively.

Table 6. 10 Results of the ANOVA

Symbol	Degree of freedom	Sum of squares	Mean square	% Contribution
A	1	1067.064	1067.064	72.25
B	1	373.804	373.804	25.31
C	1	36	36	2.43
Error	0	0	-	
Total	3	1476.868		100%

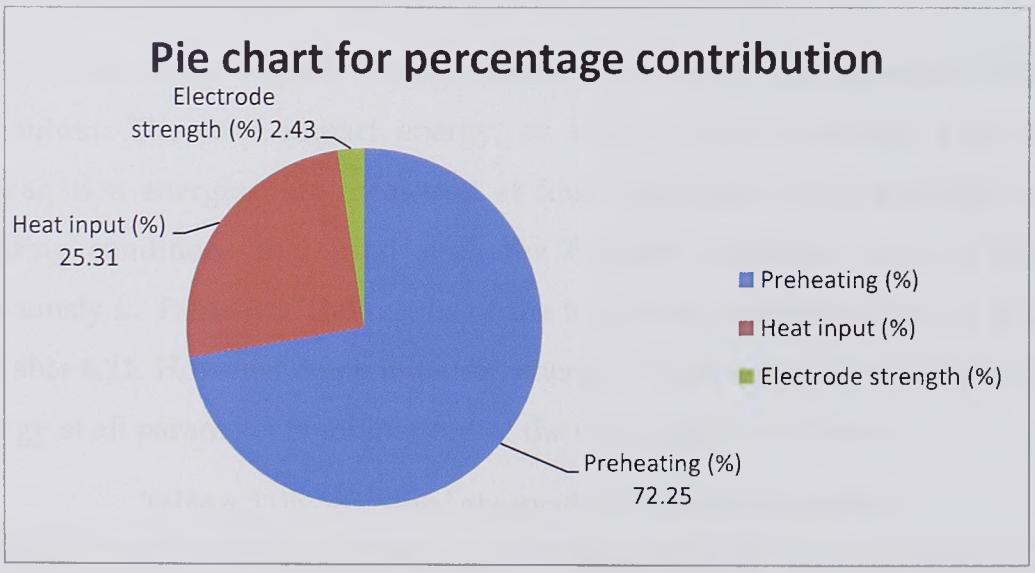

Figure 6. 3 Percentage contributions of parameters

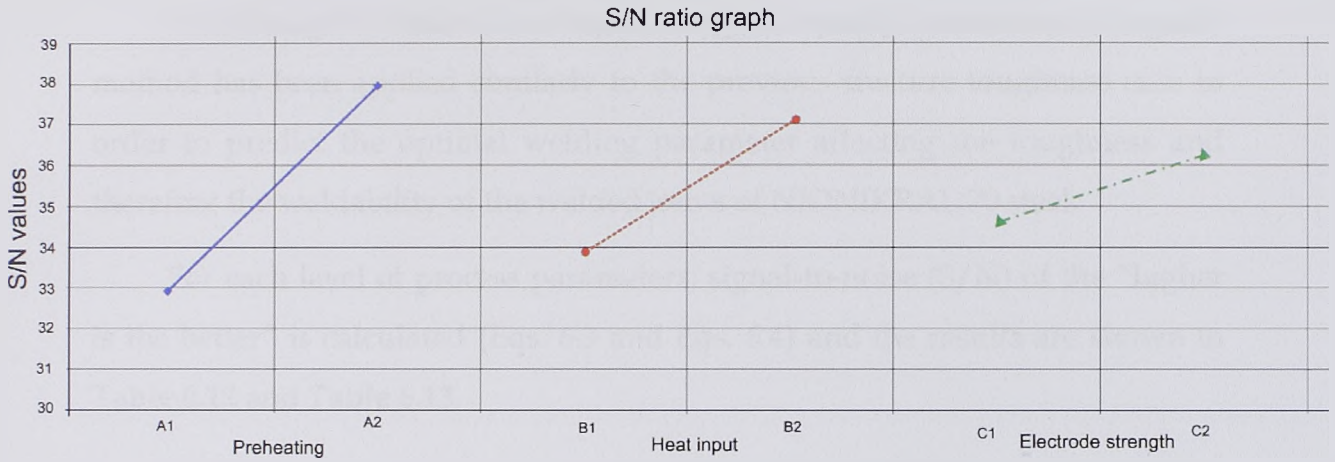

Figure 6. 4 S/N Ratio graph for fracture toughness case

6.3.4 Taguchi method of toughness quality characteristic

In this study impact testing results obtained by instrumented Charpy pendulum. The total impact energy, as well as crack initiation and crack propagation energies, are measured at four experiment trials with the same welding conditions that used with the fracture toughness case as shown previously in **Table 6.5**. The results of the toughness measurements are shown in **Table 6.11**. However crack initiation energy is higher than crack propagation energy at all parameter combinations of the four experiment trials.

Table 6. 11Experimental observations of impact toughness

Trial number	Initiation Energy (J)	Propagation Energy (J)	Total Energy (J)
1	24	16	40
2	36	26	62
3	45	32	77
4	58	43	101

Considering the obtained total impact energy as a quality characteristic, Taguchi method has been applied similarly to the previous fracture toughness case in order to predict the optimal welding parameter affecting the toughness and therefore the weldability of the welded joints of NIONIKRAL 70 steel.

For each level of process parameters, signal-to-noise (S/N) of the "higher is the better" is calculated (Eqs. 6.3 and Eqs. 6.4) and the results are shown in **Table 6.12** and **Table 6.13**.

Taguchi cannot judge [93] and determine effect of individual parameters on entire process while percentage contribution of individual parameters can be well determined using ANOVA. However to investigate effect of process parameters (preheating temperature, heat input and electrode strength) on quality characteristic (toughness) ANOVA has been obtained and the results are shown in **Table 6.14**.

Table 6. 12 S/N ratio of experimental fracture toughness results

Trial number	S/N (db)
1	32.0412
2	35.8478
3	37.7298
4	40.0864

Table 6. 13Mean S/N ratio for the parameters

Level	Factor A	Factor B	Factor C
1	33.9445	34.8855	36.0638
2	38.9081	37.9671	36.7888

Table 6. 14 Results of the ANOVA for impact toughness

Symbol	Degree of freedom	Sum of squares	Mean square	% Contribution
A	1	1444	1444	73.15
B	1	529	529	26.79
C	1	1	1	0.05
Error	0	0	-	
Total	3	1974		100%

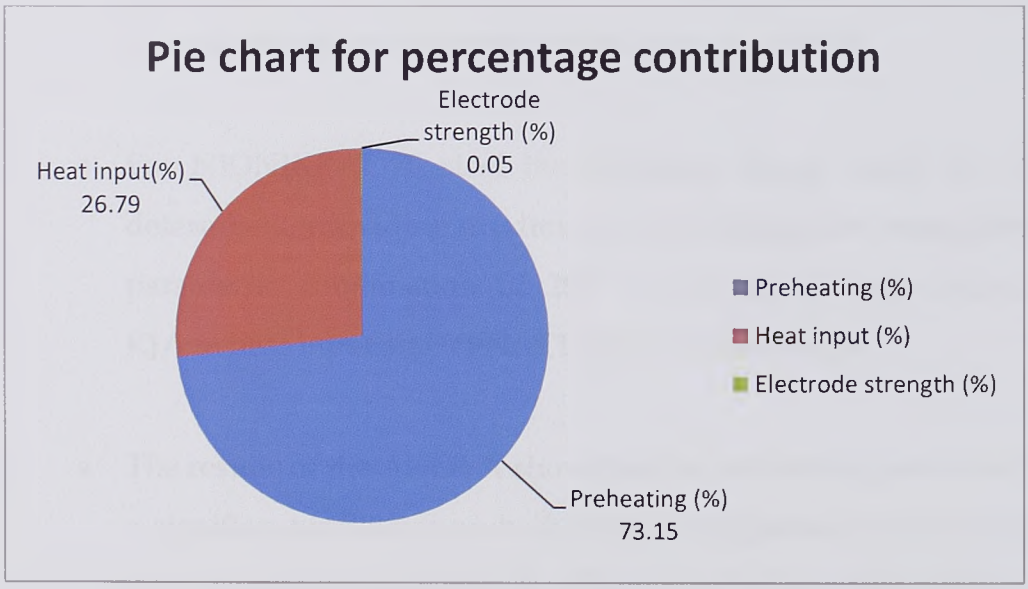

Figure 6. 5 Percentage contributions of parameters

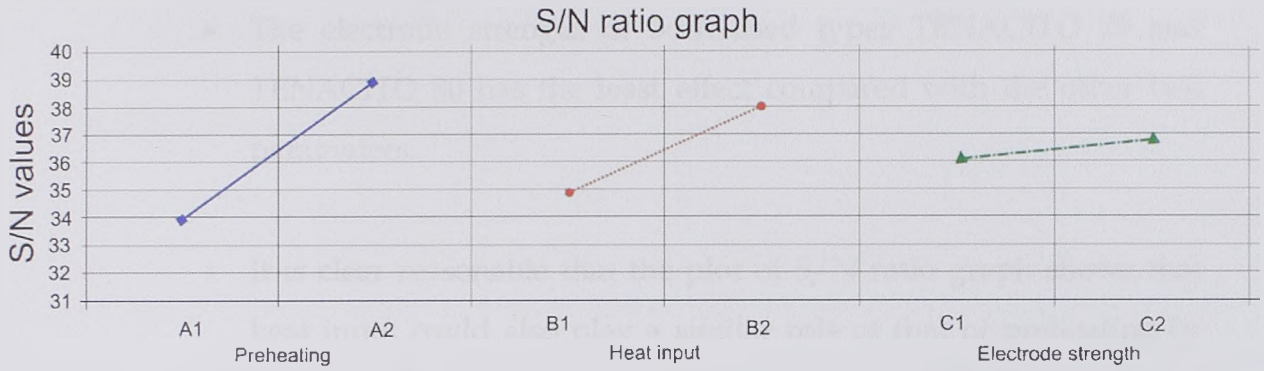

Figure 6. 6 S/N Ratio graph for impact toughness case

6.5 Conclusion

- The optimization of manual metal arc (MMA) welding process parameters of NIONIKRAL-70 steel welds using the recommendation of Taguchi method was successful.

- For NIONIKRAL-70 steel the optimum energy input has been determined, providing maximum crack propagation energy due to parametric combination of 200 °C preheating temperature, 15 KJ/cm heat input and TENACITO-80 electrode type.

- The results of the ANOVA show that the preheating parameter has a significant influence on both fracture toughness by (72.25%) and on the impact toughness by (73.15%) of HSLA NIONIKRAL 70 steel welds compared with the other two parameters.

- However this result is correlated with that of chapter 5 as shown in figure 5.18 where the preheating of 200 °C gave the most ductile microstructure compared with other lower temperatures.

- The electrode strength of both used types TENACITO 75 and TENACITO 80 has the least effect compared with the other two parameters.

- It is clear reasonable that the plot of S/N ratio graph shows that heat input could also play a similar role of that of preheating by reducing the cooling rate resulting more ductile microstructure which is more preferable to avoid cold cracks.

- Despite that the orthogonal array L4 (2^3) to design experiments with three 2-level/factors which used in this work has the less trials among the other arrays in the standard of the Taguchi approach it has shown an accepted and reasonable results with less time and effort which are the most important goals of applying the technique of product design optimization.

7. Conclusions and Future Work

7.1 Summary of Conclusions

The objectives of this thesis have required to cover knowledge of very wide and different areas such as welding engineering, metallurgy engineering and materials science. The mix of this theoretical requirement with the responsibility to design and implement the weldabilty tests in a laboratory to fulfill the experimentation necessities of this thesis work, has lead to a meticulous investigation exploiting several research lines in parallel. Each one of these research lines were developed in different chapters that, in conjunction, lead to one important and general conclusion: the weldability control of HSLA steels is entirely feasible and can produce very good performance crack-free results, if the main characteristics of this type of welding defect are taken into account and ad-hoc welding parameters are carefully chosen. Going more in detail, each one of the different working lines has provided important conclusions that are worth to mention. These conclusions are divided by chapters in the following paragraphs:

Chapter 2: "Literature Review"

- The study of the different previous work in this field reviews that preheating is necessary in welding some steel types to avoid cold cracking but it is also possible to weld without preheating in some other cases. According to the researchers results cold cracks had the higher percentage of the weld cracks in actual steel structures and the higher crack susceptibility was observed in the thickest welded metal plates. Some researchers concluded that the susceptibility toward cold cracking can be eliminated by using low hydrogen welding process and consumables.

- Moreover researchers observed that cracking was always associated with hard, martensitic regions adjacent to the fusion boundary. However other researchers emphasized that lower diffusible hydrogen level, lower weld metal strength, lower fusion boundary and HAZ hardness are quite important factors to prevent cold cracks. Some researches indicated that the presence of cracks in the welded metals with the combination of increased hardness 230 HV and the formation of high contents of acicular ferrite (above 93 %).

- It is clear that the resistance to cold cracking has generally improved in many different high strength steel types and the steps needed to avoid cold cracking through control of the welding parameters are well established.

- In brief, chapter 2 reviews the conceptual/theoretical dimension and the methodological dimension of the literature in cold cracking avoidance and discovers research questions or hypotheses that are worth researching in later chapters.

Chapter 3: "Fundamentals of HSLA Steel"

- Chapter 3 has been constructed to cover the most important issues concerning properties, applications, and processing of HSLA steel. From the wide range of information source used which exceeds 90 different references of the last three decades, it could be concluded that HSLA steel is one of the most important types of structural steels and still used in many different applications such as, pressure vessels, bridges, cars, trucks, cranes, platforms and other structures.

- HSLA steels vary from other steels in that they are made to meet all requirements for ductility, weldability and toughness. These steels have yield strengths which can be anywhere between 250-590 MPa with an increased strength-to-weight ratio over standard steels.

Chapter 4: "Weldability and Welding Rules of HSLA Steels"

This chapter has tackled different aspects as a strong theoretical background related to the main goal of this thesis work especially from HSLA steel weldability point of view. The main conclusions of this chapter are the following:

- Cracks that form in and around the weld can be distinguished into two main categories, hot cracks and cold cracks.

- The most serious problem with hydrogen induced cracking is difficulty in detecting the presence of a crack.

- Many different reasons could cause cold cracking such as a susceptible (brittle) microstructure, the presence of hydrogen in the weld metal, tensile stresses in the weld areas and higher carbon equivalent.

- The importance of preheating technique increases with the thickness of the base metal because of the rapid self quenching capability, and with the rigidity of the welded structure because of the derived constraints. Preheating is more favorable for limiting martensite formation and its hardness, hopefully contributing to higher quality crack-free welds.

- High strength low alloy HSLA steels can be welded by the entire commonly used arc welding process. Shielded metal arc, gas metal arc, flux cored arc, and submerged arc welding are used for most applications. Low hydrogen practices should be employed with all processes when carbon equivalents values indicate susceptibility towards cracking.

Chapter 5: "Weldability Testing-Experimental Procedure"

- Based on the susceptibility testing of NIONIKRAL-70 steel to cold cracking it could be concluded that for this HSLA steel there is a risk of cold cracking.

- Although CTS testing probe did not indicate such a conclusion, further investigations of intersection probe showed that it is more sensitive than CTS probe and the occurrence of cold cracking in welded joints of NIONIKRAL-70 steel can occur.

- The increased preheating temperature of 200 ° C in Y-Groove test causes a clear reduction in the hardness distribution which was in the range (250-270 HV) in both weld metal and HAZ of the welded joints of (batch 180079 electrode Tinacito-80, ⌀4 mm) which could reduce the probability of having such a crack.

- Through the "Y" probe investigating this study indicates some (minimal) differences in behavior of testing batches 180 080 and 180 079.

- "Y" probe, carried out at different preheating temperatures proved to be selective and gave a realistic picture of the behavior of

welded joints. Based on the results, "Y" probe were observed (albeit minimal) benefits of batch 180 080 compared with 180 079 and electrode batch TENACITO-80 compared with TENACITO-75, from the standpoint of susceptibility to cold cracking. According to the values of carbon equivalents (CE, Ce and Pp) and the results obtained by various technological tests; we can say that there is a risk of cold cracking.

- Cabelka-Million test probe results unequivocally demonstrated that batch of 180 079 more sensitive to the phenomenon of delayed cracking than batch 180 080. In any case, the fact remains that when welding NIONIKRAL-70 steel should take precautions to reduce the risk of occurrence of cold cracking.

- Analysis of results shows that the NIONIKRAL -70 steel within the limits of chemical composition and thickness up to 30 mm with other mechanical and technological characteristics puts the newly conquered steel the most promising high-strength steel meant for shipbuilding and manufacture of pressure vessels.

Chapter 6: **"Evaluation of HSLA Steel Wedability using Taguchi Method for DOE"**

- The optimization of manual metal arc (MMA) welding process parameters of NIONIKRAL-70 steel welds using the recommendation of Taguchi method was successful.

- For NIONIKRAL-70 steel the optimum energy input has been determined, providing maximum crack propagation energy due to

parametric combination of 200 °C preheating temperature, 15 KJ/cm heat input and TENACITO-80 electrode type.

- The results of the ANOVA show that the preheating parameter has a significant influence on both fracture toughness by (72.25%) and on the impact toughness by (73.15%) of HSLA NIONIKRAL 70 steel welds compared with the other two parameters.

- However this result is correlated with that of chapter 5 as shown in figure 5.18 where the preheating of 200 °C gave the most ductile microstructure compared with other lower temperatures.

- The electrode strength of both used types TENACITO 75 and TENACITO 80 has the least effect compared with the other two parameters.

- The plot of S/N ratio graph shows that heat input could also play a similar role of that of preheating by reducing the cooling rate resulting more ductile microstructure which is more preferable to avoid cold cracks.

- Despite that the orthogonal array L4 (2^3) to design experiments with three 2-level/factors which used in this work has the less trials among the other arrays in the standard of the Taguchi approach it has shown an accepted and reasonable results with less time and effort which are the most important goals of applying the technique of product design optimization.

7.2 Future work

- Following the investigations described in this thesis, and because of the variation of the factors which are affecting this serous welding problem, thus it is still a research field as mentioned in other research works (e.g. that of R. Capriotti and M. Colavita 2000, A D Batte and P J Boothby and FERA 2000), number of suggestions could be taken up:

- In order to find more accurate solutions for this welding phenomenon. In particular, some preliminary analysis carried out during this thesis, have shown that the cracks could not be completely avoided. Thus, it is necessary to perform more experiments about these factors such as welding parameters to discover the true link between these factors and the occurrence of cold cracking and, moreover, if these relationships can be unified with the other studies proposed in the research literature.

- Based on the possibility to weld HSLA steel using any welding process, it is strongly recommended to use more welding processes comparing with the results of this thesis work and the research literature as well.

- Beside the weldability tests such as, CTS and Y-Groove tests which have been used in this thesis work to test the susceptibility of HSLA NIONIKRAL-70 steel toward cold cracking, it could be also suggested to apply other new methods such as GOBP test comparing the results.

- To test the performance of other types of electrodes such as BOHLER type and to extend the results of the TENACITO electrodes which used in this thesis.

- To apply Taguchi method for DOE using other orthogonal array type with more trials, welding parameters and levels.

List of references:

[1] International Molybdenum Association 4Healthfied Terrace London W4 4JE UK (1989).

[2] Understanding The Weldability Of Niobium-Bearing HSLA Steel By, A D Batte, P J Boothby And A Rothwell (2001).

[3] ASM International (Alloying, Understanding The Basics) Code#06117G (2001).

[4] The Metallurgy, Welding, And Qualification Of Microalloyed (HSLA) Steel Weldments. Editors (J.T.Hickey, D.G.Howden, And M.D.Randall (1990).

[5] ASM Specialty Handbook Carbon And Alloys Steels Edited By, J.R Davis Associates (1999).

[6] Welding imperfections, www.marinewiki.org.

[7] Hydrogen Embrtittlement An Over View From A Mechanical Fastenings Aspect, FERA 17 Northwick Crescent Solihull West Midlands B91 3TU (2000)

[8] Weld Metal Hydrogen Cracking In Pipeline Girth Welds, Proc. 1st International Conference, Wollongong, Australia, Published By Welding Technology Institute Of Australia (Wtia), By Phm Hart, Granta Park, Great Abington (1999).

[9] Jssc Guidance Report On Determination Of Safe Preheating Conditions Without Weld Cracks In Steel Structures, Kunimihiko Satoh, Shigetomo Matsui (1973).

[10] Hydrogen embrittlement detection on HSS by means of XRD Residual Stress Determination Technique R. Capriotti and M. Colavita Aeronautica Militare, Centro Sperimentale di Volo, Reparto Chimico Pratica di Mare (Roma), Italy I-00040 (2000).

[11] Understanding The Weldability Of Niobium-Bearing Hsla Steels By A D Batte, P J Boothby And A B Rothwell, Uk Transcanada Pipelines, Calgary, Canada (2012).

[12] Journal of ship production, volume 19, number3, pp.159-164(6) 1 August (2003)

[13] Predictive model for the prevention of weld metal hydrogen cracking in high strength multipass welds, Pekka Nevasmaa, University of Oulu Finland (2003).

[14] Control of weldability, Per Hansson, Royal institute of technology Stockholm (2004).

[15] Microstrucral parameter controlling weld metal cold cracking, J.S. Seo, H.J.Kim, H.S.Ryoo, Korea institute of industrial technology, Volume 27 issue 2 April (2008).

[16] Progress in low transformation temperature (LTT) filler wires, G.Cam, O.Ozdemir and Kocak, International conference of the international institute of welding, , Istanbul, Turkey11-17 July (2010).

[17] Hydrogen degradation of high-strength steels, J.Cwiek, Journal of achievements in materials and manufacturing engineering, volume 37 issue, Poland 2 December (2009).

[18] One step further-500 MPa yield strength steel for offshore constructions, F.Hanus, J.Schutz and W.Shutz, OMAE- Dillingen Germany (2002).

[19] Effect of shielding gas mixture on gas metal arc welding of HSLA steel using solid and flux-cored wires, S. Mukhopadhyay, T.K. Pal, London 2005.

[20] The weld cracking susceptibility of high hardness armour steel, S.J. Alkemade, DSTO-TR-0320 (1996).

[21] Determination of necessary preheat temperature to avoid cold cracking under varying ambient temperature, Tadashi Kasuya and Nobutaka Yurioka, Nippon steel corporation May 26 Japan (1995).

[22] Fukuhisa Matsuda, Hiroji Nakagawa, Kenji Shinozaki. Criterion of alternative initiation of cold cracking in HAZ or weld metal for root pass welds of high strength steels, published by welding research institute of OsakaUniversity,Ibaraki,Osaka567, apan 31 October,Vol.12,No.21983(1983).

[23] Tadashi Kasuya Nobutaka Yurioka, Makoto Okumura, Methods for predicting maximum hardness of heat-affected zone and selecting necessary preheat temperature for steel welding, Nippon steel technical report No. 65 April (1995).

[24] Raimundo Carlos Silverio Freire Junior , Theophilo Moura Maciel , evaluation of cold crack susceptibility on HSLA steel welded joints, Federal University of Paraiba - center of science and technology - department of mechanical engineering, CEP 58.109-970, Campina Grande, PB, Brazil (2003).

[25] M. D. Rowe, T. W. Nelson, J. C. Lippold, Hydrogen-induced cracking along the fusion boundary of dissimilar metal welds, Supplement to the welding journal, February (1999).

[26] Jose Hilton Ferreira da Silva, Hipolito Carvajal Fals, Proposal of a new G-BOP test to evaluate cracks in weld beads in thin sheets,12November 2008 published online: 9 December 2008 - ASM International (2008).

[27] Yoni Adonyi, Weldability of high performance steels, Le Tourneau University.

[28] Richard E. Smith, David W. Gandy, Ambient temperature preheat for machine GTAW tempered applications, EPRI repair & replacement applications center (PRAC) 1300 W. T. Harris Boulevard Charlotte, NC 28262,GC 111050, November (1998).

[29] Jae Hak Kim, Jun Seok Seo, Effect of Weld Metal Microstructures on Cold Crack Susceptibility of FCAW weld metal, Metals and Materials International, Vol. 14, pp. 239~245 No. 2 (2008).

[30] D. D. Harwig, D. P. Longenecker, J. H. Cruz, Effects of welding parameters and electrode atmospheric exposure on the diffusible hydrogen content of gas shielded flux cored, Edison Welding Institute, Columbus, Ohio and ´ Tower Automotive, Milwaukee, Wis, November (1999).

[31] R. Pargeter, Evaluation of necessary delay before inspection for hydrogen cracks, welding journal 321-S, November (2003).
[32] B. Swieczko-Zurek, S. Sobieszczyk, J.Cwiek, Evaluation of susceptibility of high strength steels to hydrogen delayed cracking, Journal of achievements in materials and manufacturing engineering, Volume 18 Issue 1-2 September (2006).
[33] G. Magudeeswaran, V. Balasubramanian and G. Madhusudhan Reddy, Cold cracking of Flux Cored Arc welded armour grade high strength steel weldments, J. Mater. Sci. Technol., Vol.25 No.4, (2009).
[34] M. Anis, Deni Ferdian. Failure analysis of 4" Elbow Pipe Weld Crack" Dept. Metallurgy and Material, Engineering Faculty University of Indonesia Kampus Baru UI Depok, 16424.
[35] J. W. Martin, J. Kittel T. Cassagne and C. Bosch 17th JTM, Milan11/15 May (2009).
[36] Http://www.keytometals.com/Articles/Art146.htm.
[37] Http://sperle.se/referenser/pdf/artiklar/V2_JK250.pdf.
[38] Http://www.matter.org.uk/steelmatter/metallurgy/7_1.html.
[39] Industrial heating the international journal of the thermal technology by George F. Vander Voort, Buehler Ltd, Lake Bluff, (2009).
[40] Http://vanitec.org/wp-content/uploads/2011/09/Overview-of-Microalloying-in-Steel.pdf.
[41] Http://www.bergpipe.com/files/ep_tp_44_02en.pdf.
[42] Development of the microalloyed constructional steels-Journal of Achievements in Materials and Manufacturing Engineering, volume 14 issue1-2 January-February (2006).
[43] High strength steels iron and steel institute, Percy Lund, Humphries& Co.Ltd London.
[44] Data-driven metallurgical design for high strength low alloy (HSLA) steel Wei Hu Iowa State University, (2008).
[45] Http://www.baosteel.com/english_n/e07technical_n/021702e.pdf5
[46] Modelling of the DP and TRIP microstructure in the CMnAISi automotive steel, A.K.Lis, B.Gajda, volume 15 issue 1-2 Mrach-April (2006).
[47] Evolution of advanced high strength steels in automotive applications, Jody N. Hall general motors company chair, joint policy council, auto/steel partnership May 18, (2011).
[48] WorldAoutoSteel, the automotive group of the world steel association, www.worldautosteel.org.
[49] New high strength steels applied to the body structure of ULSAB-AVC, Blake K. Zuidema and Stephen G.Denner, National Steel Corporation, (2001).
[50] IMOA,international molybdenum association, HSLA steel, www.imoa.info.
[51]DOE program merit review meeting southern regional center for lightweight innovative design (SRCLID)advanced high strength steel project June 7-11,(2010).

[52] High Strength Low Alloy (HSLA) Steel, IMOA, issue 8-July (2012).
[53] Weldability and defects in weldments, Suranaree University of Technology- Sep-Dec (2007).
[54] http://en.wikipedia.org/wiki/Weldability.
[55] Introduction to the selection of carbon and low-alloy steels, Bruce R. Somers, Lehigh University.
[56] Http://app.eng.ubu.ac.th/~edocs/f20061122Suriya106.pdf.
[57] Welding options in steel construction Dr. Jayanta k Saha, Dy.General managerInstitute for steel development & Growth, Kolkata, India.
[58] Http://mme.uwaterloo.ca/~camj/pdf/49_07_1629.pdf.
[59] Solidification and phase transformations in welding, Suranaree University of Technology Sep-Dec (2007).
[60] Control of weldability, Department of Production Engineering Royal Institute of Technology Stockholm (2004).
[61]Http://www.struers.co.uk/resources/elements/12/97489/Application%20Notes%20Welding%20English.pdf.
[62] Http://www4.hcmut.edu.vn/~dantn/Weld%20pool/truehaz.htm.
[63] WJM Technology excellence in material joining, Girish P. Kelkar, Ph.D. www.welding-consultant.com.
[64] Cold cracks, causes and cures, www.kobelkoweldingtoday.com.
[65] A.Radovic- metalluragy and weldability problems, proceedings of internationally-counseling,, Vranje 85, Belgrade (1985).
[66] A.Radovic– Lectures on postgraduate studies, subjects weldability target and safety of welded structures 19781978/79 godina.
[67] A. Radovic–Defining technological weldability of high strength steels, VTI, Belgrade.
[68] Hydrogen embrittlement of welded joints for the heat-treatable XABO 960 steel heavy plates, M. Opiela- volume 38 issue 1 January (2010).
[69] A review on effect of preheating and/or post weld heat treatment (PWHT) on mechanical behavior of ferrous metals, BIPIN KUMAR SRIVASTSVA. et. al. / International journal of engineering science and technology Vol. 2(4), 2010, 625-631.
[70] SSAB Oxelosund - a subsidiary of SSAB Swedish Steel Group, www.ssabox.com.
[71] Single nozzle preheating on long seam pipe, www.youtube.com.
[72] Taking your weld's temperature, North American Steel Construction Conference, R. Scott Funderburk, (2000).
[73] Methods for predicting maximum hardness of heat-affected zone and selecting necessary preheat temperature for steel welding; Tadashi Kasuya, Nobutaka Yurioka and Makoto Okumura, Nippon steel technical report No. 65 April (1995).
[74] Preheat calculator- non alloyed and low alloy steels, www.gowelding.com

[75] The hydrogen-induced cracking resistance of consumables for use in the fabrication of the Collins class Submarines,James L. Davidson-Commonwealth of Australia (1996).
[76] American Welding Society (AWS) 550 N.W.LeJenue Road Miami, FL 33126.
[77] High heat input/reduced preheat welding of HSLA welding HSLA—100100 Provo, Utah Provo, Utah April 4 April 4--5, 20065, (2006).
[78] High Heat Input/Reduced Preheat Welding of HSLA welding HSLA--100100Provo, UtahProvo, UtahApril 4April 4--5, 20065, (2006).
[79] Solidification cracks in HSLA steel joints after controlled thermal severity tests, Campus del Mar. Dr. Fleming, Cartagena 30202, Spain(2000).
[80] Hot-cracking mitigation technique for welding high-strength aluminum alloy, by Y. P. Yang, P. Dong, J. Zhang and X. Tian (2000).
[81] Hot crack images ww.google.co.uk/search? q=hot + cracking+ mages.
[82]Lamellartearing.Www.Ewf,Copyrigth.Http//Www.Deletals.Com/Fr/Fdf/Http//Www.Delmetal.Com/Fr/Pdfs/C-Hemicanical_Alloying of Steelpdf (2007).
[83]http://www.delmetals.com/fr/pdfs/CChemicalComp_AlloyingOfSteel.pd
[84] Key Concepts In Welding Engineering, By R. Scott Funderburk Selecting Filler Metals: Low Hydrogen, Welding Innovation Vol. XVII, No. 1, (2000).
[85] Kobelco welding today, IIW Doc. XII-1647-00, (2000).
[86] DOE-I basic design of experiments, by Nutek, Inc. 3829 Quarton Road Bloomfield Hills, Michigan 48302, USA, http://nutek-us.com.
[87] Process parameter optimization in ARC welding of dissimilar metals, Lenin N., Sivakumar M. and Vigneshkumar D, Thammasat Int. J. Sc. Tech., Vol. 15, No. 3, July-September (2010).
[88] Design Of Experiments Ittdelhi, P M V Subbarao, Professor, Indian Institute Of Technology Delhi, Mechanical Engineering Department.
[89] Indian Institute Of Technology Bombay, Lecture 4 Approach To Robust Design (2009).
[90]Http://www.google.rs/search?q=taguchi+images&tbm=isch&tbo=u&source=univ&sa=X&ei=kDtpUqQLqOe4gS5g4GADA&ved=0CC4QsAQ&biw=1366&bih=667.
[91] Optimization Of Welding Parameters For Maximization Of Weld Bead Widths For Submerged Arc Welding Of Mild Steel Plates. International Jornal Of Engineering &Technology (Ijert) Issn: 2278-0181 Vol.1 Isuu 4, June-(2012).
[92] Http://Www.Corrosionpedia.Com/Definition/544/Fracture-Toughness
[93] Taguchi method and ANOVA, Bala, Biswanath and Sukamal, Journal of Scientific & Industrial Research vol.68, , pp.686-695 August (2009).

Biography

Abdalla S. Ahmed Tawengi was born on January, 24, 1971 in Surman Libya, he graduated in 1997 and got his BSc. in Mechanical Engineering from Zawia University, Faculty of Engineering of Sabratah . From 1999 to 2001 he worked as a departmental assistant at the same department. He got his MSc. degree from Budapest University, the Department of Materials Science and Engineering (2002-2006). Then he went back to Libya and worked at the previous department as an assistant lecturer for the period 2006-2008. He taught some subjects like workshop technology, technical report writing, fluid mechanics Lab, and supervised a final BSc. project. In 2008 he got his IELTS certificate from British council of Kuala Lumpur branch in Malaysia. He started doing his PhD program in 2009 at the Faculty of Mechanical Engineering in Belgrade University and, passed all exams by platform of these studies. He also participated in an international scientific journal and international conference.

Appendix A

Appendix A shows the standrad details of the Y-Groove test according to the mentioned reference in the appendix document.

E6. Oblique Y-Groove Test

1. Scope

1.1 The Oblique Y-groove test (Tekken Test) is a single-pass, restrained groove weld test used to evaluate susceptibility to hydrogen and weld metal solidification cracking of steel weldments.

1.2 This standard is applicable to the following, when specified:

(1) Qualification of materials and welding procedures

(2) Information, basis for acceptance and manufacturing quality control

(3) Research and development

1.3 The use of this test is restricted as follows:

(1) Base-metal thickness limited to 13 mm or greater.

(2) Test results are applicable only to the base-material thickness tested.

1.4 When this standard is used, the following information shall be furnished:

(1) Test number

(2) Welding procedure specification and procedure qualification record numbers (if applicable)

(3) Base-metal identification: specification, heat number, mill test chemistry and heat treatment

(4) Base-metal thickness

(5) Welding process

(6) Filler metal identification, specification and diameter

(7) Filler metal preweld conditioning (e.g., baking)

(8) Shielding gas identification: type, dew point, and flow rate

(9) All welding parameters

(10) Weld preheat temperature

(11) Maximum interpass temperature

(12) Acceptance criteria, if any

1.5 Safety Precautions. Safety precautions shall conform to the latest edition of ANSI Z49.1, *Safety in Welding, Cutting, and Allied Processes*, published by the American Welding Society.

Note: This standard may involve hazardous materials, operations, and equipment. The standard does not purport to address all of the safety problems associated with its use. It is the responsibility of the user to establish appropriate safety and health practices. The user should determine the applicability of any regulatory limitations prior to use.

2. Applicable Documents

Reference should be made to the latest edition of the following documents:

AWS A2.4	Standard Symbols for Welding, Brazing, and Nondestructive Examination
AWS A3.0	Standard Welding Terms and Definitions
AWS A4.3	Standard Methods for Determination of the Diffusible Hydrogen Content of Martensitic, Bainitic, and Ferritic Steel Weld Metal Produced by Arc Welding

The source for these documents is the following:

American Welding Society (AWS)
550 N.W. LeJeune Road
Miami, FL 33126

3. Summary of Method

3.1 The test is performed using a set of three flat plate test assemblies welded under identical conditions. Welds are deposited on each side of the test area to provide restraint. A single test weld is deposited in the restrained, machined groove of each assembly.

3.2 The combination of welding amperage, voltage and travel speed shall be such that the specified heat input range is obtained.

3.3 Each test weld is examined for the presence of hydrogen-assisted cracks, not less than 48 hours after depositing the test weld. Test welds are sectioned as required for internal examination.

3.4 Testing is usually conducted using several test sets welded identically over a range of preheat temperatures so that 100 percent cracking occurs at the lowest temperature tested and 0 percent cracking occurs at the highest temperature tested. Resulting data is useful as a comparative measure of the susceptibility of the material to cracking.

4. Significance

This test is used as a comparative measure to assess the susceptibility to hydrogen and weld metal solidification cracking of steel weldments.

5. Definitions and Symbols

The welding terms used in this section are in accordance with the latest edition of AWS A3.0, *Standard Welding Terms and Definitions.*

6. Apparatus

6.1 A simple fixture is used to hold the test plates so the restraining welds can be deposited. Water-cooled mechanical means are used to section completed test assemblies for internal examination for the presence of cracks. Metallographic equipment is required for polishing, etching, and examining specimens.

7. Specimens

7.1 Test assembly configuration is shown in Figure E19. All weld joint surfaces shall be machined to 4 micrometers R_a minimum. When it is possible to identify the rolling direction of the material being tested, the parts should be cut and assembled with the rolling direction perpendicular to the weld groove, unless otherwise specified.

7.2 The test assembly is fabricated by depositing welds on each end of the weld groove to provide the necessary restraint, as shown in Figure E19, Section A-A. Low-hydrogen-type mild steel filler metal is normally used. Welds shall be deposited by a suitable welding process, using a deep penetrating arc and a weave-bead technique to fill the joints with a minimum number of weld beads. Care shall be taken to minimize angular distortion during welding. Weld reinforcement should be approximately 2 mm. Maximum interpass temperature should be in accordance with steel manufacturers recommendations as applicable to the steel type being joined.

7.3 Each test assembly shall be dimensionally inspected after cooling to ensure the proper configuration as shown in Figure E19, Section B-B. The groove root opening dimension shall be within tolerance.

7.4 Fabricate a minimum of three test assemblies per set.

8. Procedure

8.1 All welding shall be performed in the flat position (1G).

8.2 Test assemblies shall be uniformly heated in an oven, to a temperature slightly higher than the desired preheat temperature. The test assembly is removed from the oven and the surface temperature near the bevel area shall be monitored. Welding shall begin when the desired preheat temperature is reached.

8.3 The single-pass test weld shall be deposited as shown in Figure E20. Welding techniques which promote good fusion and crater fill shall be employed. Following welding, the assembly shall be allowed to cool in still air. It shall be left at ambient temperature for a minimum period of 48 hours before examination for cracks.

8.4 The test weld area shall be examined for surface cracks. If surface cracks are visible, no further examination is required. If cracking is not visible, the weld shall be sectioned and examined microscopically.

8.5 When sectioning is required, the test weld should be sectioned at the one-fourth, one-half, and three-fourth length positions. Water-cooled mechanical means shall be used to section the test welds. Assemblies shall be securely clamped in such a manner that the cutting process does not contribute to weld root cracking. Sectioned specimens shall be polished, etched and examined at 20X for cracks.

8.6 When the test is used to evaluate susceptibility to hydrogen cracking, a diffusible hydrogen determination shall be performed for each welding process and consumable in accordance with AWS A4.3. The diffusible hydrogen determination shall be performed under the same conditions as the test weld.

9. Report

9.1 The test results that typically are reported include:

(1) Test number

(2) Welding procedure specification and procedure qualification record numbers (if applicable)

(3) Base metal identification

(4) Base metal thickness

(5) Filler metal identification

(6) Filler metal diameter

(7) Shielding gas identification

(8) All welding parameters necessary to completely define the procedure and heat input

(9) Weld preheat temperature

(10) Ambient temperature and relative humidity at time of welding

(11) Maximum interpass temperature allowed during welding of restraining welds (if applicable)

(12) Any observation of unusual characteristics of the test specimen, weld profile, section surface or procedure

(13) Results of Diffusible Hydrogen tests.

9.2 Test data should be recorded on a Test Results Sheet similar to Figure E21.

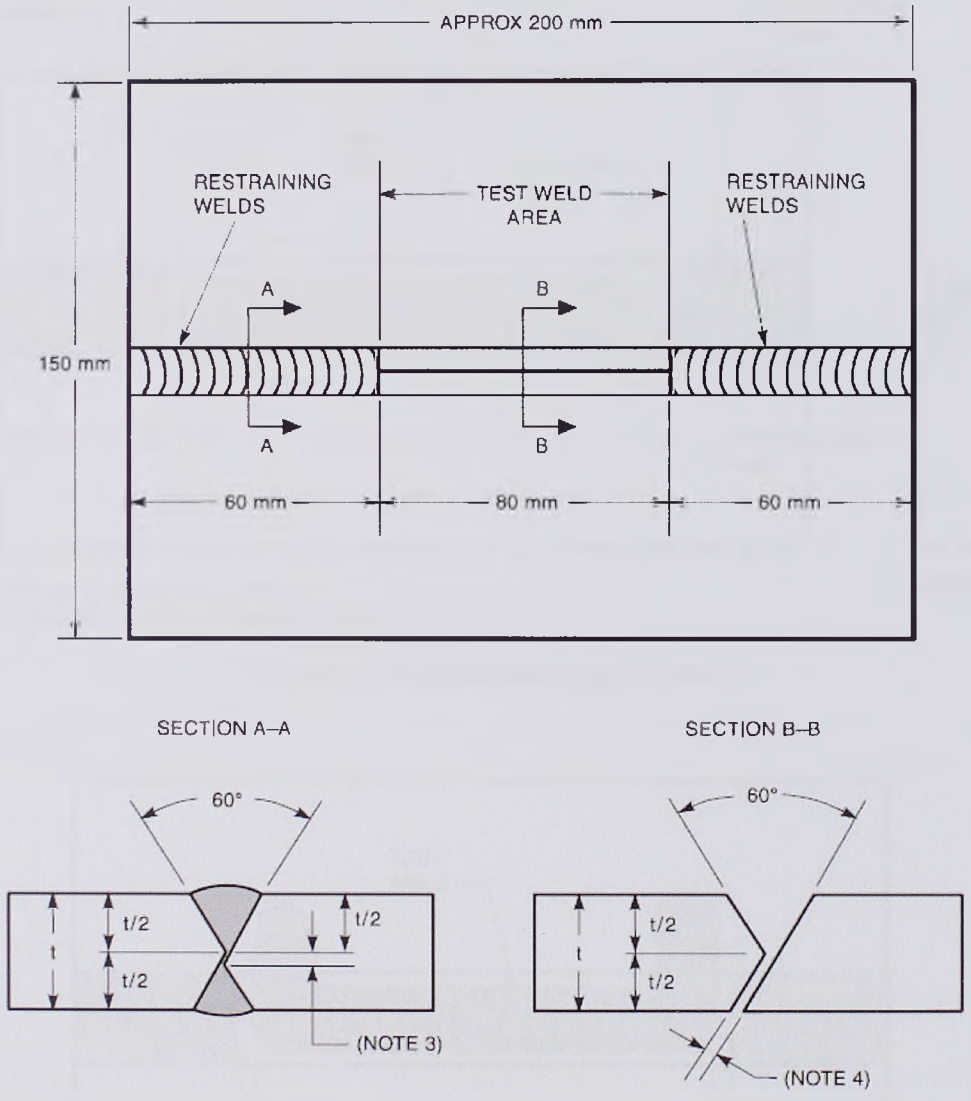

Notes:
1. Base metal outer edges may be thermally cut (not required to be machined).
2. Joint groove preparation shall be made by machine cutting. Surfaces should be no rougher than 4 micrometers R_a. It is recommended that the lay of the surface roughness be oriented parallel with the longitudinal axis of the specimen.
3. Dimension shall be 3 mm prior to depositing restraining welds.
4. Final dimension shall be 2 ± 0.2 mm after restraining welds are deposited. However, contraction caused during anchor welding must be considered prior to machining and assembly; typically approximately 0.3 mm shrinkage.

Figure E19—Oblique Y-Groove Test Assembly

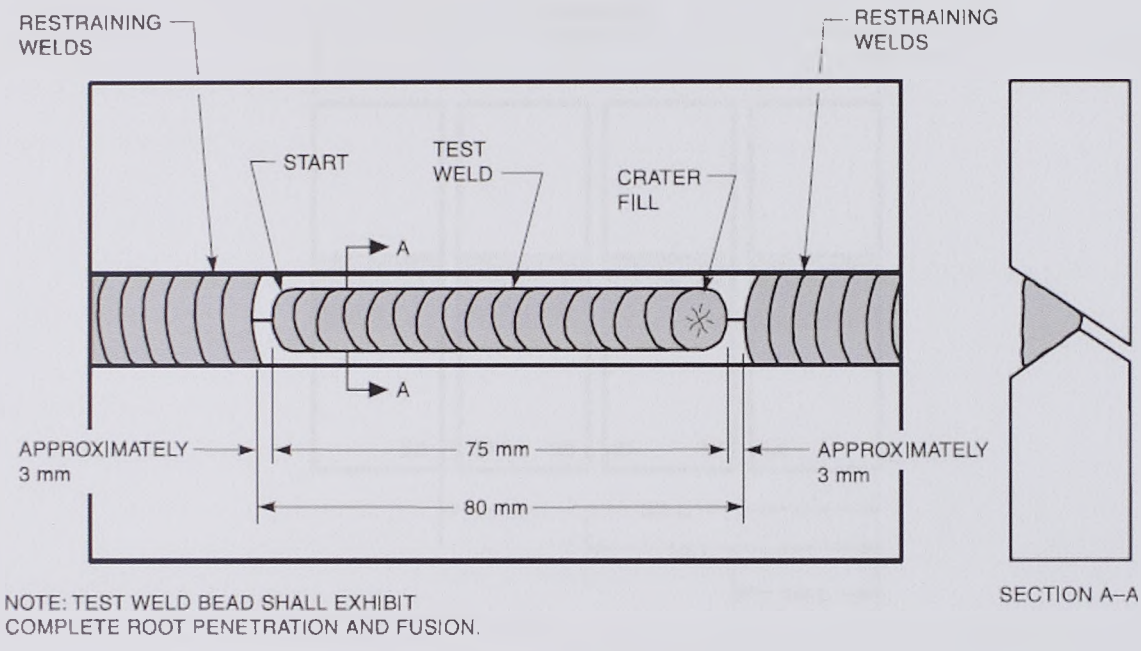

NOTE: TEST WELD BEAD SHALL EXHIBIT COMPLETE ROOT PENETRATION AND FUSION.

(A) TEST PLATE FOR MECHANIZED WELDING

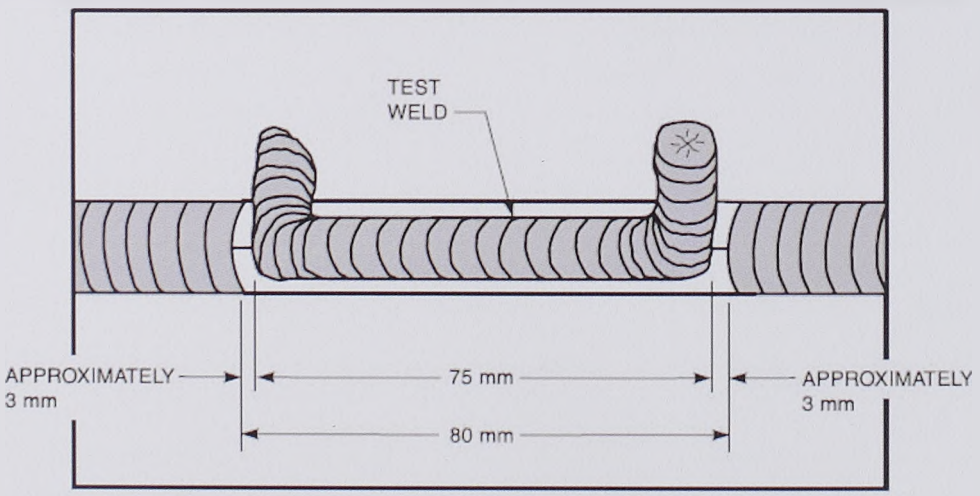

(B) TEST PLATE FOR MANUAL WELDING

Figure E20—Oblique Y-Groove Test Weld Configuration

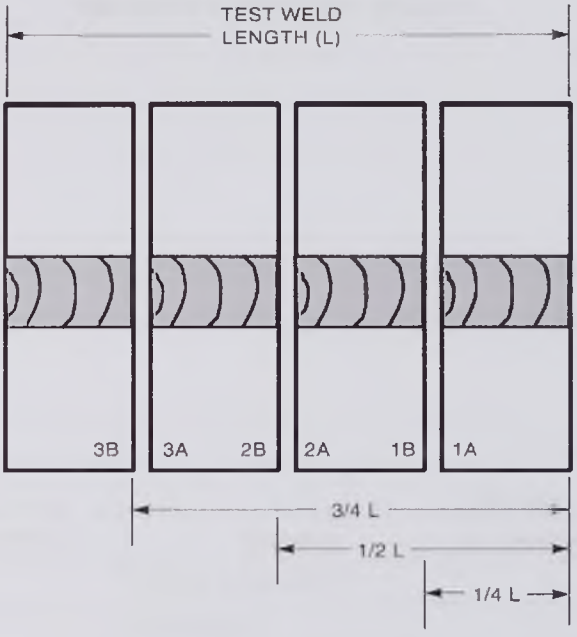

(C) SECTIONING OF TEST PLATE

Figure E20 (Continued)—Oblique Y-Groove Test Weld Configuration

OBLIQUE Y-GROOVE TEST RESULTS

Company Name _____ Date _____

Job/Test No. _____ Sheet _____ of _____

Description of Investigation _____

Material Identification _____

Material Thickness _____ Rolling Direction Indicated Y / N

Material Heat Treatment _____

Applicable Welding Procedure No. _____

Welding Details _____ Process _____

Date of Welding _____ Time Lapse—Welding to Testing (hrs) _____

Parameters	Test Weld	Parameters	Anchor Weld	Test Weld
Electrode/Wire Dia.		Welding Consumable ID		
Amperage		Specification		
Voltage		Classification		
Polarity		Baking Treatment		
Travel Speed		Shielding Gas Type, Medium		
Preheat Temperature		Shielding Gas Dew Point		
Heat Input		Max. Interpass Temp.		
Humidity (RH)		Measuring Method		
Ambient Temp.				
Hydrogen Determination Method		Date	Result	
EXAMINATION				
	Surface		Section	
Assembly No.	Inspection Method	Results (C or NC)	Inspection Method	Results (C or NC)

No. of Test Assemblies Inspected _____ Total % Cracking _____

Remarks _____

_____

Tested By _____

Signature _____ Date _____

Figure E21—Suggested Data Sheet for Oblique Y-Groove Test

Appendix B

The appendix B shows the information of both electrodes, TENACITO 75&TENACITO 80 respectively.

TENACITO 75

OERLIKON

MMA Electrodes
High-strength steels

Basic coated electrode producing tough and crack-free welded joints. Weld deposit is of extremely high metallurgical purity and very low hydrogen content. Due to its double coating (up to 3,2 mm), the electrode features a stable and concentrated arc, making it well-suited for positional welding. Welds are of X-ray quality.

Classification	
AWS	A5.5: E10018-G-H4
EN	757: E 69 6 Mn2NiCrMo B 42 H5

Approvals	Grades
DB	
DNV	
GL	
RS	
TÜV	

see Appendix, Classification Society Approvals, for details pag. 521

Analysis of all-weld metal (Typical values in %)

C	Mn	Si	P	S	Cr	Ni	Mo	Nb	V	N	Cu
0.06	1.40	0.50	≤ 0.020	≤ 0.012	0.40	2.20	0.40	-	-	-	-

All-weld metal Mechanical Properties

Heat Treatment	Yield Strength N/mm²	Tensile Strength N/mm²	Elongation A5 (%)	Impact Energy ISO - V (J) - 60 °C	Hardness
As Welded	≥ 720	760-900	≥ 17	≥ 60	-

Materials

S620-S690; P690; L415-L555

Storage and redrying

Keep dry and avoid condensation.
HD ≤ 5: Re-dry at 340-360 °C for 2 hours, 5 times max.

Current condition and welding position

DC+

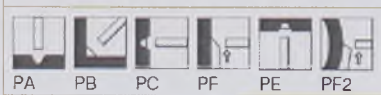

Packaging data

Diameter (mm)	Length (mm)	Current (A)	Electrode average weight (g)	Weld metal weight per electrode (g)
2,5	350	65-95	19,8	12,8
3,2	350	90-140	34,3	22,2
4,0	450	140-185	70,3	45,2
5,0	450	180-240	109,9	70,0

TENACITO 80

OERLIKON

MMA Electrodes
High-strength steels

Basic coated electrode producing tough and crack-free welded joints. Weld deposit is of extremely high metallurgical purity and very low hydrogen content. Due to its double coating (up to 3,2 mm), the electrode features a stable and concentrated arc, making it well-suited for positional welding. Welds are of X-ray quality.

Classification	
AWS	A5.5: E11018-G-H4
EN	757: E 69 6 Mn2NiCrMo B 42 H5

Approvals	Grades
ABS	
GL	
RS	
TÜV	

see Appendix, Classification Society Approvals, for details pag. 521

Analysis of all-weld metal (Typical values in %)

C	Mn	Si	P	S	Cr	Ni	Mo	Nb	V	N	Cu
0.06	1.80	0.50	≤ 0.020	≤ 0.012	0.35	2.20	0.40	-	-	-	-

All-weld metal Mechanical Properties

Heat Treatment	Yield Strength N/mm²	Tensile Strength N/mm²	Elongation A5 (%)	Impact Energy ISO - V (J) - 60 °C	Hardness
As Welded	≥ 800	850-960	≥ 16	≥ 60	-

Materials

S(P)690; L415-L555

Storage and redrying

Keep dry and avoid condensation.
HD ≤ 5: Re-dry at 340-360 °C for 2 hours, 5 times max.

Current condition and welding position

DC+

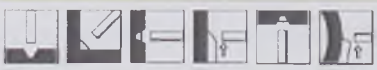

PA PB PC PF PE PF2

Packaging data

Diameter (mm)	Length (mm)	Current (A)	Electrode average weight (g)	Weld metal weight per electrode (g)
2,5	350	65-95	19,8	12,8
3,2	350	90-135	34,3	22,2
4,0	450	140-185	67,0	45,2
5,0	450	180-240	107,5	70,0

Прилог 1.

Изјава о ауторству

Потписани-а Abdalla S. Ahmed Tawengi

број уписа D 43/09

Изјављујем

да је докторска дисертација под насловом

EVALUATION OF WELDABILITY OF HSLA STEEL USING TAGUCHI METHOD FOR DESIGN OF EXPERIMENT

OdređivanjezavarljivostiniskolegiranihčelikapovišenečvrstoćeprimenomTagučij evemetodeplaniranjaeksperimenta

- резултат сопственог истраживачког рада,
- да предложена дисертација у целини ни у деловима није била предложена за добијање било које дипломе према студијским програмима других високошколских установа,
- да су резултати коректно наведени и
- да нисам кршио/ла ауторска права и користио интелектуалну својину других лица.

Потпис докторанда

У Београду, / /2014

Прилог 2.

Изјаваоистоветностиштампане и електронске верзиједокторског рада

Име и презиме аутора: **Abdalla S. Ahmed Tawengi**

Број уписа: D 43/09

Студијски програм: Doktorskestudije

Наслов рада :

EVALUATION OF WELDABILITY OF HSLA STEEL USING TAGUCHI METHOD FOR DESIGN OF EXPERIMENT

OdređivanjezavarljivostiniskolegiranihčelikapovišenečvrstoćeprimenomTagučij evemetodeplaniranjaeksperimenta

Ментор : Prof. Dr. Aleksandar Sedmak

Потписани : Abdalla S. AhmedTawengi

изјављујем да је штампана верзија мог докторског рада истоветна електронској верзији коју сам предао/ла за објављивање на порталу **Дигиталног репозиторијума Универзитета у Београду.**

Дозвољавам да се објаве моји лични подаци везани за добијање академског звања доктора наука, као што су име и презиме, година и место рођења и датум одбране рада.

Ови лични подаци могу се објавити на мрежним страницама дигиталне библиотеке, у електронском каталогу и у публикацијама Универзитета у Београду.

Потпис докторанда

У Београду, / /2014

Прилог 3.

Изјава о коришћењу

Овлашћујем Универзитетску библиотеку „Светозар Марковић" да у Дигитални репозиторијум Универзитета у Београду унесе моју докторску дисертацију под насловом:

EVALUATION OF WELDABILITY OF HSLA STEEL USING TAGUCHI METHOD FOR DESIGN OF EXPERIMENT

OdređivanjezavarljivostiniskolegiranihčelikapovišenečvrstoćeprimenomTagučij evemetodeplaniranjaeksperimenta

која је моје ауторско дело.

Дисертацију са свим прилозима предао/ла сам у електронском формату погодном за трајно архивирање.

Моју докторску дисертацију похрањену у Дигитални репозиторијум Универзитета у Београду могу да користе сви који поштују одредбе садржане у одабраном типу лиценце Креативне заједнице (Creative Commons) за коју сам се одлучио/ла.

1. Ауторство

2. Ауторство - некомерцијално

3. Ауторство – некомерцијално – без прераде

4. Ауторство – некомерцијално – делити под истим условима

5. Ауторство – без прераде

6. Ауторство – делити под истим условима

(Молимо да заокружите само једну од шест понуђених лиценци, кратак опис лиценци дат је на полеђини листа).

Потпис докторанда

У Београду, / /2014

1. Ауторство - Дозвољавате умножавање, дистрибуцију и јавно саопштавање дела, и прераде, ако се наведе име аутора на начин одређен од стране аутора или даваоца лиценце, чак и у комерцијалне сврхе. Ово је најслободнија од свих лиценци.

2. Ауторство – некомерцијално. Дозвољавате умножавање, дистрибуцију и јавно саопштавање дела, и прераде, ако се наведе име аутора на начин одређен од стране аутора или даваоца лиценце. Ова лиценца не дозвољава комерцијалну употребу дела.

3. Ауторство - некомерцијално – без прераде. Дозвољавате умножавање, дистрибуцију и јавно саопштавање дела, без промена, преобликовања или употребе дела у свом делу, ако се наведе име аутора на начин одређен од стране аутора или даваоца лиценце. Ова лиценца не дозвољава комерцијалну употребу дела. У односу на све остале лиценце, овом лиценцом се ограничава највећи обим права коришћења дела.

4. Ауторство - некомерцијално – делити под истим условима. Дозвољавате умножавање, дистрибуцију и јавно саопштавање дела, и прераде, ако се наведе име аутора на начин одређен од стране аутора или даваоца лиценце и ако се прерада дистрибуира под истом или сличном лиценцом. Ова лиценца не дозвољава комерцијалну употребу дела и прерада.

5. Ауторство – без прераде. Дозвољавате умножавање, дистрибуцију и јавно саопштавање дела, без промена, преобликовања или употребе дела у свом делу, ако се наведе име аутора на начин одређен од стране аутора или даваоца лиценце. Ова лиценца дозвољава комерцијалну употребу дела.

6. Ауторство - делити под истим условима. Дозвољавате умножавање, дистрибуцију и јавно саопштавање дела, и прераде, ако се наведе име аутора на начин одређен од стране аутора или даваоца лиценце и ако се прерада дистрибуира под истом или сличном лиценцом. Ова лиценца дозвољава комерцијалну употребу дела и прерада. Слична је софтверским лиценцама, односно лиценцама отвореног кода.